HETEK

A System for estimation of Chloride ingress into Concrete
Theoretical background

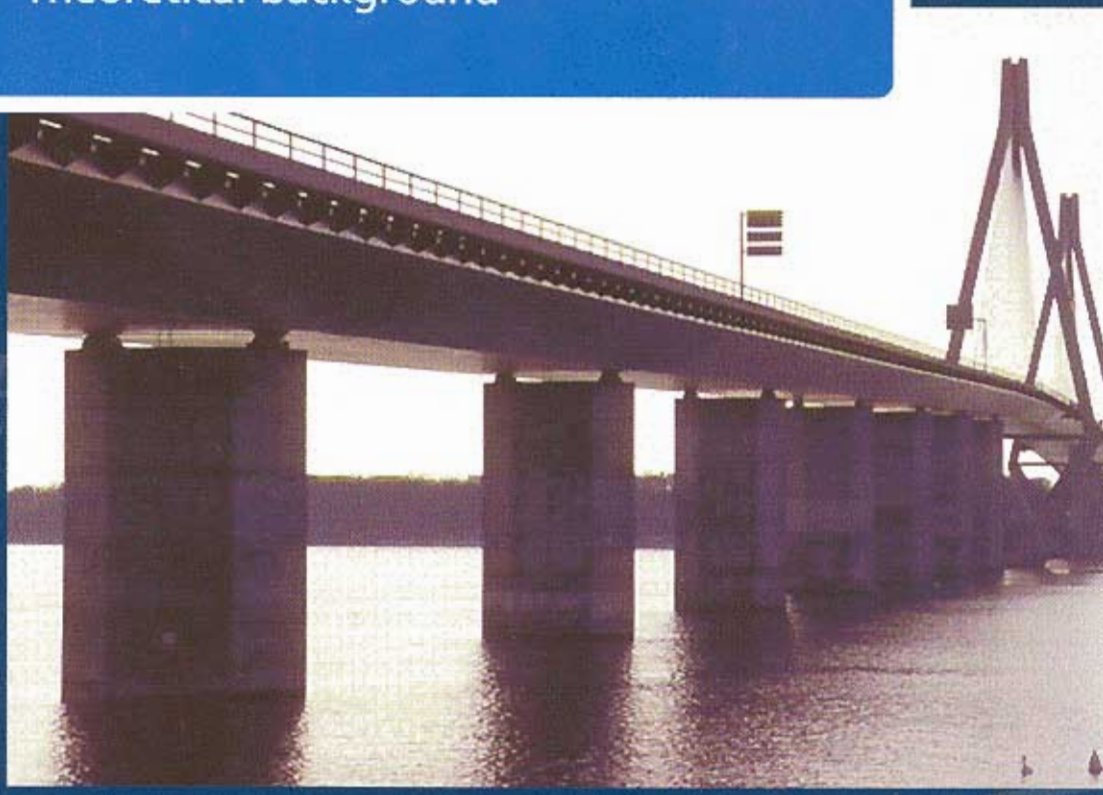

Report No.83
1997

Road Directorate Denmark Ministry of Transport

IRRD Information

Title:	HETEK, A system for estimation of chloride ingress into concrete, Theoretical background	
Authors:	L.-O. Nilsson, P. Sandberg, E. Poulsen, Tang L., A. Andersen & J.M. Frederiksen	
Subject classification:	Field 32: Concrete	
Key words:	Concrete	4755
	Chloride	7314
	Brigde	3455
	Salt (de-icing)	2598
	Moisture content	5920
	Suction	5771
	Drying	5184
	Diffusion	6769
	Cracking	5211
	Environment	2455
	Denmark	8028
Uncontrolled terms:	Threshold value	

Abstract:

This report is part of a series of reports generated in the research project HETEK headed by the Danish Road Directorate. The present sub-task is concerning chloride transport into concrete and this report presents a system for estimation of the service life of bridge structures exposed to de-icing salts and/or marine environment.

The report gives detailed descriptions of two different ways for predicting the chloride ingress into concrete. One model is the scientifically based numerical model *ClinConc* developed by Tang and the other one is the empirically based analytical model developed by Mejlbro and Poulsen. The models are compared, the result is discussed and suggestions for adjustments are given.

A simple model for convection of chlorides is presented. The model may be suitable for explaining chloride ingress into concrete exposed to an environment with wetting, drying and a discontinuous chloride exposure. The model can explain why chloride ingress sometimes do not proceed.

The report also deals with the problems of cracks on chloride penetration and corrosion initiation. A theoretical way of handling different crack intensities is presented.

Experiences from natural exposure in the road environment and in the marine environment are compiled and trends are extracted for more general use. Also chloride threshold levels in different environments and different types of concrete are presented.

UDK:	691.32
ISBN:	87 7491 783 8
ISSN:	09 09 4288

List of Contents

1 Preface

HETEK is covering 8 topics. The present project is dealing with chloride penetration into concrete. The consortium ACCE consists of AEC, Chalmers and Cementa. This report is structured into three main parts: Models, Data, Design.

1.1 Background

The Road Directorate in Denmark has launched a number of research projects in 1995 to be performed and completed during 1996. The package of projects has been given the name HETEK, which is short, in Danish, for High quality concrete, the Contractors TEChnology. The projects cover eight topics:

1. Test methods for chloride resistance of high quality concrete
2. Test methods for freeze/thaw durability of high quality concrete
3. Self-desiccation
4. Curing Technology
5. Casting and compaction
6. Curing treatment
7. Guidance in trial castings
8. Remedial measures during the execution phase

The projects are to give a state-of-the-art report, identify the need for further research, perform some of that research and finally give guidelines for the contractor.

The state-of-the-art report on Chloride penetration was first completed, cf. Nilsson et al. [1996]. The first research report describes the experimental study on the effect of *w/c* ratio on chloride penetration, cf. Frederiksen et al. [1996]. The second report describes the road environment from field investigations of chloride and moisture conditions in a number of road bridges, cf. Andersen [1996]. The present report summarises the theoretical background to the final result of the project: A system for estimation of the service-life of concrete structures exposed to chloride from sea water or de-icing salt.

1.1.1 About HETEK-1

The research consortium ACCE was given the first project HETEK-1 on chloride resistance of high quality concrete. The task for this project is to re-evaluate existing methods, and develop new ones, for determination of chloride penetration in high quality concrete. The methods must consider the differences in environmental actions on the concrete structure. Quantitative criteria for approval shall be laid down to ensure compliance with the durability requirements and the economy of the methods shall be estimated.

The research consortium ACCE consists of the three partners: AEC, Chalmers University of Technology and Cementa AB.

1.1.2 About the research consortium

AEC Consulting Engineers (Ltd.) A/S is a private consultant company in Denmark. AEC mainly works in the field of concrete structures and topics related to the repair, durability and maintenance of those. The typical clients of AEC are other consultants, contractors, building owners, insurance companies, cement producers and suppliers and also producers of materials for concrete repair and maintenance. The company has two departments: a structural department and a materials department. The structural department offers constancy regarding specialised construction problems and conventional consultancy in civil engineering. The materials department, the AEC-laboratory, assesses deterioration of concrete structures, prescribes and develops repair methods and evaluates repair materials. In addition, research and development regarding concrete durability tasks are solved for clients and/or financed by fundings.

Chalmers University of Technology educate civil engineers and researchers and do research in a number of basic and applied sciences and technologies. The department of Building Materials at the School of Civil Engineering, is participating in HETEK-1. The main research area is transport processes in porous building materials, mainly cement-based and wooden-based materials and surface materials on such materials. Examples of concrete research are: Moisture binding and flow properties of concrete, self-desiccation and drying of hardening high performance concrete, plastic shrinkage and early age cracking, chloride penetration into structures exposed to sea water and de-icing salts. The relationships between mix design, micro and pore structure and properties are experimentally studied and the behaviour in different environments are modelled and verified on concrete structures.

Cementa AB is a cement producer in Sweden. The activities of Cementa regarding concrete research are as follows: High Performance Concrete, i.e. high strength, low water content and low permeability. Concrete and environment, i.e. problems regarding moisture in concrete and emissions from concrete. Durable Concrete, i.e. long time experiments regarding chloride ingress, permeability, strength evolution and carbonation. No Slump Concrete, i.e. rheological aspects of making pre-cast concrete products.

1.2 Scope

The scope of this report is to give the theoretical background for the recommendations to a system for estimation of the service-life of concrete structures exposed to chloride containing environments. The recommendations will not contain any background information, only the instructions of how to proceed to make a service-life design of concrete structures with regard to reinforcement corrosion initiated by chloride penetrating through the concrete cover. In order to support those recommendations, the theoretical justification for the choice of the system for service-life estimation is summarised in the present report. The recommendations are given in Report No. 87: "Manual for the Design, Execution and Maintenance of Reinforced Concrete Infrastructures Exposed to Chloride", cf. Poulsen & Frederiksen [1997].

1.3 Structure

The report is structured into three main parts surrounded by an introduction and a conclusion:

Part A. Models
Part B. Data
Part C. Design

In the first part, the models that have been used in the project are described in details. The latest developments of the empirical and the scientific models are displayed and the two models are compared. A comparison between predictions and measurements in accelerated tests is also given in this part. A description is made of a new model that includes the effect of convection of chloride, i.e. the movement of chloride with the liquid moisture flow. Preliminary predictions of a number of basic cases where convection is a significant part of the mass transport are reported.

The effect of cracks is also analysed in part A. The effect of crack intensity and crack depth on the penetration of chloride by diffusion is theoretically examined by two-dimensional computer calculations. The effect of cracks on corrosion is summarised in one chapter in part A.

In part B available data on chloride threshold levels are summarised. Additionally, the environments and data from marine and road structures are analysed and compiled into a description of the boundary conditions for the models to be used in the service-life design.

In the third part instructions and examples of how to use the data and models for design are given. A description and classification of typical chlorine environments is given in the first chapter in part C. A detailed example of how to use the scientific model for service-life design of the submerged part of a marine structure is presented. Several examples of how to use the empirical model show the applicability for marine structures, both for the design of new structures and for the design of the remaining service-life of existing structures. Also an example of how to calibrate the models is presented

At last a list of the notation used throughout the report is given and the literature references are listed in alphabetical order.

The main authors of the various sections were:
A Andersen: 11
J M Frederiksen: 3, 6.6, 12, 13, 16-20
L-O Nilsson: 1, 2, 4, 5, 6.1-6.5, 6.7-6.8, 7, 8, 14
E Poulsen: 3, 12, 15, 16, 17
P Sandberg: 9, 10
Tang L: 4, 14
J M Frederiksen edited and H E Sørensen & J M Frederiksen performed the quality assurance.

1.4 Limitations

The report does not give the complete theoretical background to the system for service-life estimations for structures exposed to chloride. Numerous references are given to Nilsson et al. [1996] that covers most of what was known by March 1996. Some of that is repeated in this report, but for detailed information on various topics, Nilsson et al. [1996] is recommended.

2 Introduction

This report gives a description of updated models for the prediction of chloride ingress into concrete and the time to initiate corrosion. Two approaches are described and in a separate volume the most relevant test methods are collected. The scope of the project is to develop a complete system for service-life design. This scope is met with this report.

2.1 Environments in question

The task is to be able to cope with 5-6 different environments were chloride exposure on bridge structures is present. Those are:

1. *Bridge structures exposed to de-icing salts*
   a. Non-sheltered structures, e.g. edge beams, close to roads that are de-iced by salting.
   b. Sheltered structures, e.g. pillars under bridge decks, close to roads that are de-iced by salting.
2. *Bridge structures exposed in a marine environment*
   a. Submerged structures, e.g. caissons and the lower parts of pillars.
   b. Structures in the splash zone, e.g. pillars.
   c. Marine atmosphere, e.g. bridge decks and the top of pillars.
3. *The combination of 1a and 2c, e.g. the deck of a marine bridge.*

2.2 Models for service-life design

When planning and designing a new concrete structure to be placed in a saline environment the following problem arise:

Provided the environment in question is known a decision on the type of concrete and the minimum cover to reinforcement shall be taken.

In Nilsson et al. [1996] the state-of-the-art for solving this task is presented. This includes two models: A scientifically based model and an empirically based model. The lack of knowledge in general and the needs in order to make it possible to solve the above problem for the environments in question are pointed out.

It was the aim to use the advantages of having both a scientific and an empirical basis. In this way it was believed that more knowledge and better results could be obtained faster and in a more cost effective way.

These models have been further developed now and additional data on material properties, test methods and environmental conditions have been collected.

2.3 Improvements of the models

There was a need to describe the *scientific* model in further detail to make it possible to better evaluate its advantages and limitations. To support that, more examples of utilisation of the model should be shown. Since accelerated test results have been produced within the project, a comparison between those measurements and predictions by the scientific models could be done.

The *empirical* model also needed some development. It was clear already in Nilsson et al. [1996] that time-dependent "achieved chloride diffusion coefficients" could give far much better predictions than the previous models with a constant diffusion coefficient. The predictions, however, could be even more improved by describing the boundary conditions in a more sophisticated way. The model was further developed and now include time-dependent chloride surface contents.

To get an estimate of the uncertainties in the present models, a comparison between the two models was performed.

2.4 The further research

Both of the models are based on pure diffusion of chloride. To evaluate the possibilities and most relevant lack of knowledge when it comes to convection of chloride, a new simple model was developed to examine the processes and conditions when part of the chloride move with the liquid water flow in concrete.

The effect of cracks was covered very briefly in the state-of-the-art report. Some new knowledge on corrosion rates has been gained since March 1996. Literature information gives contradictory conclusion on the effect of cracks on chloride penetration. An additional examination was required.

Data on chloride conditions are many for marine structures. A thorough analysis and compilation into boundary conditions for prediction models are missing, however. For the road environment, data on the chloride conditions is scarce and of low quality. New, better data was collected within the project. An analysis and compilation of that data had to be done.

In spite of all the research summarised in the state-of-the-art report on chloride threshold values for initiation of reinforcement corrosion, an updated revision is needed.

The state-of the-art report gave only scattered examples of how to use the previous prediction models for service-life design. There is a need to give a complete description of how to describe various environments as boundary conditions for the new models. Additionally, a systematic selection of examples of how to use the models for design are given.

The requirements summarised in the previous paragraphs are to be covered in this report of the third sub-task in the HETEK-1 project. That will serve as a theoretical background for the recommendations to be given as the final result of the project.

PART A. MODELS

Part A covers chapters 3-9, describing the further development and verification of the models to be used for service-life estimation

3 Details of the Mejlbro-Poulsen model

Parts of the Mejlbro-Poulsen model for prediction of chloride ingress into concrete has been published earlier. Here a complete description of the basis for the model is given.

The empirical model, the so-called "Mejlbro-Poulsen Model", is a result of many comparisons and predictions made on basis of laboratory experiments, observations from marine exposure stations, and examination of marine structures. The model is based upon Fick's general law of diffusion which implies only one assumption, namely that the flow of chloride in concrete is proportional to the gradient of the chloride concentration in the concrete. The solution of this mathematical model implies the initial and boundary conditions found and predicted by pre-testing the concrete and environment in question. Thus, the model tackles the problem of how to translate findings in the laboratory to findings in the field and visa versa.

The obvious advantage of the model is the straight forward utilisation of observed chloride profiles from concrete structures.

3.1 Achieved chloride profiles of concrete

The chloride profile at each point of a concrete surface which is exposed to a chloride-laden environment is defined as the concrete structure's response to the environment. The chloride profiles develop with time and the scope of the following description is to advise a method for the prediction of this development.

A chloride profile is here described by the following four parameters:

- The initial chloride concentration C_i of the concrete.
- The chloride concentration C_{sa} of the exposed concrete surface.
- The achieved chloride diffusion coefficient D_a of the concrete.
- The exposure time $\Delta t = t - t_{ex}$ of the concrete.

A typical example of an achieved chloride profile is shown in Figure 3.1:1. The profile is achieved during 37 years of exposure and is observed in the splash zone of a concrete sheet pile.

The best fit of the error function solution to Fick's 2nd law is shown. Deviation, which might be systematic, is seen between the observed chloride profile and the error function complement. Such deviations are not dealt with here, but the reader is requested to read the thesis of Østerdal [1995] for more details.

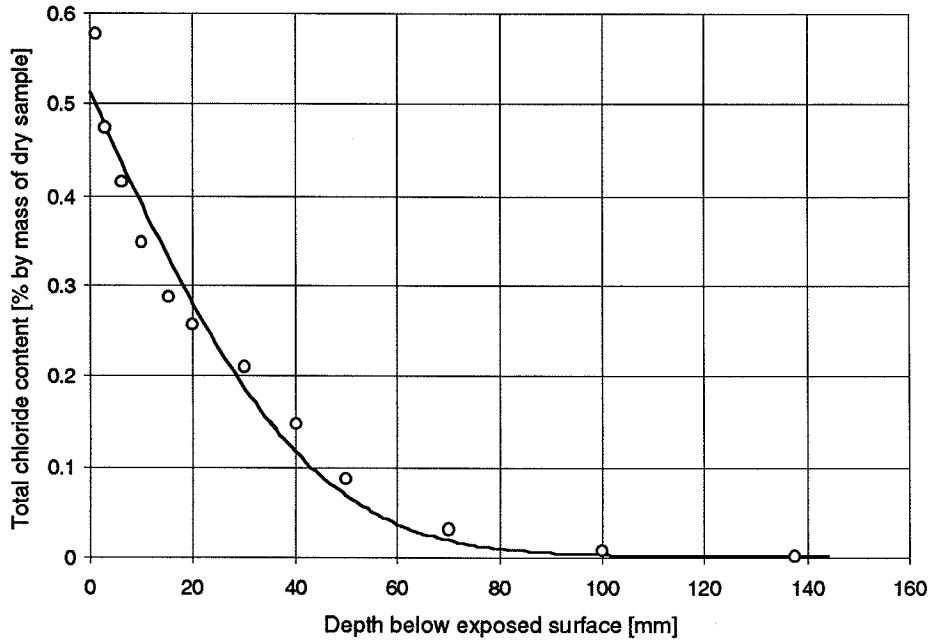

Figure 3.1:1. A typical example of a chloride profile as measured in concrete exposed in a marine splash zone in a harbour on Jutlands West coast. The age of the structure at the time of the profile measurement is 37 years. The curve presents the best fit of the "error function solution" to Fick's 2nd law.

3.2 Formulation of the Mejlbro-Poulsen model

Fick's second law of diffusion is a partial differential equation which cannot be solved without specifying the material parameter, i.e. the chloride diffusion coefficient D (the physical condition), the initial and boundary conditions of the case in question. Inspection of marine concrete structures has shown that:

- The achieved chloride diffusion coefficient D_a is time-dependent.
- The achieved chloride concentration C_{sa} of the exposed concrete surface is time-dependent.
- The initial chloride concentration C_i of the concrete is constant and independent of time and the distance x from the chloride exposed concrete surface.

A few comments shall be given in order to understand the presupposition of the Mejlbro-Poulsen Model of chloride ingress into concrete by diffusion.

3.2.1 Diffusion coefficients of concrete

In the Nordic countries it has been put into practice to describe a concrete's chloride diffusivity by three types of chloride diffusion coefficients:

- The potential chloride diffusion coefficient D_p measured by means of NT Build 443. D_p is not a materials constant since it is time-dependent. However, D_p is often (like the concrete compressive strength) specified as D_{pex} at a maturity age of 28 M-days before the concrete is tested according to NT Build 443.

- The achieved chloride diffusion coefficient D_a of the concrete of a marine concrete structure measured by means of APM 207. D_a is not a materials constant since it is time-dependent and dependent of the environmental load.
- The real chloride diffusion coefficient D of the concrete. It is not possible to measure D directly, but there is a relation between D_a and D from which D may be derived.

Potential chloride diffusion coefficient

Concrete cast with a Danish low alkali sulphate resisting Portland cement and without addition of fly ash, silica fume, slag etc. has shown a potential chloride diffusion coefficient at 28 M-days which obeys:

$$D_{pex} = 50{,}000 \exp\left(-\sqrt{\frac{10}{w/c}}\right) \qquad (3.2.1:1)$$

cf. Frederiksen et al. [1996]. The unit of D_{pex} is mm^2/year and w/c is the mass ratio of the concrete's water to cement ratio. Figure 3.2.1:1 shows the graph of (3.2.1:1) and the corresponding observations.

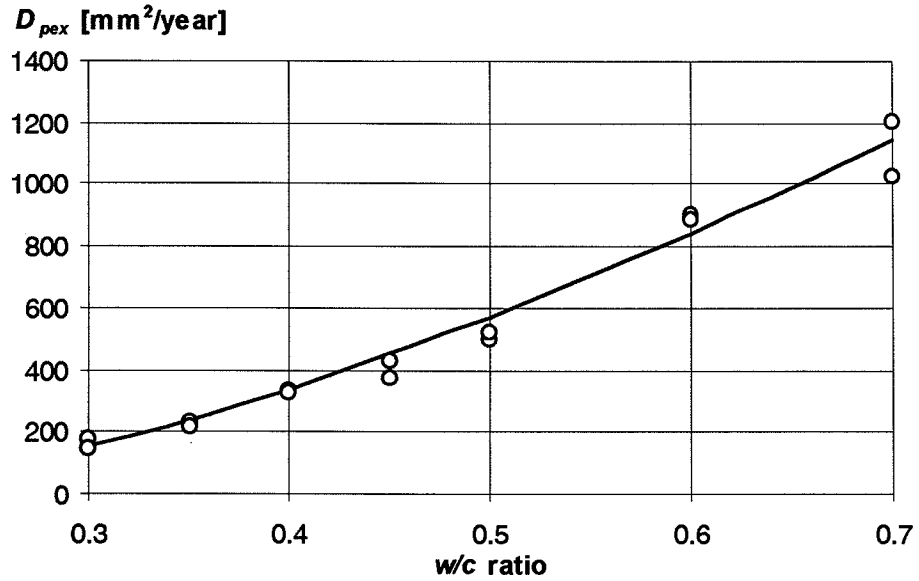

Figure 3.2.1:1. The potential chloride diffusion coefficient D_{pex} (acc. to NT Build 443) versus the w/c ratio. Valid for concrete made with Danish low alkali sulphate resisting Portland cement having a maturity of 28 days when exposed to chloride, Frederiksen et al. [1996].

Other types of concrete containing pozzolanic materials as e.g. fly ash, silica fume and slag and other types of Portland cement do not obey (3.2.1:1). Therefore, tests according to NT Build 443 must be carried out in order to determine D_{pex} or one must know or be able to estimate the values of the efficiency factors for the binder composition in question.

Achieved chloride diffusion coefficient

The definition of the achieved chloride diffusion coefficient at time t is: "The value of a virtual chloride diffusion coefficient which, when remaining constant, theoretically spoken will result in the chloride profile achieved when the observed chloride concentration of the chloride exposed concrete surface is kept constant". As seen the achieved chloride diffusion coefficient $D_{aex} = D_a(t_{ex})$ at the time of the first chloride exposure t_{ex} is not defined (a singular point).

Takewaka et al. [1988] proposed to describe $D_a(t)$ as a power function of time. Later this has been supported by observations made by Maage et al. [1994], Mangat et al. [1994] and Sandberg [1995]. Maage et al. [1995] have proposed to write the achieved chloride diffusion coefficient as the following power function:

$$D_a(t) = D_{aex}\left(\frac{t_{ex}}{t}\right)^{\alpha} \tag{3.2.1:2}$$

In the case where the chloride concentration of the chloride exposed concrete surface is constant the chloride profile is described by the well-known error-function complement, also when the achieved chloride diffusion coefficient $D_a(t)$ is time-dependent, cf. Poulsen [1993]:

$$C(x,t) = C_i + (C_{sa} - C_i)\mathrm{erfc}\left(\frac{0.5x}{\sqrt{(t-t_{ex})D_a(t)}}\right) \tag{3.2.1:3}$$

It is observed in practice that $D_a(t)$ is a monotone decreasing function of time t. This means that in (3.2.1:2) we have that $\alpha \geq 0$.

The special case $\alpha = 0$ covers cases where the achieved chloride diffusion coefficient $D_a(t)$ remains constant.

A reference value of the chloride concentration C_r (e.g. 0.1 % by mass concrete) is chosen. At time $t = t_{in}$ the abscissa corresponding to C_r is x_r. If the chloride penetrates the concrete x_r must be an increasing function of time and in case the chloride ingress is "self-blocking" x_r will remain constant. In order to see how this influences α (3.2.1:3) is re-written in the following way:

$$\mathrm{erfc}\left(\frac{0.5x_r}{\sqrt{(t-t_{ex})D_a(t)}}\right) = \frac{C_r - C_i}{C_{sa} - C_i} = \text{constant} \tag{3.2.1:4}$$

In the case of a "self-blocking" chloride ingress the product $(t - t_{ex})D_a(t)$ must remain constant, i.e.:

$$D_a(t) = \frac{k}{t - t_{ex}} \approx \frac{k}{t_{ex}}\left(\frac{t_{ex}}{t}\right)^{1} \tag{3.2.1:5}$$

From this it is seen that in the case of "self-blocking" chloride ingress we have $\alpha \approx 1$ and that α could not exceed 1. Thus, when chloride ingress takes place we have that $0 \leq \alpha \leq 1$.

3.2.2 Achieved chloride concentration of the surface

Uji et al. [1990] observed that the chloride concentration of the exposed concrete surface of a marine structure was time-dependent. On the basis of the observations Uji et al. [1990] proposed to assume that C_{sa} increases with the square root of time. That was the most convenient choice since Crank [1986] has published a solution of Fick's second law of diffusion under that condition. Besides Uji et al. [1990] this solution has been applied by Purvis [1994], Gautefall [1993] and Amey et al. [1996].

However, Swamy et al. [1995] has published a comprehensive amount of observations showing that C_{sa} not always increases with the square root of time. From the observations made by Swamy et al. [1995] it is concluded, that a better model of the increase of C_{sa} with time is a power function or the like, cf. Figure 3.2.2:1.

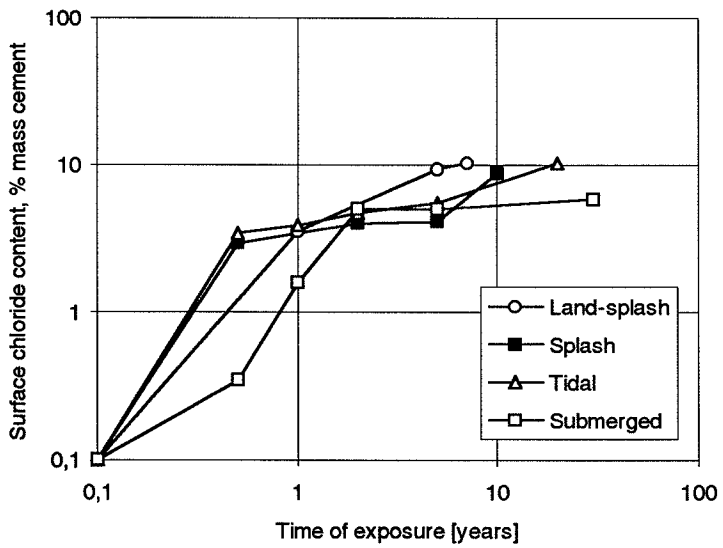

Figure 3.2.2:1. Surface chloride concentration versus the time of exposure to seawater, Swamy et al. [1995]. Note that the observations do not form a straight line indicating that a power function is not valid for describing the time-dependence of C_{sa}.

Observations from many marine concrete structures and concrete specimens exposed at marine exposure stations indicate, cf. Uji et al. [1990] and Mangat et al. [1995], that C_{sa} also depends on the concrete.

Proposal by Mejlbro

Mejlbro [1996] proposes that C_{sa} ought to be described by the following family of functions:

$$C_{sa} = C_i + S \times [(t - t_{ex}) \times D_a(t)]^p \qquad (3.2.2:1)$$

By this formula the following three main conditions are fulfilled:

- C_{sa} becomes a function of time t and this function proves to be flexible enough to fit the time-dependency found by e.g. Swamy et al. [1995] and others.
- C_{sa} becomes dependent of the properties of the concrete through $D_a(t)$, i.e. dependent of mainly the concrete's *w/c* ratio and type of binder.
- There exists a simple solution of Fick's second law of diffusion and this solution could be tabulated and is easy to apply, e.g. by simple handling of spread sheet and by programming of pocket computers.

The factor S in (3.2.2:1) depends of the chloride aggressiveness of the environment and the cement type and the composition of the binder of the concrete. The exponent p depends on how fast C_{sa} increases with time, i.e. mainly on the type of binder and the environment.

The relation (3.2.2:1) is of a general form. Especially if (3.2.1:2) is valid for $D_a(t)$, the relation (3.2.2:1) yields:

$$C_{sa} = C_i + S \times \left((t - t_{ex}) \times D_{aex} \times \left(\frac{t_{ex}}{t} \right)^{\alpha} \right)^{p} \qquad (3.2.2:2)$$

or:

$$C_{sa} = C_i + S_p \times \tau^p \qquad (3.2.2:3)$$

where:

$$S_p = S \times (t_{ex} D_{aex})^p \qquad (3.2.2:4)$$

and:

$$\tau = \left(\frac{t}{t_{ex}} \right)^{1-\alpha} - \left(\frac{t_{ex}}{t} \right)^{\alpha} \qquad (3.2.2:5)$$

Figure 3.2.2:2 illustrates the flexibility of (3.2.2:3) for $0 \leq p \leq 1$ and C_{sa} fixed to a value of 1.0 % by mass concrete at t = 100 years.

On the basis of observations made by Maage et al. [1995] it is concluded, that the worst case in practice is covered by the following boundary conditions:

$$C_{sa} = C_i + 0.5\tau^{0.2} \qquad (3.2.2:6)$$

cf. Figure 3.2.2:3.

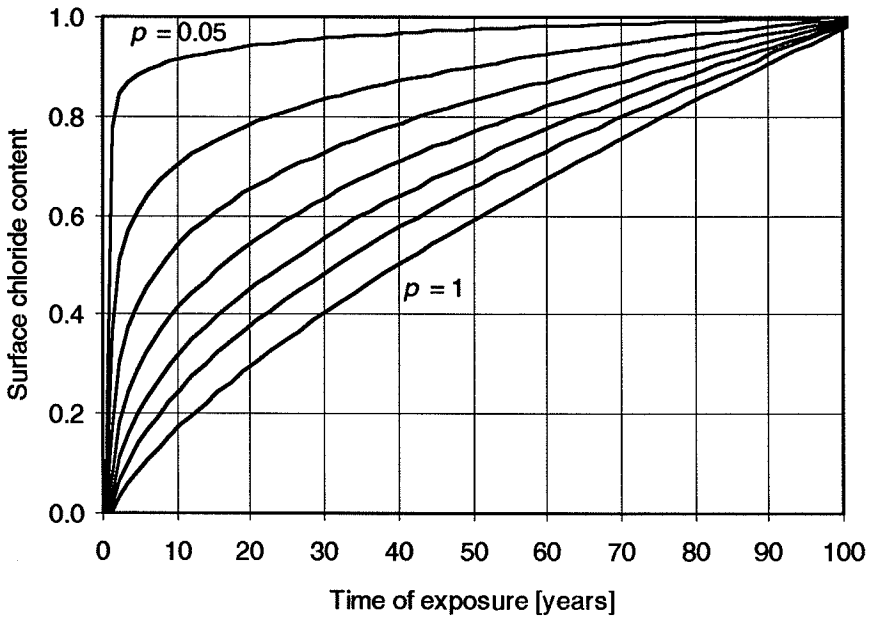

Figure 3.2.2:2. Curves representing the flexibility of (3.2.2:3). The values of the parameters are: α= 0.30; $C_{sa}(t=100)$ = 1.0; t_{ex} = 0.1 year. The lowest curve represents p=1, then follow p= 0.8; 0.65; 0.5; 0.35; 0.2; 0.05.

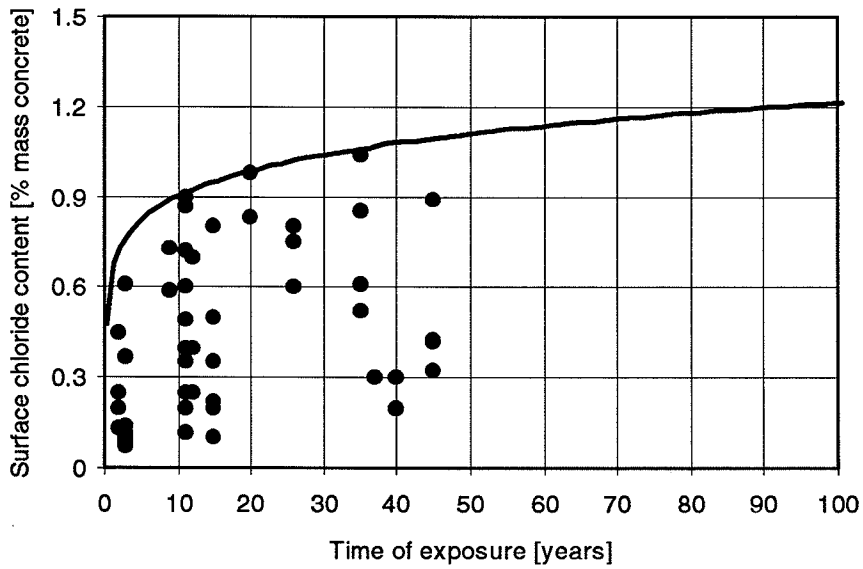

Figure 3.2.2:3. Observed concentration of chloride in concrete surfaces in marine environments, mainly splash zones. The curve illustrates the upper boundary of C_{sa} and is based upon (3.2.2:6).

3.2.3 The Mejlbro Ψ-functions

The above given conditions are necessary and sufficient for solving the problem of predicting the chloride ingress into the concrete.

Equations of the problem

In mathematical terms the problem of chloride ingress into concrete can be formulated as follows: Fick's second law of diffusion yields (valid when the diffusion coefficient is time-dependent):

$$\frac{\partial C}{\partial t} = D(t) \cdot \frac{\partial^2 C}{\partial x^2} \qquad (3.2.3:1)$$

The achieved chloride diffusion coefficient's time dependency is assumed to obey the relation (3.2.1:2). The initial condition (i.e. the initial chloride content of the concrete) is:

$$C(x, t_{ex}) = C_i = \text{constant} \qquad (3.2.3:2)$$

When applying (3.2.1:2) the boundary condition (i.e. the chloride concentration of the exposed concrete surface) is according to Mejlbro (3.2.2:2).

The chloride profile

The solution of the equations given above yields, cf. Mejlbro [1996]:

$$C(x,t) = C_i + (C_{sa} - C_i) \times \Psi_p(z) \qquad (3.2.3:3)$$

where:

$$z = \frac{0.5x}{\sqrt{(t - t_{ex}) D_a(t)}} = \frac{0.5x}{\sqrt{\tau \times t_{ex} D_{aex}}} \qquad (3.2.3:4)$$

and, cf. Mejlbro [1996]:

$$\Psi_p(z) = \sum_{n=0}^{+\infty} \frac{p^{(n)} (2z)^{2n}}{(2n)!} - \frac{\Gamma(p+1)}{\Gamma(p+0.5)} \sum_{n=0}^{+\infty} \frac{(p-0.5)^{(n)} (2z)^{2n+1}}{(2n+1)!} \qquad (3.2.3:5)$$

Figure 3.2.2:4 shows the graphs of Mejlbro's Ψ-functions.

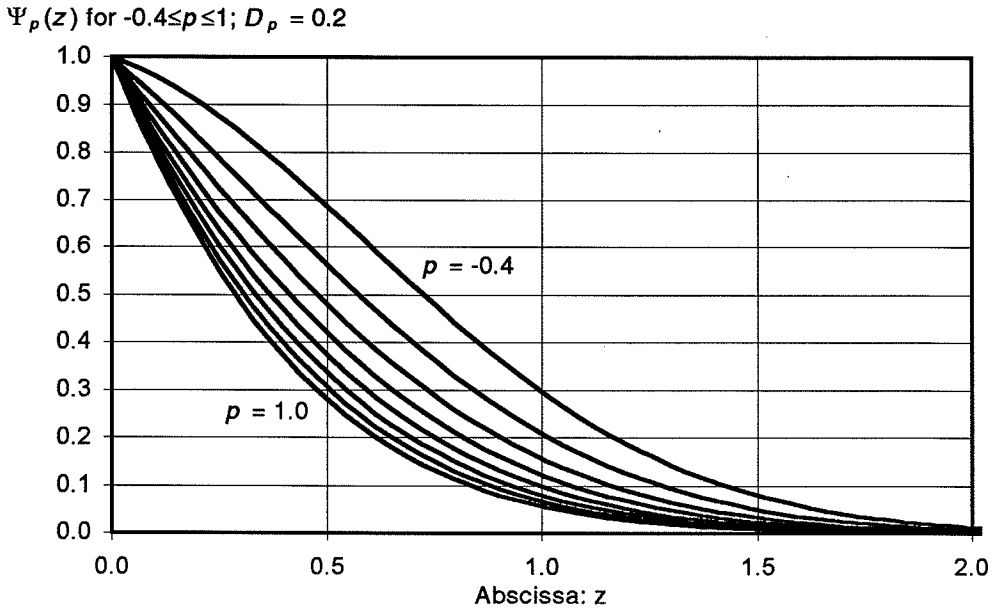

Figure 3.2.2:4. Graphs of typical Mejlbro Ψ-functions.

In (3.2.3:5) $\Gamma(y)$ is the Gamma function defined as:

$$\Gamma(y) = \int_0^{+\infty} u^{y-1} \exp(-u) du \tag{3.2.3:6}$$

for $y \geq 0$. The notation used in (3.2.3:5) should be noted:

$$p^{(0)} = 1;\ p^{(1)} = p;\ p^{(2)} = p \times (p-1);\ldots\ p^{(n)} = p \times (p-1) \times \ldots \times (p-n+1) \tag{3.2.3:7}$$

where $p^{(n)}$ has $n \geq 1$ factors.

3.3 Practical applications of the Mejlbro-Poulsen model

The equation (3.2.2:6) of the chloride profile is suitable for the following types of predictions:

- Prediction of the achieved chloride profiles at a specified time when the parameters t_{ex}, D_{aex}, α, S and p are known.
- Prediction of the ingress into concrete versus time of a reference chloride concentration C_r when the parameters t_{ex}, D_{aex}, α, S and p are known.
- Prediction of the initiation time t_{cr} of chloride corrosion when the threshold value of the chloride in concrete C_{cr} and the parameters t_{ex}, D_{aex}, α, S and p are known.
- Design of the thickness of the necessary concrete cover c of reinforcing bars when the threshold value of the chloride in concrete C_{cr} and the parameters t_{ex}, D_{aex}, α, S and p are known and the initiation time and safety level are specified.

The way of handling these predictions are dealt with in Part C of this report.

3.3.2 Advantages

The most important advantage of the Mejlbro-Poulsen Model is the direct applicability of measured chloride profiles from field exposure. If sampled and measured in a sufficiently systematically and reproducible way, information of the chloride profiles with respect to life-time predictions can be extracted and used in the model. This frees the model from assumptions regarding the concretes response to the environmental load.

3.3.3 Limitations

The Mejlbro-Poulsen Model do not model the actual physical and chemical processes involved in the chloride ingress into concrete. The aim of the model is to describe the *result* of these physical and chemical processes of this transport, i.e. the chloride profiles. The model is dependent of good measurements from the environment and the concrete type in question. The measurements must represent a fairly long time of exposure to improve the predictions. These drawbacks will be overcomed with time when the experience grow. The model is very sensitive to the quality of the measurements therefore many of the existing measurements must regarded as unsuitable for prediction purposes with this model.

As seen the most obvious limitations of the model is the available experience in the actual situation. Thus the experiences for the time being are limiting the most easy application of the model.

4 Details of *ClinConc*

***ClinConc* is the name of a scientifically based model for chloride penetration into concrete. So far *ClinConc* only covers constantly submerged conditions. The scientific basis is presented in this chapter.**

One of the most advanced models for predicting chloride penetration into concrete, *ClinConc*, has been developed by Tang [1996a]. The *ClinConc* model for prediction of chloride profiles is based on the current knowledge on the transport and binding processes in concrete. By using a Finite Difference Method (FDM) numerical approach, most of the factors involved in chloride penetration are considered in a relevant and scientific way. The description is meant to be as close to the real physical and chemical processes as is relevant without introducing a great number of parameters that cannot be measured. The ambition is to use as input data only those parameters that can be measured independently without relying upon any curve-fitting procedure. The ambition is also to model the full chloride profile in order to be able to compare predicted and measured ones. A comparison with the chloride threshold values for corrosion can then be done, in terms of total chloride, free chloride or the Cl/OH ratio, to design for service-life of a structure.

The details of the model are thoroughly described by Tang [1996a]. This chapter is based on his thesis.

The model consists of two main procedures:

- Simulating transport of free chloride through the pore solution in concrete.
- Calculating the distribution of the total chloride content in concrete into a "free" part and a "bound" part.

It is essentially important that the various dimensions in the calculation should be clearly specified.

4.1 The mass balance equation

The mass balance equation for chloride is solved by using separate terms for chloride diffusion and for chloride binding. The background to the equation is graphically shown in Figure 4.1:1.

The flux of chloride q_{Cl} is different at different positions in the concrete. The difference in chloride flux to and from an infinitesimal slice of concrete with a thickness dx will change the total amount of chloride c_{tot} in such a slice. The change in total chloride content per unit of time will be equal to the difference in chloride flux to and from the slice, divided by the thickness of the slice.

The change in total chloride content will be split into a change in free chloride dissolved in the pore water and a change in bound chloride in such a way that equilibrium will be maintained between free and bound chloride. Since the chloride flux occurs in the pore water, the change in chloride content will first occur as change in free chloride. An almost "instant" change in bound chloride will follow, since the rate of chloride binding is fairly high.

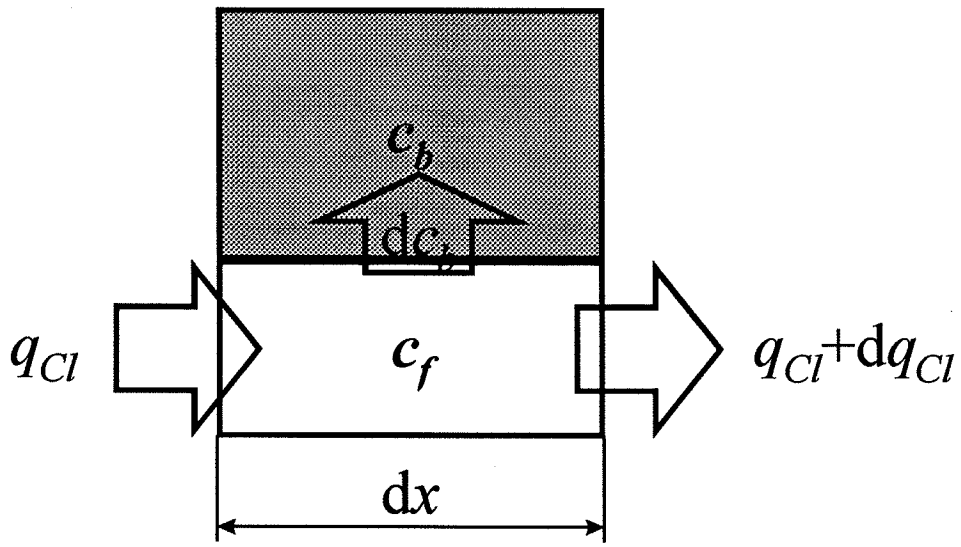

Figure 4.1:1. A visual description of the mass balance equation for free and bound chloride.

Mathematically the mass balance equation is expressed as the change with time of the chloride concentrations

$$\frac{\partial c_{tot}}{\partial t} = \frac{\partial c_f}{\partial t} + \frac{\partial c_b}{\partial t} = \frac{\partial c_f}{\partial t}\left(1 + \frac{\partial c_b}{\partial c_f}\right) = -\frac{\partial q_{Cl}}{\partial x} = \frac{\partial}{\partial x} D_0 \frac{\partial c_f}{\partial x} \qquad (4.1:1)$$

Tang's approach to describe the mass balance equation numerically, for a concrete slice with a unit area and thickness Δx, is in a first procedure to calculate the net flow of free chloride $\Delta Q(diff)$, in $\frac{\mathrm{kg_{Cl}}}{\mathrm{m^3_{concrete}}}$, at the position x_i in a time interval Δt. The flow can be calculated by the following equation:

$$\Delta Q_{i,j}(diff) = A_{i,j}(diff) \times D_{i,j} \frac{c_{i-1,j-1} - 2c_{i,j-1} + c_{i+1,j-1}}{\Delta x^2} \Delta t_j \qquad (4.1:2)$$

where the subscriptions i and j denote the depth position and the time step, respectively; and $A(diff)$ is the effective diffusion path with a dimension of

$$\frac{\mathrm{m^2_{solution}}}{\mathrm{m^2_{concrete}}} \text{ or } \frac{\mathrm{m^2_{solution}} \cdot \mathrm{m}_x}{\mathrm{m^2_{concrete}} \cdot \mathrm{m}_x} = \frac{\mathrm{m^3_{solution}}}{\mathrm{m^3_{concrete}}},$$

which is related to the water content in concrete. In the water saturated condition, $A(diff)$ simply is assumed to be equal to the capillary porosity of concrete $\varepsilon_{capillary}$, that is,

$$A(diff) = \varepsilon_{capillary} = 1 - \sum \frac{m}{\rho} - 0.75W_n - \varepsilon_{air} \qquad (4.1:3)$$

where m and ρ are the mass and density of solid materials in concrete, respectively. Calculating the non-evaporable water content W_n involves calculating the degree of hydration α_h. Both calculations of W_n and α_h are described in Tang [1996a].

In the second procedure, the total quantity of chloride $Q(total)$ in the concrete slice of thickness Δx becomes:

$$Q_{i,j}(total) = Q_{i,j-1}(total) + \Delta Q_{i,j}(diff) \qquad \left[\frac{\mathrm{kg_{Cl}}}{\mathrm{m^3_{concrete}}}\right] \tag{4.1:4}$$

4.2 Diffusion coefficient

The basic diffusion coefficient is the "true" chloride diffusion coefficient D_{FI}, evaluated from the D_{CTH} from the CTH migration test method. Additionally, the effect of depth from a cast surface is taken into account. The effect of age is also considered.

The diffusion coefficient $D_{i,j}$ in equation (4.1:2) is a function of temperature, age and depth:

$$D_{i,j}(Cl) = D_0|_{T_0} f_D(T_j) g(t_j) f(x_i) \qquad \left[\mathrm{m_x^2/s}\right] \tag{4.2:1}$$

where D_0 is the intrinsic diffusion coefficient, cf. Tang [1996a]. If the rapid CTH migration test method is used for determining diffusivity, the intrinsic diffusion coefficient is obtained from

$$D_0|_{T_0} = D_{CTH}|_{T_0}\left(1 + K_b \frac{W_{gel}}{\varepsilon}\right) \qquad \left[\mathrm{m_x^2/s}\right] \tag{4.2:2}$$

The functions $f_D(T_j)$, $g(t_j)$ and $f(x_i)$ can be calculated by equations (4.2:3), (4.2:4) and (4.2:5), respectively. The influence of temperature on chloride diffusivity can be expressed by the Arrhenius law:

$$f_D(T) = \frac{D_0}{D_0|_{T_0}} = e^{\frac{E_D}{R}\left(\frac{1}{T_0} - \frac{1}{T}\right)} \tag{4.2:3}$$

where $f_D(T)$ and E_D can be identified as the temperature-dependent coefficient and the activation energy for chloride diffusivity, respectively. A few data of the activation energy are available.

The age-dependent function $g(t)$ can be calculated from

$$g(t) = \begin{cases} \left(\dfrac{t_0}{t}\right)^{\beta_t} & t < t_0 \\ 1 & t \geq t_0 \end{cases} \tag{4.2:4}$$

where t_0 is the age when the diffusivity becomes constant and β_t is a constant.

The depth dependent effect $f(x)$ can be expressed as:

$$f(x) = \begin{cases} \varphi + (1-\varphi)\left(\dfrac{x}{x_s}\right)^{\beta_x} & x < x_s \\ 1 & x \geq x_s \end{cases} \qquad (4.2:5)$$

where φ is the relative diffusivity in the surface zone, $\varphi = D_{surface}/D_{inner}$; x_s is the thickness of the surface zone and β_x is a constant.

4.3 Total chloride distribution into free and bound chloride

The chloride binding is described with a non-linear binding isotherm. There is no parameter involved, only the amount of gel as calculated from the concrete mix composition. The effect of temperature is considered with an Arrhenius equation. Lack of knowledge on the temperature effect is provisionally dealt with by fitting field data from the surface near region to predictions for a number of field studies. The pH effect is based on available measurements.

Since the free chloride concentration c is dependent on the quantity of total chloride, the chloride binding isotherm, and the water content in concrete, each new free chloride concentration $c_{i,j}$ should be found out by solving the following equation:

$$Q_{i,j}(total) = c_{i,j}(W_s)_{i,j} + Q_{i,j}(bound) \qquad \left[\frac{\mathrm{kg_{Cl}}}{\mathrm{m^3_{concrete}}}\right] \qquad (4.3:1)$$

where W_s is the water content in the concrete slice with a dimension of $\mathrm{m^3_{solution}/m^3_{concrete}}$, and $Q(bound)$ is the quantity of bound chloride. Considering available data, cf. Tang [1996a], we can obtain

$$Q_{i,j}(bound) = e^{\alpha_{OH}\left(1-\frac{[OH]_{i,j-1}}{[OH]_{initial,j-1}}\right)} e^{\frac{E_b}{R}\left(\frac{1}{T_j}-\frac{1}{T_0}\right)} W_{i,j}(gel)\frac{f_b}{1000}c^B_{i,j} \qquad (4.3:2)$$

where $W(gel)$ has a dimension of $\dfrac{\mathrm{kg_{gel}}}{\mathrm{m^3_{concrete}}}$, and $\dfrac{f_b}{1000}c^B_{i,j}$ has a dimension of $\dfrac{\mathrm{kg_{Cl}}}{\mathrm{kg_{gel}}}$, so as for $Q(bound)$ to obtain a dimension of $\dfrac{\mathrm{kg_{Cl}}}{\mathrm{m^3_{concrete}}}$.

4.4 Leaching of alkalis

Diffusion of hydroxides contributed by alkalis is described in a similar way as diffusion of chloride to model the leaching process. Leaching of calcium hydroxides is not yet included, i.e. a drop in pH from some 13.5-14 to some 12.5 is modelled to be able to properly describe the chloride binding. For long exposure times and high w/c ratio the

leaching of hydroxides to pH below 12.5 should be included. That is, however, of minor importance for high quality concrete having low *w/c* ratio.

The initial hydroxide concentration is calculated from the alkali content and pore content in concrete. A hydroxide concentration of 0.043 moles/l as in saturated lime water can be used as the boundary concentration, assuming the leaching of $Ca(OH)_2$ is limited. The consequent hydroxide concentration could be estimated by a formula similar to equation (4.1:2). Since the knowledge of hydroxide diffusivity in a pore solution is very limited, at present it may be estimated by the following equation:

$$D(OH) = \frac{D_{OH}}{D_{Cl}} \frac{D_0|_{T_o}}{1 + K_b(OH)} \qquad \left[\mathrm{m}_x^2/\mathrm{s}\right] \tag{4.4:1}$$

where D_{OH} and D_{Cl} are the ion diffusion coefficients in the bulk solution, $D_{OH} = 5.26\times10^{-9}$ $\mathrm{m}_x^2/\mathrm{s}$, and $D_{Cl} = 2.03\times10^{-9}$ $\mathrm{m}_x^2/\mathrm{s}$, respectively; and $K_b(OH)$ can be called the hydroxide binding coefficient, assuming $K_b(OH) = 20$.

4.5 Environmental conditions

The exposure conditions are described as a chloride concentration in the sea water in contact with the concrete surface, with a variation between a maximum and minimum value, and a temperature variation during e.g. a year cycle. Since the temperature has a tremendous effect on chloride binding, the temperature variations will strongly affect the predicted free chloride profiles.

The temperature T_j may be expressed by a periodic function:

$$T_j = \frac{T_{\max} + T_{\min}}{2} + \frac{T_{\max} - T_{\min}}{2} \sin\left(2\pi \frac{t_j - t_0^T}{365}\right) \qquad [\mathrm{K}] \tag{4.5:1}$$

The chloride concentration in sea water may also be expressed by a periodic function similar to equation (4.5:1):

$$c_{0j} = \frac{c_{0\max} + c_{0\min}}{2} + \frac{c_{0\max} - c_{0\min}}{2} \sin\left(2\pi \frac{t_j - t_0^c}{365}\right) \qquad \left[\frac{\mathrm{kg\,Cl}}{\mathrm{m^3_{solution}}}\right] \tag{4.5:2}$$

where t_0^T and t_0^c are the initial time for the sine function, individually.

4.6 Description of the *ClinConc* software

It can be seen from Sections 4.2 and 4.3 that in this numerical model most of the factors affecting chloride penetration have been considered. The main input data include concrete mix design, workmanship and exposure conditions. The only parameter one needs to measure is the chloride diffusion coefficient by using the rapid CTH test method. The chloride binding data, which have strong effect on chloride penetration profiles, are stored in a database for numerical calculation. The model is schematically shown in

Figure 4.6:1. Based on this model a Windows program called *ClinConc*, *Chloride in Concrete*, has been developed, as presented in Figure 4.6:2 from Tang [1996a].

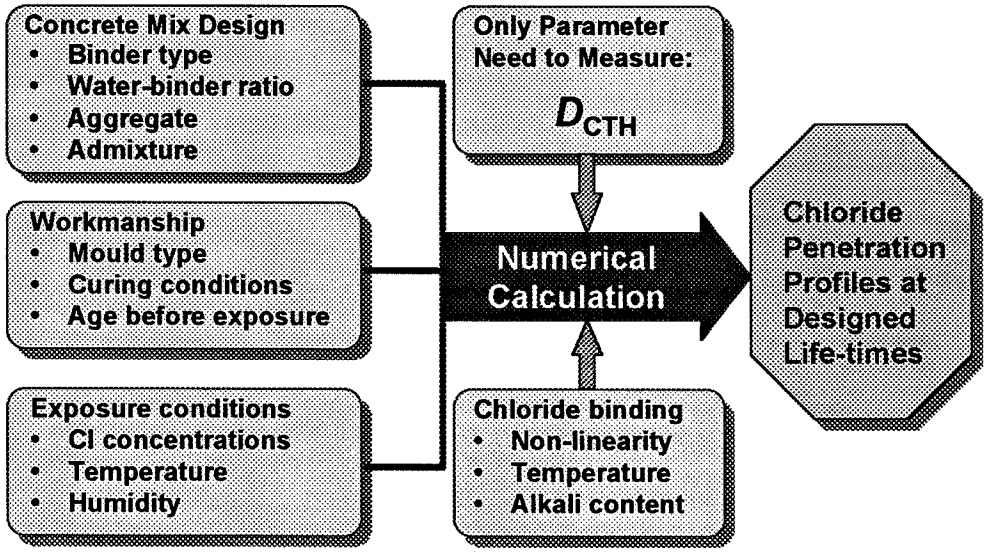

Figure 4.6:1. Schematic presentation of the CTH model for prediction of chloride penetration, Tang [1996a].

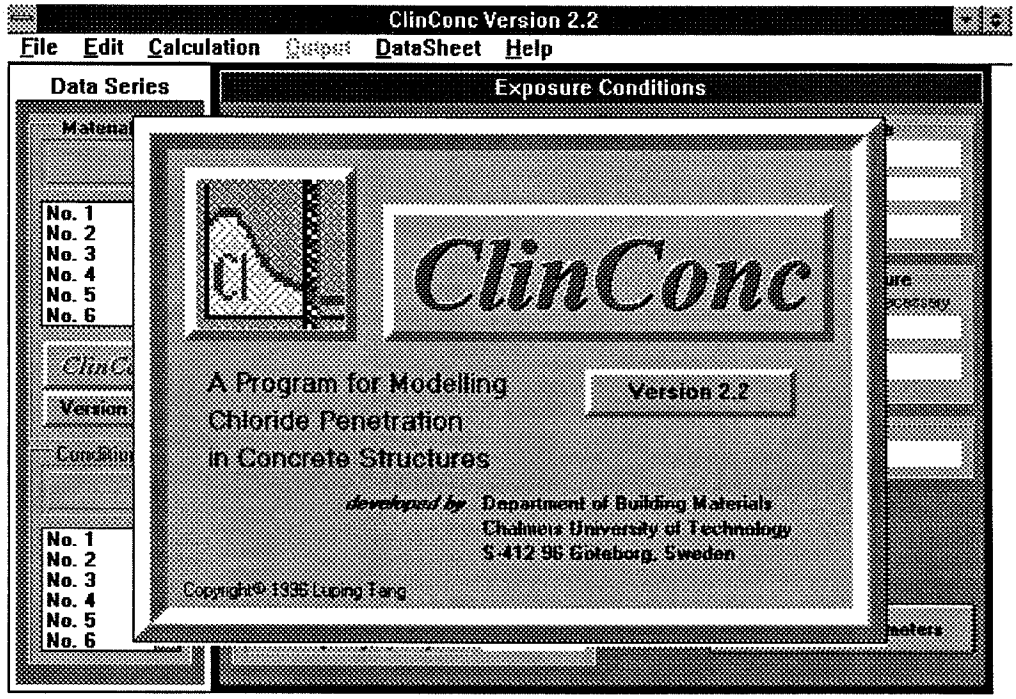

Figure 4.6:2. A Windows program ClinConc for prediction of chloride penetration, Tang [1996a].

The program mainly includes the following windows:

- *Material parameters window* for the material parameters input including material type, mix design, casting and curing conditions. A database is connected with this window. In many cases the user needs just to choose a proper parameter from the database.
- *Exposure conditions window* for input of the parameters related to the exposure environment, including the essential factors: temperature and chloride concentration. The parameters, environmental moisture and wet-dry cycles, are designed for the future use, e.g. predicting chloride penetration in a splash zone.
- *Calculation window* for choosing different exposure times. The user can also choose either semi-infinite or limited thickness according to the selected structure. A small depth increment gives a good calculation precision, but requires a long calculation time.
- *Graphics window* for graphically presenting the calculation results. The user can choose one of five different profiles including total chloride, free chloride, moisture, free hydroxide and the ratio of free chloride to hydroxide concentrations. The user can also choose different types of criteria and different scales for the axes.
- *Results window* for numerically presentation of the calculation results. The user can print and copy these results, or export them as a text file.

4.7 Limitations and advantages

Since the chloride transport is modelled by pure diffusion, the model so far may only predict the chloride penetration at submerged conditions with little influence of water transport. Of course it is possible to make predictions with an "equivalent" or "achieved" chloride concentration at the surface, as done with analytical prediction models, but that is to exceed the limits of the relevance of the scientific-based model. Further development of the model to include convection of chloride and non-saturated conditions is going on in order to be able to model the conditions in the splash zone and in structures exposed to de-icing salt.

The *ClinConc* model is unique in several ways. Since it includes most relevant factors in a sophisticated way, without large simplifications, it actually predict, to a large extent, the true nature of the combined processes involved when chloride penetrates into concrete in a structure.

Temperature variations give a maximum in predicted profiles and a counter-diffusion of chloride during summer periods!

Examples of these effects were shown in Nilsson et al. [1996]. The strong temperature dependence of chloride binding causes some of the bound chloride to dissolve when the temperature rises, resulting in a large increase in concentration of free chloride in summer time. The concentration at the surface, however, does not change very much during a year. Consequently, the profile of free chloride shows a larger concentration in the concrete pores than in the surrounding sea water. The predicted profiles also show a maximum of free chloride at a certain depth, i.e. a counter-diffusion of chloride out of the concrete, during the summer period! The shape of chloride profiles depends on what time of the year the cores were taken according to the predictions by *ClinConc*!

Another unique feature in the *ClinConc* model is the small number of parameters to be inserted into the model. Actually only one parameter has to be determined, the diffusion coefficient of the particular concrete at a certain age, and that one is determined in an independent test and no curve-fitting is involved. The other parameters in the model follow from the mix composition and the exposure conditions. At this stage the most uncertain part is the temperature effect on chloride binding, since available data are scarce.

In conclusion, the *ClinConc* model for chloride penetration is very promising for predicting actual chloride profiles in structures. The required input data is very limited but a short term test method has been developed and can be standardised to determine it. The predicted results are meant to be used for direct comparisons with measured profiles without involving curve-fitting. Any discrepancies found will immediately indicate where the most important lack of knowledge is to be looked for.

So far, however, the possible application is limited. More binding data is needed for concretes other than OPC concrete and the effects of special form-work, special aggregates and cracks have to be studied to widen the range of possible applications. The knowledge and understanding of the processes in the non-saturated conditions in structures exposed to the splash of sea water or de-icing salts must be improved before they can be added to the model.

5 Comparison of chloride profiles predicted by *ClinConc* and measured by NT Build 443

Profiles as measured by NT Build 443 can be predicted by *ClinConc*. Do the profiles coincide? If not, what has to be improved?

5.1 Introduction

A test of the ability of the scientific model *ClinConc* to correctly predict measured chloride profiles is available within this project. A great number of chloride profiles were determined in the accelerated test of several concrete qualities by the immersion test method NT Build 443, cf. Frederiksen et al. [1996]. The chloride penetration during such a test should be possible to predict by the use of *ClinConc*. A comparison with measured profiles would give an estimate of the prediction error in very delicate cases. Any discrepancy could identify lack of knowledge and give hints on where improvements are needed.

To predict the penetration during an accelerated test is of course a very delicate task and a perfect agreement would not be expected.

5.2 Available information from the tests

In the accelerated tests concretes with *w/c* ratios from 0.3 to 0.7 were tested with the NT Build 443 immersion test with a very high chloride concentration in the solution. In additional tests the chloride diffusion coefficients D_{CTH} were independently determined for the same concretes with the rapid CTH migration test method.

The concretes with *w/c* ratios of 0.3, 0.4 and 0.7 have been selected for a comparison. The relevant parts of the test conditions in the NT Build 443 tests are summarised in Table 5.2:1. The test results from the rapid CTH migration tests are given in Table 5.2:2.

Table 5.2:1. Test conditions in the NT Build 443 immersion tests relevant for predictions.

Specimen	Cut exposed surface	1D penetration
Curing temperature	20	°C
Curing conditions	sealed for 28 days	
Age at exposure	28	days
Test temperature	22-23	°C
Chloride concentration	100	g/l
Initial pH in test solution	7-8	
Duration of test	35	days

Table 5.2:2. Test results from the CTH migration tests , Frederiksen et al. [1996].

w/c	D_{CTH} (10^{-12} m^2/s)	
0.3	7.8 & 7.8	
0.4	13.8 & 14.9	
0.7	39.0 & 41.5	
Age during testing	28-29	days

The cement and concrete compositions are given in Frederiksen et al. [1996].

5.3 Recalculation of D_{CTH}

The required input data for the *ClinConc* model is the diffusion coefficient D_{CTH} at an age of at least six months. The test results are valid for an age of 28 days, however. A recalculation has to be performed.

5.3.1 Age-dependent diffusion coefficients

The true time-dependency of the chloride diffusion coefficients is reported by Tang [1996a], cf. Figure 5.3.1:1 The time-dependency is an age-dependency during the first six months and it depends on the concrete quality, the *w/c* ratio and the type of binder.

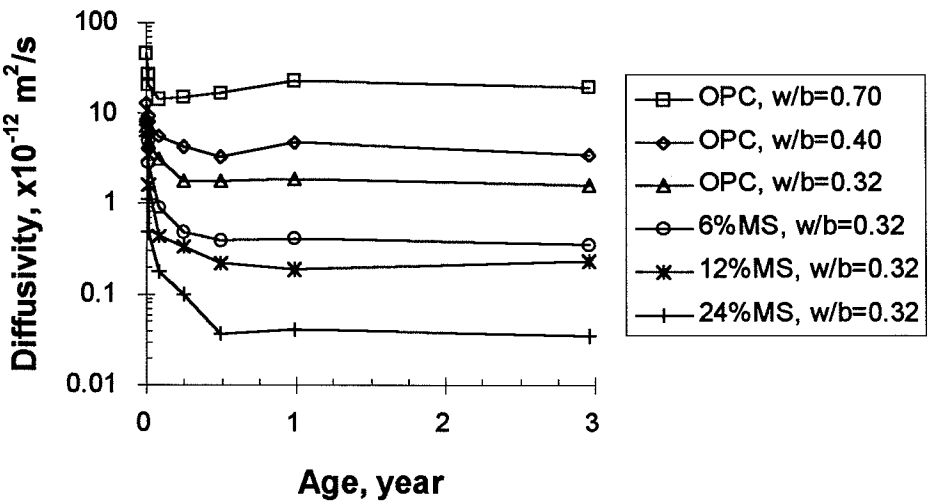

Figure 5.3.1:1. Age-dependent diffusion coefficients reported by Tang [1996a].

Tang [1996a] suggests an age-dependency of the diffusion coefficient D_{CTH} measured by the CTH-method according to equation (5.3.1:1).

$$\begin{cases} \dfrac{D_{CTH}(t)}{D_{CTH}(t_0)} = \left(\dfrac{t_0}{t_{ex}+t'}\right)^{\beta} & t_{ex} < t_0 - t' \\ \dfrac{D_{CTH}(t)}{D_{CTH}(t_0)} = 1 & t_{ex} \geq t_0 - t' \end{cases} \qquad (5.3.1:1)$$

where

t is the age of the concrete

t_0 is the age when the diffusion coefficient has reached a constant value; usually six months for OPC concrete.

t' is the duration of the exposure to chloride

t_{ex} is the age at exposure

β is a parameter

An evaluation of the data from Tang & Nilsson [1992], by interpolation and extrapolation, gives the values in Table 5.3.1:1 for the parameter β.

Table 5.3.1:1. β-values in the equation for age-dependent diffusion coefficients.

w/c	0.3	0.35	0.4	0.45	0.5	0.6	0.7	0.75
β	0.37	0.33	0.3	0.282	0.27	0.25	0.237	0.23
	t_0=180 days							

By use of the values in Table 5.3.1:1, the age-dependency of the diffusion coefficients can be estimated from (5.3.1:1). The numbers are shown in Table 5.3.1:2 and in Figure 5.3.1.2. The relation between the diffusion coefficients at ages of 28 days and 180 days is shown in Figure 5.3.1.3.

Table 5.3.1:2. Calculated relation between diffusion coefficients (D_{CTH}) at different ages.

age=$t'+t_{ex}$	*w/c*			$D(t)/D(t_0)$				
(days)	0.3	0.35	0.4	0.45	0.5	0.6	0.7	0.75
1	6.83	5.54	4.74	4.32	4.06	3.66	3.42	3.30
2	5.28	4.41	3.85	3.55	3.37	3.08	2.90	2.81
4	4.09	3.51	3.13	2.92	2.79	2.59	2.46	2.40
7	3.33	2.92	2.65	2.50	2.40	2.25	2.16	2.11
14	2.57	2.32	2.15	2.05	1.99	1.89	1.83	1.80
28	1.99	1.84	1.75	1.69	1.65	1.59	1.55	1.53
56	1.54	1.47	1.42	1.39	1.37	1.34	1.32	1.31
90	1.29	1.26	1.23	1.22	1.21	1.19	1.18	1.17
112	1.19	1.17	1.15	1.14	1.14	1.13	1.12	1.12
180	1	1	1	1	1	1	1	1

t_0=180 days. β-values according to Table 5.3.1:1.

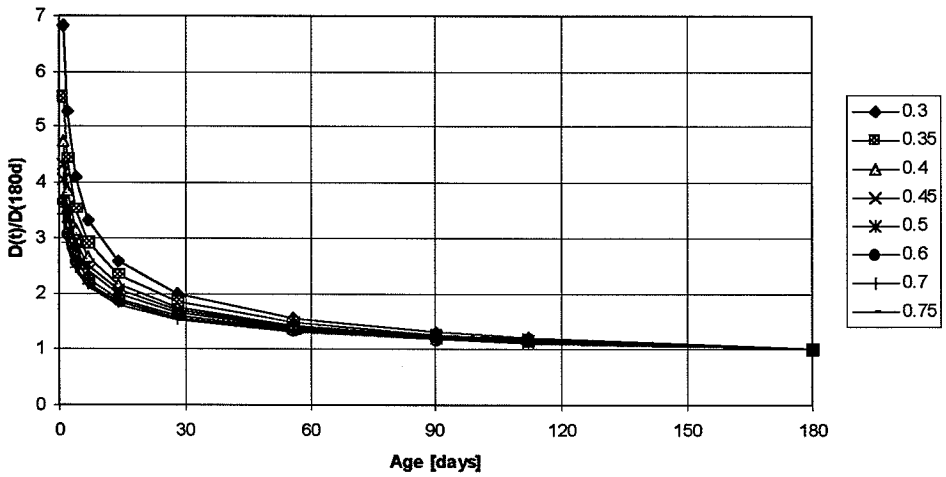

Figure 5.3.1.2. The age-dependency of the diffusion coefficients (D_{CTH}) according to equation 5.3.1.1 for the values in Table 5.3.1:2.

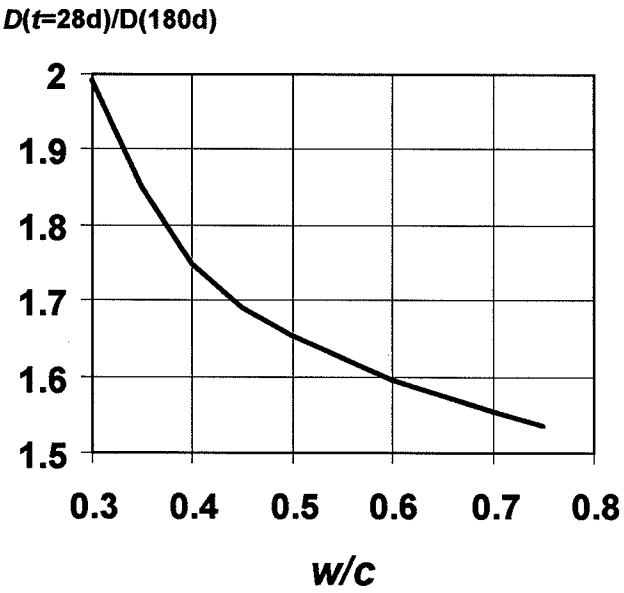

Figure 5.3.1.3. The calculated relation between the diffusion coefficients (D_{CTH}) at ages of 28 and 180 days respectively.

5.3.2 Recalculated D_{CTH}

For the three concretes that were chosen for the comparison, D_{CTH} is calculated according to the principles given in Section 5.3.1. The results are shown in Table 5.3.2:1.

Table 5.3.2:1. Measured and recalculated D_{CTH} for the concretes in the comparison.

w/c	D_{CTH} (10^{-12} m^2/s)	
Age	28-29 days	180 days
0.3	7.8 & 7.8	3.9
0.4	13.8 & 14.9	8.5
0.7	39.0 & 41.5	25.1

5.4 Predictions

By using D_{CTH} at an age of 180 days for the three concretes and the mix design according to Frederiksen et al. [1996], all required input data is available. The environmental conditions are the ones given in Table 5.2:1.

Predictions are done with two versions of the *ClinConc* model, versions 1.2 and 2.2 respectively. The major difference between the two versions is that the time-dependency is not included in the present version of *ClinConc 2.2*. Consequently version 2.2 should give somewhat lower depths of penetration during the first months.

5.5 Prediction results compared to measured profiles

The predicted chloride profiles are given in % by mass of binder. With the cement content and an estimation of the dry density of the concretes, the chloride profiles are transformed into % by mass of concrete as the test results are expressed.

The prediction results and the test results are compared in Figures 5.5.1-5.5.3.

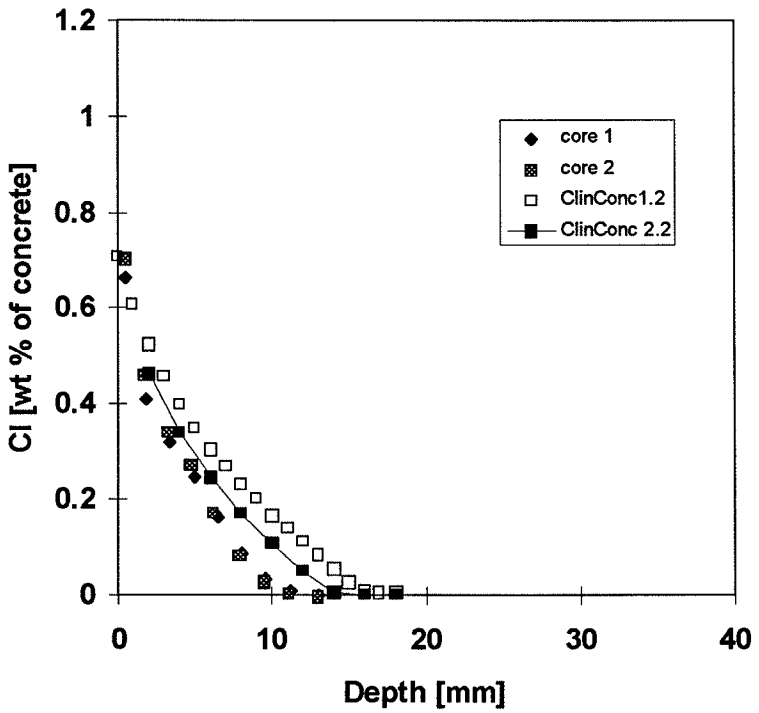

Figure 5.5.1. A comparison of predicted and measured chloride profiles for an accelerated immersion test of an SRPC concrete with w/c = 0.3. Age at exposure 28 days. Duration of test 35 days (NT Build 443).

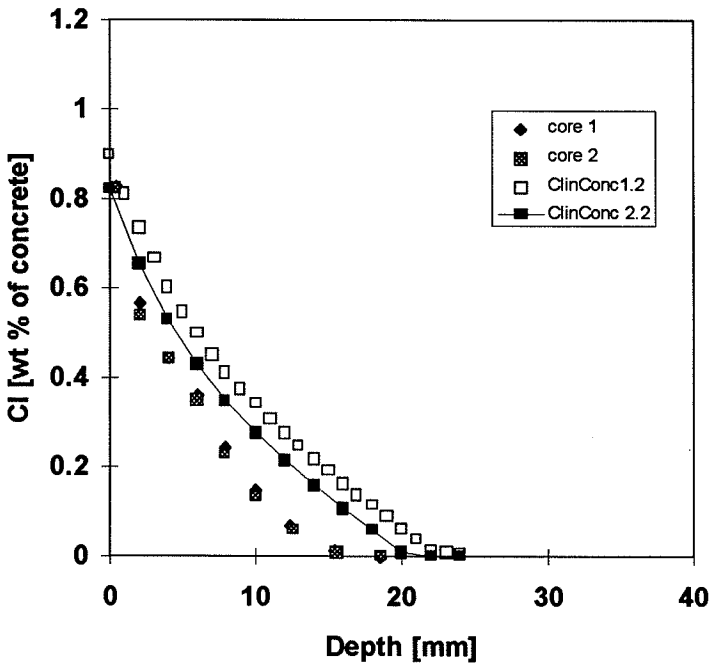

Figure 5.5.2. A comparison of predicted and measured chloride profiles for an accelerated immersion test of an SRPC concrete with w/c = 0.4. Age at exposure 28 days. Duration of test 35 days (NT Build 443).

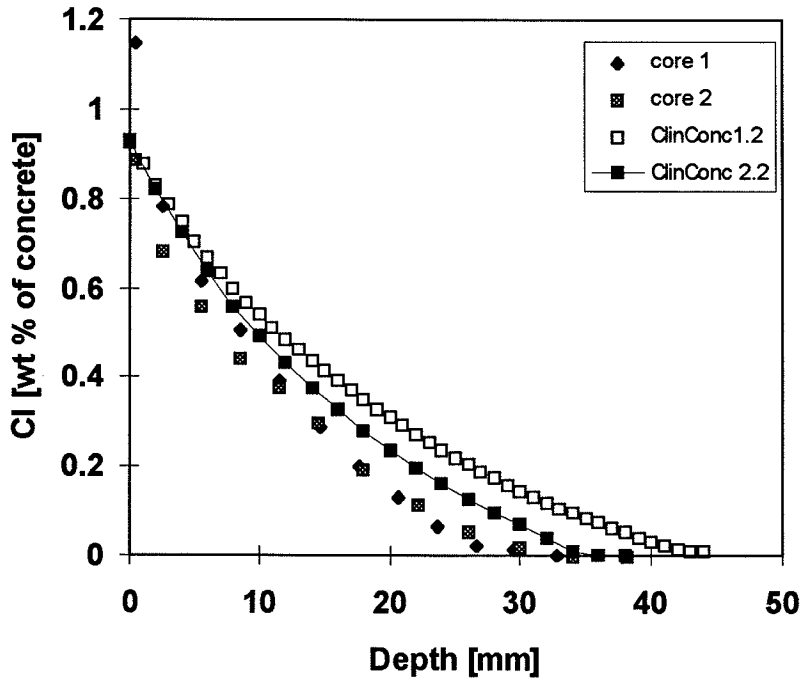

Figure 5.5.3. A comparison of predicted and measured chloride profiles for an accelerated immersion test of an SRPC concrete with w/c = 0.7. Age at exposure 28 days. Duration of test 35 days (NT Build 443).

5.6 Discussion and conclusion

The *ClinConc* model gives a certain over-estimation of the penetration of chloride during the test. The chloride concentrations at the surfaces are predicted almost exactly, i.e. the general description of the chloride binding properties of SRPC concrete seems to be valid also for the cement used in the tests.

The predictions with the two versions of *ClinConc* give somewhat different results. Predictions by *ClinConc 2.2* are closer to the measured profiles, but this is only natural since the age-dependency is not included in that version. Consequently, the predictions are done with diffusion coefficients valid for ages of 180 days. The age-dependency between 28 and 180 days is obviously not enough to explain the differences between the predicted and measured profiles.

One possible explanation could be that the age-dependency of the true diffusion coefficient is different from the age-dependency of the D_{CTH}. The D_{CTH} includes not only the true diffusion coefficient but also a certain chloride binding capacity activated during such a test. That chloride binding capacity should be proportional to the amount of reaction products, i.e. proportional to the degree of hydration. The change in chloride binding capacity between 28 and 180 days could be large for certain binders. This would counteract the decrease in D_{CTH} during that time. Consequently the true diffusion coefficient may not decrease as much as the D_{CTH} according to Section 5.3.

It seems, however, as if the true diffusion coefficients are even smaller than the ones estimated from the CTH-method at an age of 180 days, in this case with the conditions as in an accelerated test. A possible explanation could be the concentration dependency of the diffusion coefficient as described in Nilsson et al. [1996]. The results by Bigas [1994] are shown in Figure 5.6.1.

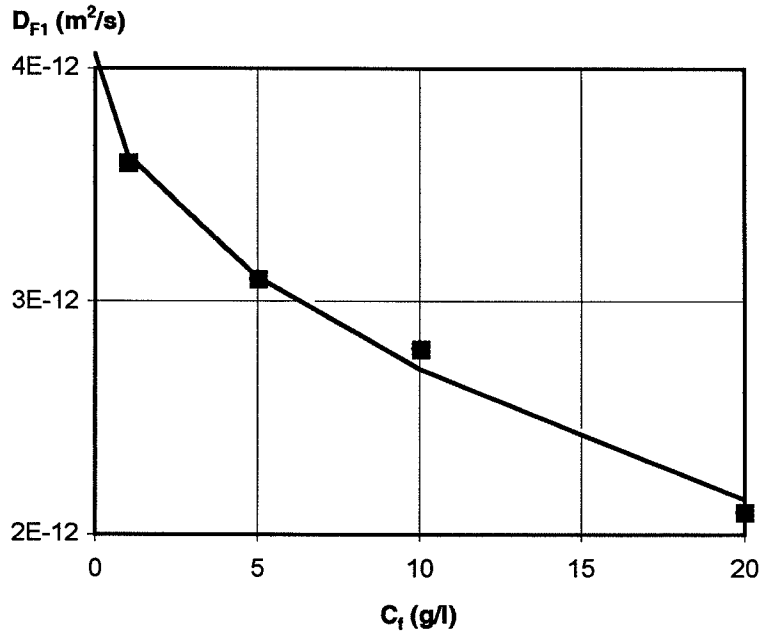

Figure 5.6.1. Average diffusion coefficients D_{F1} (c1) (points) for a w/c = 0.6 mortar as a function of the concentration in the upstream cell in a series diffusion cell experiments, Bigas [1994].

The diffusion coefficients should be very much lower at high chloride concentrations according to this hypothesis. In the NT Build 443 immersion test the concentration of chloride is 100 g/l. At this concentration the diffusion coefficient could be lower than at the conditions where D_{CTH} is measured. Obviously more research is needed to improve the accuracy in predictions at early ages and elevated conditions.

6 Comparison of the empirical and the scientific models

The scientific model is so far only valid in the submerged zone, where field data for the empirical model is scarce. Can a comparison be done and if so, how much will the predictions diverge?

6.1 Introduction

Two models have been presented, a "scientific" model and an "empirical" model. These two models are quite different and use quite different information as input for a prediction. A comparison of predictions with the two models would give an estimate of the present uncertainties in predicting chloride penetration into concrete structures.

However, the two models cannot be used in any situation. They have certain limitations that are different for the two methods. Consequently, a special case has to be chosen for a comparison where input data for both models are available.

The limitations for the models are described in the next section. Then possible alternative concretes and environments are discussed and one concrete and one environment are chosen. The predictions with the two models are then described and finally the prediction results are compared and the differences are discussed.

Predictions of chloride profiles are made for exposure times of 1, 3, 10, 30 and 100 years.

6.2 Requirements for structures to be compared

The *ClinConc* model is only applicable for a submerged part of a structure and only under the following conditions

1. a concrete where D_{CTH} has been measured according to the rapid CTH migration test method, preferably at ages over six months
2. a concrete where the chloride binding properties are known or possible to estimate, such as modern SRPC-concrete
3. an environment where the chloride concentration and the sea water temperature are known

The empirical model is applicable under the following conditions

1. a concrete where D_{pex} has been measured according to NT Build 443 (earlier APM 302)
2. a concrete and an environment similar to the conditions where the time-dependency of the achieved diffusion coefficient and the time-dependency of the achieved chloride surface content have been evaluated earlier, or
3. a concrete and an environment where data exist for a number of exposure times.

Of course the best evaluation of the model uncertainty would be gained if a concrete and an environment could be chosen where the "result" is known, i.e. where accurate chloride profiles have been measured after long-term exposure.

6.3 Choice of concrete

With the restrictions given in section 6.2 any concrete used in the BMB-project ("Beständighet Marina Betongkonstruktioner" - a Swedish research programme) could be used. However, field experience of these concretes is limited to four years (for the Öland Bridge concrete) or to two years (for the concretes at the field exposure sites in Träslövsläge).

A possible choice could be the concrete used in the repair of the Öland Bridge in Kalmarsund. The concrete was called "#1-40" and "Ö" in the BMB-project.

Concrete #1-40 and Ö contains SRPC-cement with 0.01 % Na_2O and 0.6 % K_2O. The concrete mix design is given in Table 6.3:1.

Table 6.3:1. Concrete mix design for concrete #1-40 and Ö in the BMB-project.

Cement	420	kg/m^3
Water	168	kg/m^3
w/c ratio	0.44	
Aggregate	1692	kg/m^3
Air content	6	% by volume

6.4 Choice of environments

The sea water conditions in the south of Sweden and in Denmark are well known. Structures in Kalmarsund, Öresund, Esbjerg harbour and Great Belt were examined in the BMB-project. Numerous specimens were exposed at a field exposure site at Träslövsläge harbour at the west coast of Sweden. Any of these waters could be chosen.

A possible choice could be the Öresund, where now a bridge is being built between Denmark and Sweden. The conditions in Öresund (and Träslövsläge) are summarised in Table 6.4:1.

Table 6.4:1. The sea water conditions in Öresund and Träslövsläge.

Chloride concentration	14±4	g/l
pH	7-8	
Temperature	11 ± 9	°C

For these conditions, and for the concrete chosen in section 6.3, chloride profiles are available for comparison after 0.6, 1 and 2 years of exposure, cf. Figure 6.4:1.

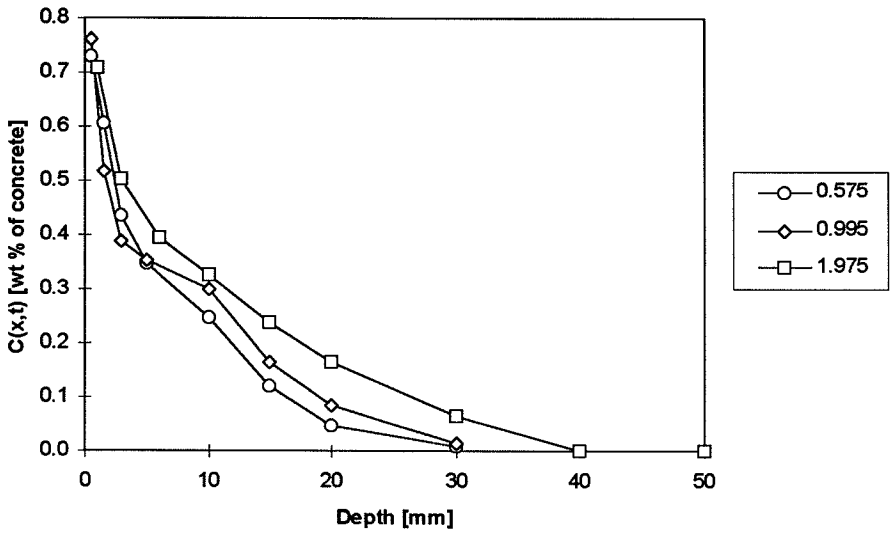

Figure 6.4:1. Chloride profiles for the submerged part of specimens of concrete #1-40 in Träslövsläge harbour after 0.6, 1 and 2 years of exposure.

6.5 Prediction with the *ClinConc* model

6.5.1 Input data

As input the *ClinConc* model needs the diffusion coefficient D_{CTH} measured with the rapid CTH migration test method at an age of six months or more. If that is missing for the particular concrete, a test result from NT Build 443 could be used, but a somewhat larger uncertainty would be introduced.

The *ClinConc* model also needs the chloride concentration and the temperature in the sea water. A constant value would do, but an annual variation could be dealt with.

The special input data for the concrete #1-40 and for the environment in Öresund are given in Table 6.5.1:1.

Table 6.5.1:1. Unique input data for ClinConc for the particular concrete and the particular environment, in addition to the concrete mix design.

D_{CTH}	7.24×10^{-12}	m^2/s
age before exposure	14	days
Cl(t)	14 ± 4	g/l
T (t)	11 ± 9	°C

ClinConc automatically uses some input data for SRPC-concrete on chloride binding, time-dependent diffusion coefficient and activation energy. Depending on the type of form-work, a depth dependency of the diffusion coefficient is included. The current prediction is done for steel form-work.

The automatically used values for input data are shown in Table 6.5.1:2.

Table 6.5.1:2. Automatically used input data for ClinConc regarding SRPC concrete and sea water environment, cf. Tang [1996a].

Slope of chloride binding isotherm	3.57	
Non-linear exponent in binding isotherm	0.38	
Exponent for age-dependent diffusion coefficient	0.3	
Activation energy for chloride binding	40	kJ/mole
Activation energy for chloride diffusivity	42	kJ/mole
pH of sea water	7-8	

Additional input to *ClinConc* is the times of exposure and the size of the cells (currently 5 mm). The input windows are shown in Figures 6.5.1:1 and 6.5.1:2.

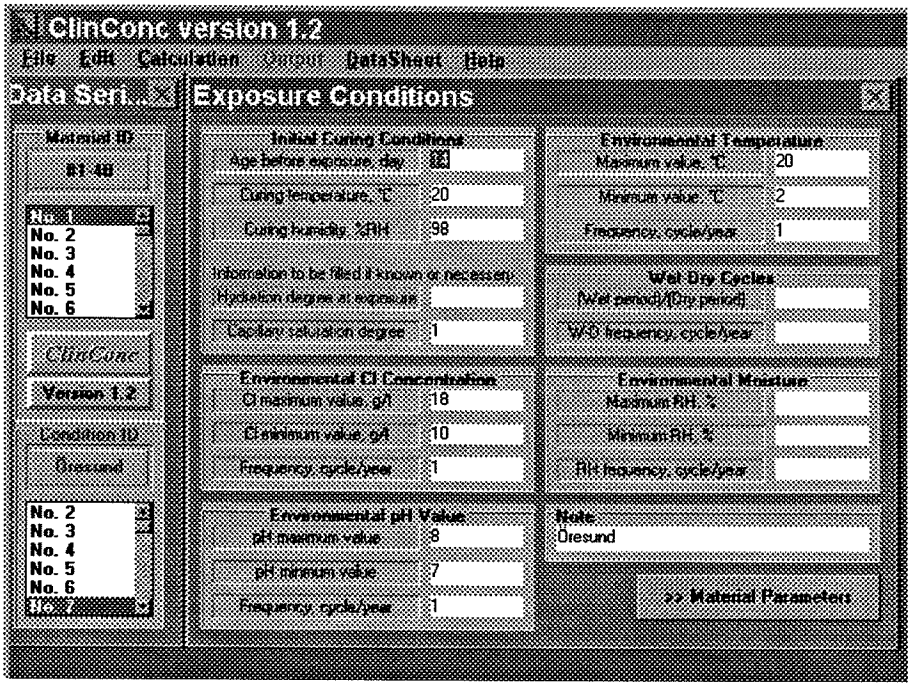

Figure 6.5.1:1. The window with input data for environmental conditions in ClinConc.

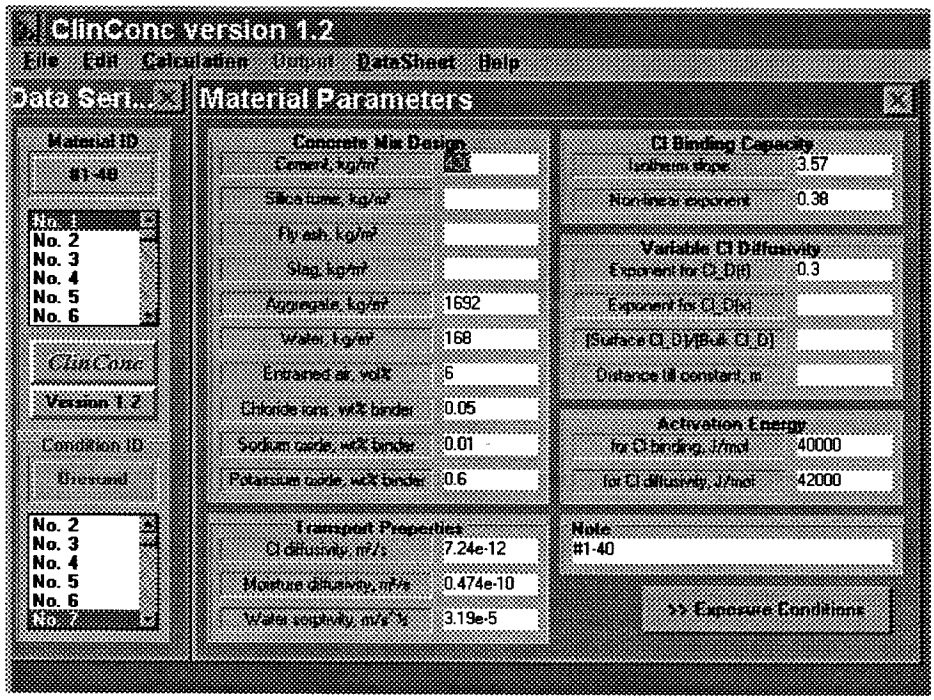

Figure 6.5.1:2. The window with input data for the concrete in ClinConc.

6.5.2 Prediction procedure

After the input data has been typed in, the calculation is started by choosing the times of exposure, size of cells and whether the prediction is for a semi-infinite case or a case with a limited thickness. The calculations takes some 10-20 minutes depending on the computer capacity since the calculations are to be run for 100 years with a constant small time step.

When the calculation is completed the output as profiles of total or free chloride, hydroxide concentration or the relation Cl/OH can be chosen in various ways, graphically or in a spread sheet. From the spread sheet the values can be used for curve-fitting if required or displayed graphically in any suitable way.

6.5.3 Prediction results

The results of the predictions for the current case are shown as profiles of total or free chloride, hydroxide concentration and the relation Cl/OH in Figures 6.5.3:1-6.5.3:4.

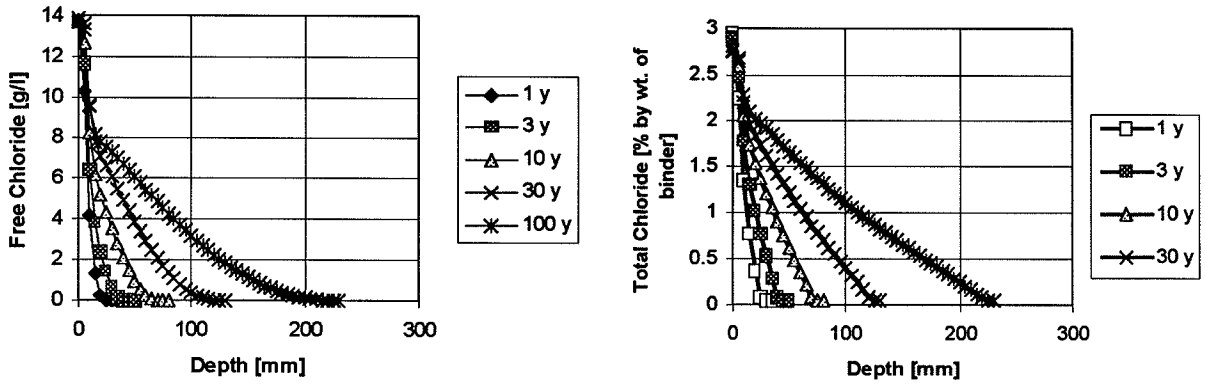

Figure 6.5.3:1 and Figure 6.5.3:2. Profiles of free chloride (left) and total chloride (right) predicted by the use of ClinConc.

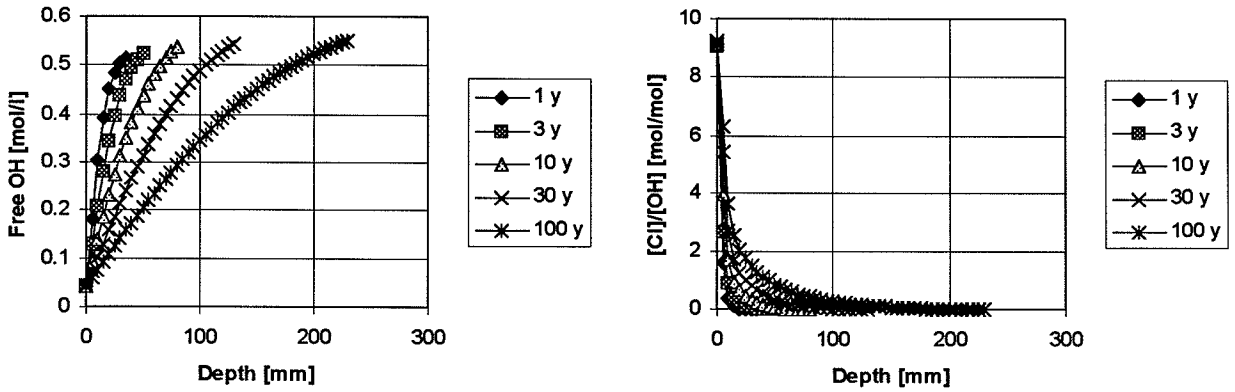

Figure 6.5.3:3 and Figure 6.5.3:4. Profiles of hydroxide (left) and the relation chloride to hydroxide (right) predicted by the use of ClinConc.

A comparison between the measured and predicted profiles of total chloride are shown in Figure 6.5.3:5.

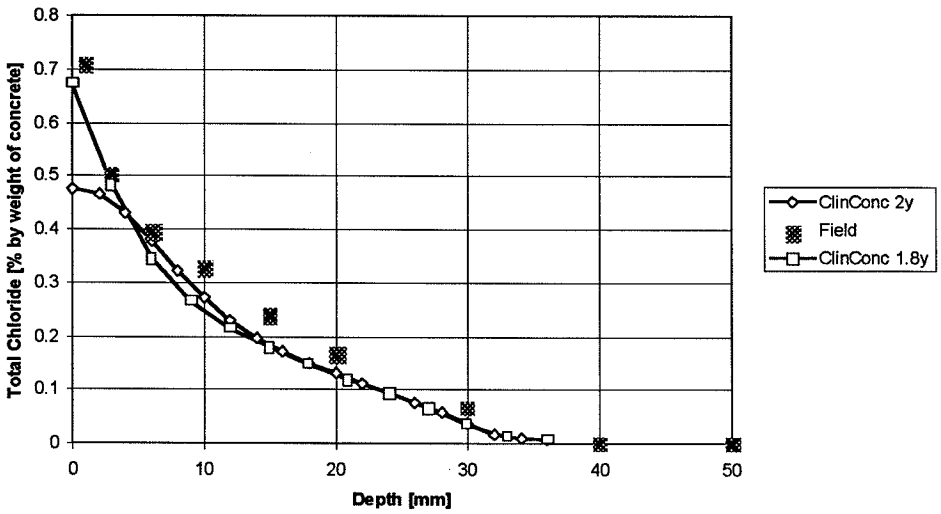

Figure 6.5.3:5. Measured and predicted profiles of total chloride in concrete #1-40 and Ö in the submerged zone in Träslövsläge harbour after 1.8 and 2 years of exposure.

The predicted and measured profiles agree fairly well. Note that no curve-fitting is involved. The predicted profiles are completely independent from the measured ones.

The predicted concentration in the surface region coincides well, but it must be remembered that the concentrations at the surface vary during a year cycle, due to temperature effect, see the profiles after 1.8 and 2 years respectively in Figure 6.5.3:5. Additionally the measured concentrations close to the surface should be higher than the predicted ones since the binder content is higher close to the surface than at larger depths.

The predicted penetration is somewhat smaller than the measured one. However, the measured profiles may have a certain inaccuracy. The inaccuracy is not known since only one profile was determined at each occasion.

In Figure 6.5.3:6 the profiles of total chloride are shown for exposure times 1, 3, 10, 30 and 100 years, expressed as a function of $x/\sqrt{t}$ to compare the profiles with each other.

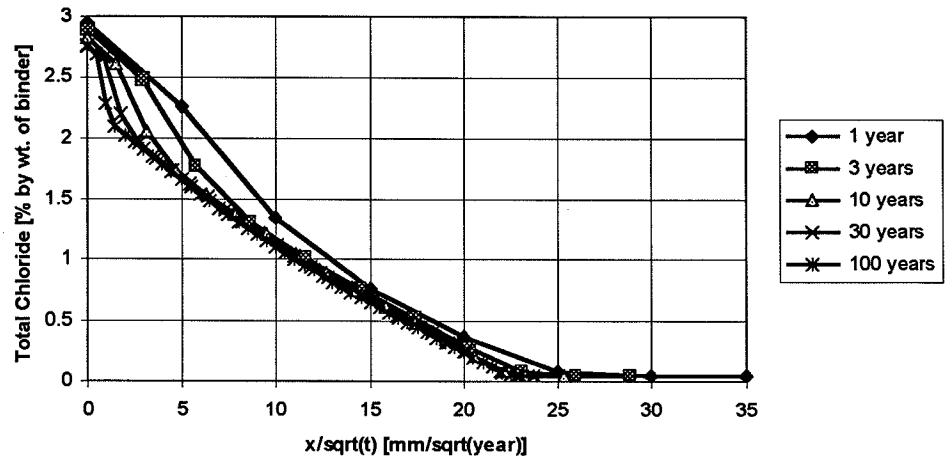

Figure 6.5.3:6. Profiles of total chloride at exposure times between 1 and 100 years predicted by the use of ClinConc.

The chloride profiles were curve-fitted to the error function solution of Fick's 2nd law. Depending on the number of points close to the surface that are "excluded" in the curve-fitting, the result of the curve-fitting will vary. Two alternatives are shown in Figures 6.5.3:7 and 6.5.3:8.

Note that the laboratory measured diffusion coefficient D_{CTH}, used as input data for the prediction, is 7.24×10^{-12} m^2/s. The "achieved diffusion coefficients" in the submerged zone obviously will be much lower than that.

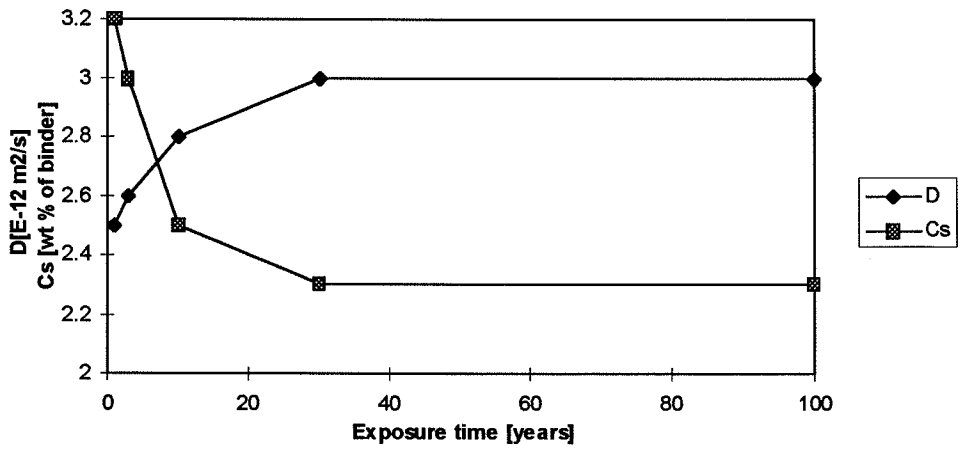

Figure 6.5.3:7. Parameters in the error function solution from curve-fitting to profiles predicted by ClinConc. Graphical curve-fitting of all values. Linear time scale.

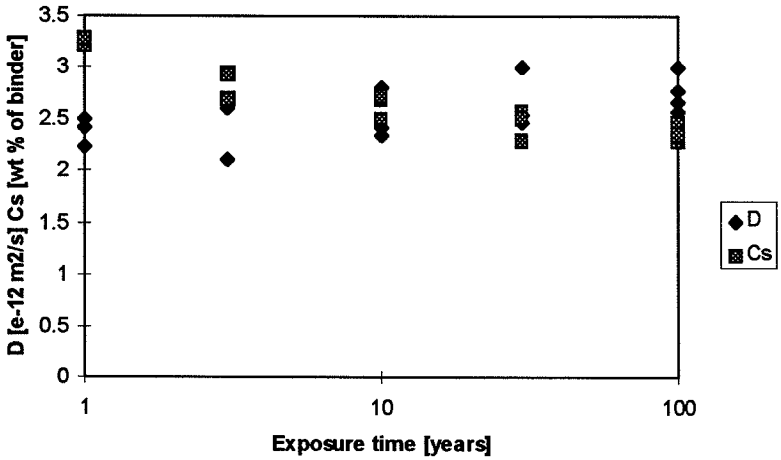

Figure 6.5.3:8. Parameters in the error function solution from curve-fitting to profiles predicted by ClinConc. Automatic curve-fitting by excluding one or more points close to the surface. Logarithmic time scale.

6.6 Prediction with the Mejlbro-Poulsen model

Here the utilisation of experiences from field exposure tests for prediction of future chloride ingress is described.

As described in Chapter 3 the Mejlbro-Poulsen model utilises measured chloride profiles as direct input for predicting the further chloride ingress into concrete. This implies that some knowledge of the concrete's response to the environment is important. The prediction will be very dependent on the quality (accuracy and planning) of the data. The more measured profiles at different times of exposure and the longer exposure time the better the predictions will be.

Because of the nature of the input data for the model, the effect of varying environmental conditions, varying concrete quality with depth, leaching and other matters are indirectly incorporated into the prediction. This of course have the adverse consequence of overestimating the effect of such matters when these are changing a lot during the first years of exposure. It is however believed to be a conservative way of handling the straightforwardness that the "experience" can be transformed into predictions.

6.6.1 Input data

The input data for the prediction with the Mejlbro-Poulsen model is the measured profiles of total acid soluble chloride in per cent of the dry sample mass. Naturally the chloride content could be expressed in another unit, it should however be kept in mind that the results always are given in the same unit as the input data.

The chloride profiles measured in the concrete marked "Ö" in the BMB project are given in Table 6.6.1:1.

Table 6.6.1:1. Measured chloride profiles in the concrete marked "Ö" in the BMB project after marine exposure in Träslövsläge harbour. The profiles represents three exposure times. Below the profile values are given the achieved diffusion coefficients and surface concentrations as found by use of the error function solution and the Mejlbro-Poulsen model respectively

Sample identification: Träslövsläge: *Ö (submerged zone)*				
Measured profiles, natural exposure				
t_{in} =	0.614	1.033	2.014	[yr]
t_{in} - t_{ex} =	0.575	0.995	1.976	[yr]
x [mm]	$C(x,t_{in} - t_{ex})$ [% mass]	$C(x, t_{in} - t_{ex})$ [% mass]	x [mm]	$C(x, t_{in} - t_{ex})$ [% mass]
0.5	0.730	0.763	1	0.710
1.5	0.607	0.517	3	0.503
3	0.434	0.389	6	0.394
5	0.348	0.354	10	0.327
10	0.247	0.300	15	0.239
15	0.121	0.166	20	0.165
20	0.048	0.084	30	0.065
30	0.009	0.014	40	0.000
			50	0,000
D_a =	106.8	114.2	90.1	[mm^2/yr]
C_{sa} =	0.609	0.515	0.555	[% mass]
$D_a(t_{in})$ =	1014.9	603.0	309.3	[mm^2/yr]
$C_{sa}(t_{in})$=	0.571	0.639	0.691	[% mass]

The profiles of the submerged zone is shown graphically in Figure 6.6.1:1 below.

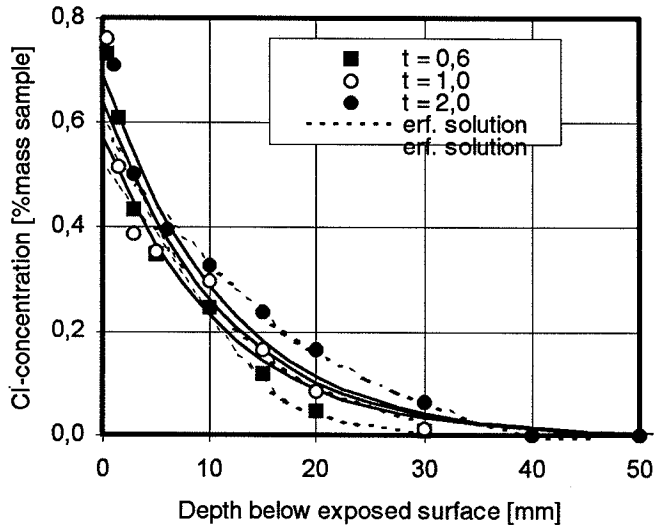

Figure 6.6.1:1. The calculated chloride profiles (acc. to the Mejlbro-Poulsen model) after 0.6, 1.0 and 2.0 compared to the measured profiles respectively. In addition the profiles fitted by the error-function solution are shown as dotted curves. The measured profiles are from the submerged zone of the specimens exposed in Träslövsläge harbour.

6.6.2 Prediction procedure

The time dependence of the transport coefficient D_a is assumed to follow (3.2.1:4). The time dependence of the surface boundary condition is believed to follow (3.2.2:2).

A multiple non-linear regression analysis (a least squares fit) was performed on the chloride profiles from the submerged zone. The task was to minimise the deviation between the modelled curves and the measured curves simultaneously by changing the parameters D_{aex}, α, p and S of the model.

In order *not* to get results that were unsupported by experiences from marine exposures and in order to reduce the flexibility of the model, restrictions were laid on certain important parameters of the model. The restrictions were as follows:

- The diffusion coefficient should be between *constant* and *decreasing* with time. The decrease however should not be allowed to exceed the situation were $D_a \times t$ is a constant, i.e. $0 \leq \alpha \leq 1$.
- The surface chloride content should not be allowed to decrease with time, i.e. $p \geq 0$.
- The surface chloride content should not exceed 2 % mass concrete, i.e. $C_{sa,100yr} \leq 2$ % by mass concrete.

Those restrictions had the expected side effect that the models ability of fitting the input data was to some extend limited.

All the above calculations were done in a Microsoft Excel 5.0 workbook using only build in standard functions and procedures.

6.6.3 Prediction result

The measured profiles are compared to the calculated profiles in Figure 6.6.1:1. The result of the prediction of the chloride ingress in the submerged zone for exposure times 5, 10, 50 and 100 years are shown graphically in Figure 6.6.3:1.

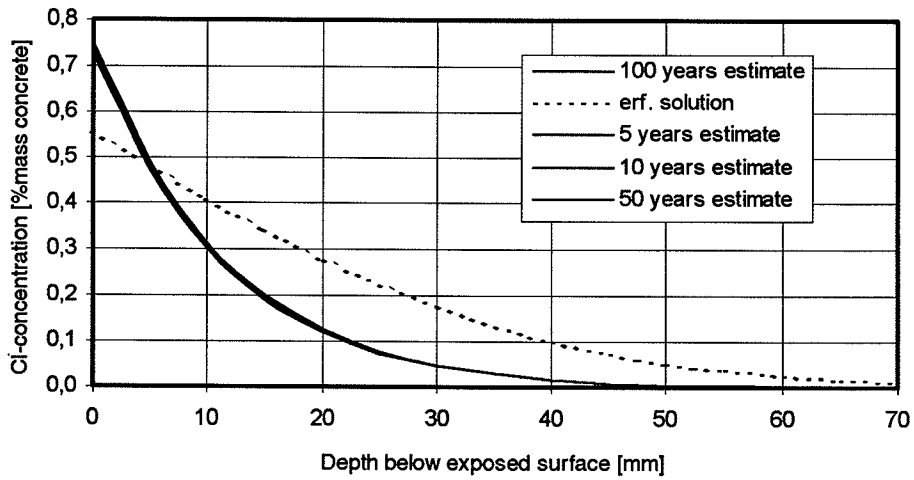

Figure 6.6.3:1. The predicted chloride profiles for 5, 10 and 100 years of submerged exposure in Träslövsläge harbour for the concrete marked "Ö" in the BMB project. The curve for the "erf.-solution" represents 100 years.

6.7 Comparison and discussion of prediction results

The chloride profiles after 5, 50 and 100 years, predicted by the two models, are compared in Figure 6.7:1.

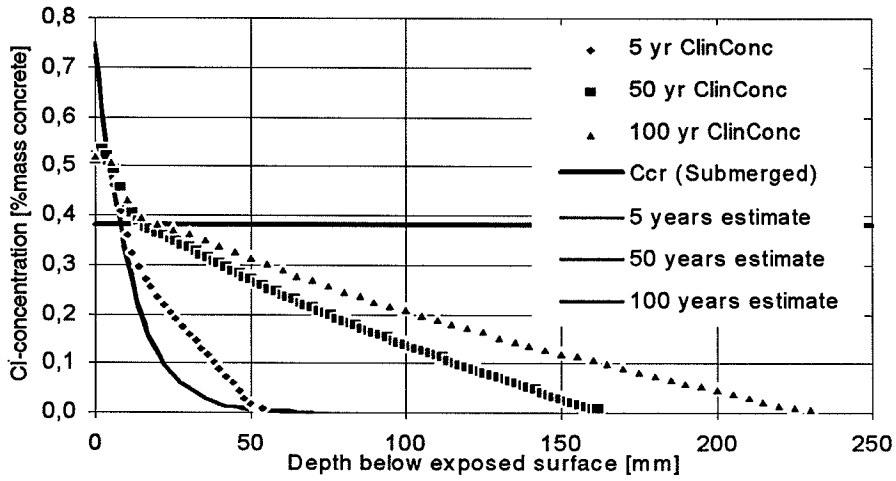

Figure 6.7:1. Chloride profiles after 5, 50 and 100 years, predicted by the two models.

There is a large difference between the prediction results. *ClinConc* gives a much lower chloride content close to the concrete surface but a much larger depth of penetration. This difference should be regarded as measure of the uncertainty in today's chloride penetration predictions.

The main explanation of the differences is of course the very much different assumptions for the surface chloride content in the two models. That difference will cause a much higher amount of bound chloride in the results predicted by the empirical model. If that was to be included in *ClinConc*, it would certainly also explain the differences in the predicted penetration depths. Consequently, the main difference between the two models is the description of the surface chloride contents.

In *ClinConc* the surface content follows from the chloride concentration in the sea water and the chloride binding isotherm. There is no large time-effect included. The surface content will change a little with time due to continuous cement hydration that produces more gel that binds more chloride. A small change with time will also be due to leaching of hydroxide that will change the pH and, consequently, the chloride binding close to the surface. At larger depths, however, leaching is small and chloride binding should not increase much with time.

In the empirical model, however, the surface chloride content may be assumed to (significantly) increase with time. The parameters in the equation for surface chloride contents are determined by curve-fitting to the measured profiles after 0.6, 1 and 2 years and was found to give some time-effect. Such a curve-fitting is of course very sensitive to small deviations in the measured profiles. Measurement errors, differences due to taking profiles at different times of the year and the higher binder content close to the surface are examples of possible sources of such deviations. Longer exposure times would give much more reliable predictions.

However, the background data for the hypothesis of the surface chloride content increasing with time seem to be very limited for the submerged zone. For the time

being, regardless of what model is chosen for predictions, the differences shown in Figure 6.7:1 is a measure of the uncertainty in the two most advanced models that exist today.

6.8 Conclusion

Predicted chloride profiles in the submerged zone, from the scientific and the empirical model respectively, agree fairly well at an exposure time of two years or less, with each other and with measured data.

At an exposure time of 100 years, however, predicted profiles from the two models are quite different. The surface chloride content and the penetration depths differ a lot. The main explanation for this difference is the different ways of describing the surface chloride contents. The difference must, however, be regarded as a measure of the uncertainty in today's models for chloride penetration.

7 A Model for Convection of Chloride

A new, simple model for convection of chloride in concrete structures exposed to splash from sea water or de-icing salts is presented.

7.1 Introduction

The distribution of chloride in concrete structures exposed to splash from sea water or de-icing salt are modelled as a non water-saturated concrete intermittently exposed to air, water and chloride solution where chloride move by diffusion and convection with the liquid moisture flow. Chloride ions are described independently of other ions present in the pore solution. Only one-dimensional cases are treated.

7.2 Mass balance equations

The chloride distributions follow from solving the mass balance equation for chloride

$$\frac{\partial c_{tot}}{\partial t} = -\frac{\partial q_{Cl}}{\partial x} \tag{7.2:1}$$

where q_{Cl} is the transported amount of chloride, t is time and x is the co-ordinate. For a small time interval Δt, the change in total chloride content may be written as differentials

$$\Delta c_{tot} = \frac{\Delta t}{\Delta x}\left(q_{Cl}(x,t) - q_{Cl}(x+\Delta x,t)\right) \tag{7.2:2}$$

where Δx is the thickness of a small element of the concrete.

The convection of chloride is governed by the moisture flow and the changes in moisture contents will change the chloride concentrations. Consequently, the moisture distributions must be predicted as well by solving the mass balance equation for moisture

$$\frac{\partial w}{\partial t} = -\frac{\partial q_{tot}}{\partial x} \tag{7.2:3}$$

where q_{tot} is the total moisture flow. That mass balance equation can be written in differentials in the same way as for chloride

$$\Delta w = \frac{\Delta t}{\Delta x}\left(q_{tot}(x,t) - q_{tot}(x+\Delta x,t)\right) \tag{7.2:4}$$

The temperature conditions are assumed to be more or less instantaneously changed to be equal to the concrete surface temperature. The energy balance equation does not need to be solved in such a case.

The two mass balance equations are coupled and must be solved together. The main part of the solution is to describe the flows of moisture and chloride. The initial conditions are trivial but the boundary conditions must be, until better data are available, a simplification of the true environmental conditions at the concrete surface.

7.3 Flow equations and flow coefficients

7.3.1 Moisture flow, vapour and liquid

The moisture flow must be divided into vapour and liquid flow since the chloride ions will be transported by convection with only the liquid flow. The vapour flow is described with the vapour concentration as the flow potential

$$q_v = -\delta_v \frac{\partial v}{\partial x} \tag{7.3.1:1}$$

where the vapour flow coefficient is assumed to be constant for a particular concrete.

The liquid flow should be described with the pore water pressure as the flow potential.

$$q_l = -k_p(w) \frac{\partial P_w}{\partial x} \tag{7.3.1:2}$$

where the water permeability is regarded as being dependent on the moisture content or degree of capillary saturation. Below a "critical" moisture content w_{cr}, the permeability is negligible.

However, since data on the permeability is scarce the "equivalent" relative humidity $\varphi_{eq}(w)$, not including the effect of the salt content, has been chosen as liquid flow potential. Utilising measured data on the total moisture flow coefficient δ_{tot}, Hedenblad [1993], one gets

$$\begin{aligned} q_l &= q_{tot} - q_v = -\delta_{tot} \frac{\partial v}{\partial x} - \delta_v \frac{\partial v}{\partial x} = \\ &= -(\delta_{tot} - \delta_v) v_s(T_{20}) \frac{\partial \varphi}{\partial x} = -k_{RH}(\varphi_{eq}) \frac{\partial \varphi}{\partial x} \end{aligned} \tag{7.3.1:3}$$

where $v_s(T_{20})$ is the vapour content at saturation in +20°C. There should be a small temperature effect on the liquid flow coefficient k_{RH} but since it is very small for the temperature variations expected in concrete structures it has been omitted here. For wider temperature ranges a factor of T/T_{20} [K/K] should be included. In this way the temperature effect will be much smaller than when using the vapour content as driving potential also for the moisture flow.

The liquid flow through the concrete surface is of course zero if the surface is not wet.

An example of the effect of φ_{eq} on the liquid flow coefficient is shown in Figure 7.3.1:1.

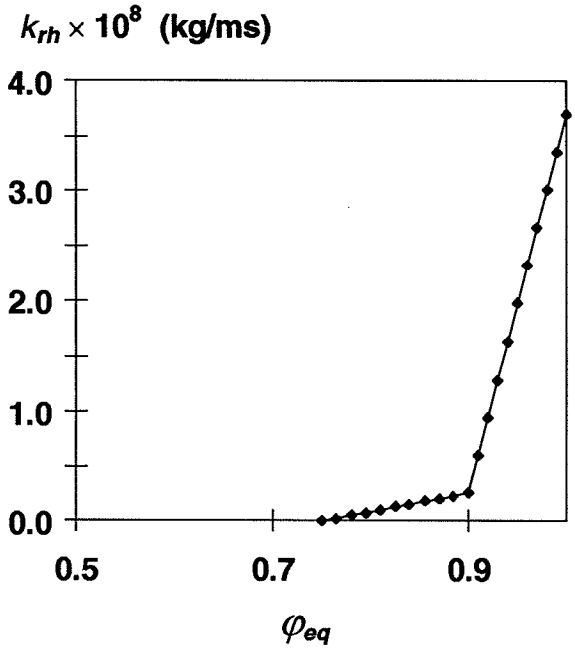

Figure 7.3.1:1. An example of the effect of φ_{eq} on the liquid flow coefficient, using data from Hedenblad [1993].

7.3.2 Chloride diffusion and convection

Chloride transport is assumed to occur as diffusion and convection. The diffusive and convective parts are described by separate terms in the chloride flow equation

$$q_{Cl} = -D_{Cl}(w,T,c_f')\frac{\partial c_f'}{\partial x} + q_l c_f' \qquad (7.3.2:1)$$

where the diffusion coefficient depends on the moisture content and is zero below a certain "critical" moisture content w_{cr}.

The chloride transport through the concrete surface is of course zero if the surface is not wet.

An example of the effect of φ_{eq} on the chloride diffusion coefficient is shown in Figure 7.3.2:1.

eq

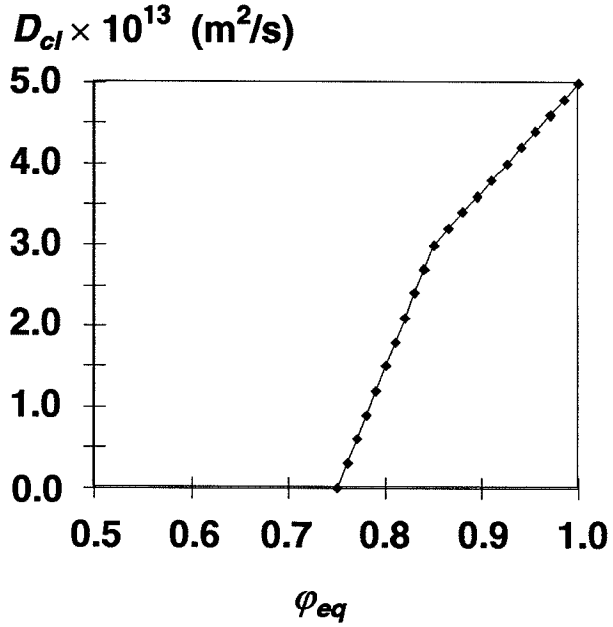

Figure 7.3.2:1. An example of the effect of φ_{eq} on the chloride diffusion coefficient.

7.4 Environmental conditions

The tidal and splash zone of concrete structures exposed to saline sea water, and the parts of road and bridge structures that are exposed to de-icing salts, are exposed to various combinations of drying and wetting from humid air, washed by rain water and contact with chloride solutions. Simultaneously, the temperature conditions vary. A reasonable simplification of the environmental conditions could be to combine periods of air with a certain "equivalent" surface relative humidity, pure water and chloride solutions with certain concentrations.

In the tidal and splash zone of marine structures the conditions could be

$$T(x = 0, t) = T_{sea} \tag{7.4:1}$$

$$\varphi(x = 0, \Delta t_1) = \varphi_{air} \tag{7.4:2}$$

$$\varphi(x = 0, \Delta t_2) = 100\% \tag{7.4:3}$$

$$c_f'(x = 0, \Delta t_3) = c_f'(sea) \tag{7.4:4}$$

with different combinations of the three types of time intervals for different parts of a structure.

At the surfaces of structures exposed to de-icing salts at a number of occasions during the winter season, a "typical year" could be described in the same way, but with the sea water temperature replaced by the air temperature and the chloride concentration replaced by the chloride concentration in a saturated solution. The time intervals are of course quite different and the sum of them is one year. An example is shown in Figure 7.4:1.

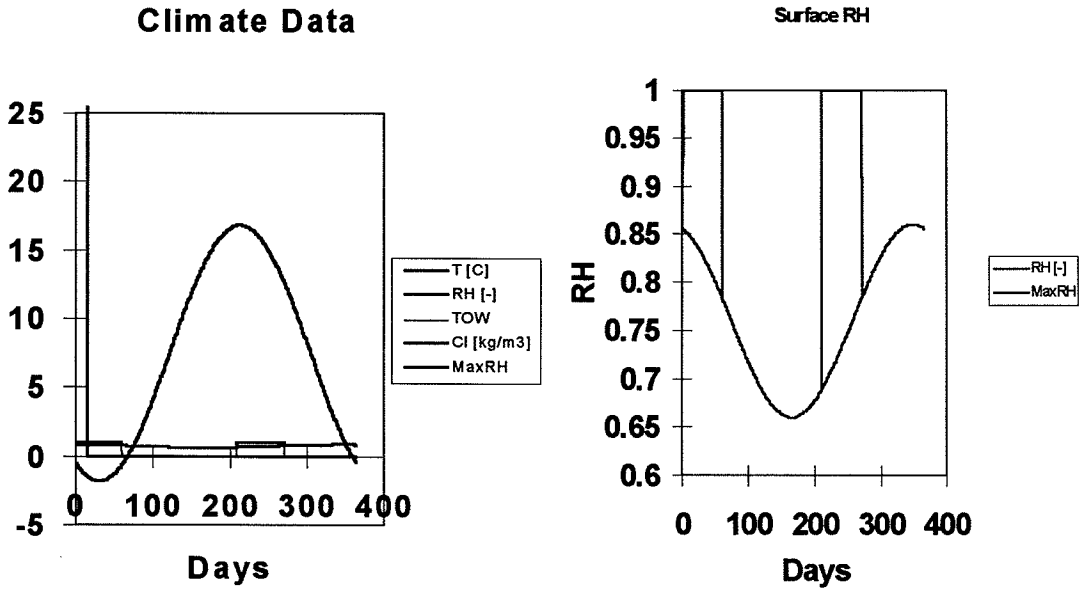

Figure 7.4:1. An example of a simple description of the environmental conditions at a concrete surface exposed to de-icing salts in wintertime with two periods of driving rain. (TOW = Time Of Wetness).

7.5 Relationships

7.5.1 Pore water pressure

The pore water pressure depends on the relative humidity (φ) and the concentration of chloride in the pore water (c'_f). From Hedenblad [1988] the pressure could be estimated by

$$P_w \approx \frac{RT}{V_w}(\ln\varphi + kc'_f) \qquad (7.5.1:1)$$

where the coefficient k depends on the molar weight, the number of ions per molecule and an osmotic coefficient. V_w is the molar volume of water (18×10^{-6} m^3/mole).

For saturated concrete P_w equals 0. Consequently φ is somewhat smaller than 100%.

$$\varphi_{sat} = e^{-kc_f'} \tag{7.5.1:2}$$

For a NaCl saturated pore solution $\varphi = 75\%$ and at +20°C the concentration of chloride is 216 g/l or 216 kg/m^3. An estimate of k consequently is $k = 1.33 \times 10^{-3}$ m^3/kg.

7.5.2 Relative humidity and moisture content

The relative humidity in the pore system is given by the moisture content, or the degree of capillary saturation, and the concentration of chloride

$$\varphi = \varphi(w, c_f') = \varphi(s_{cap}, c_f') \tag{7.5.2:1}$$

The moisture content w or the degree of capillary saturation is the inverse of $\varphi(w)$

$$w(\varphi, c_f') = s_{cap}(\varphi, c_f') w_{cap} \tag{7.5.2:2}$$

The potential for the liquid flow φ_{eq}, the equivalent relative humidity, is only a function of the moisture content

$$\varphi_{eq} = \varphi_{eq}(w) \tag{7.5.2:3}$$

With the sorption isotherm approximated to a straight line in the upper region, a moisture binding capacity of $dw/d\varphi$ and an "offset" from $\varphi = 100\%$ due to the chloride concentration, simple relationships could be used

$$\varphi(w, c_f') = \varphi_{sat} - \frac{w_{cap} - w}{\frac{dw}{d\varphi}} \tag{7.5.2:4}$$

At low levels of relative humidity a straight line to $\varphi(w_{nsol}) = 0.11$ is used (w_{nsol} is defined in section 7.5.4). The value of φ_{eq}, is obtained from the same expression with $\varphi_{sat} = 1$.

An example of sorption isotherms for different chloride contents is shown in Figure 7.5.2:1.

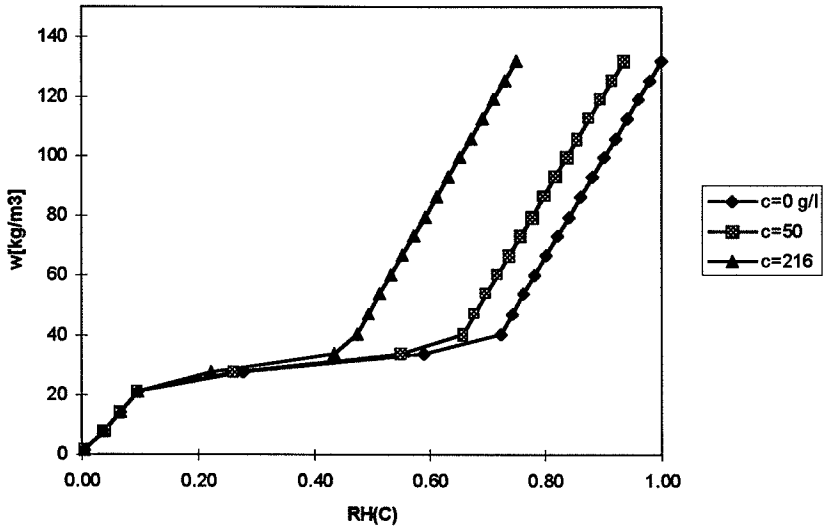

Figure 7.5.2:1. An example of sorption isotherms for different chloride contents at 20°C.

7.5.3 Vapour concentration

The vapour content at saturation is very much temperature dependent.

$$v = \varphi v_s(T) \tag{7.5.3:1}$$

where approximate values for up to +30°C could be derived from

$$v_s(T) = 10^{-3} e^{-\frac{1}{a_1}\left(a_0 - \frac{1}{T}\right)} \quad [\text{kg/m}^3] \tag{7.5.3:2}$$

with T in K. For $T > 0$°C, $a_1 = 1.976\times10^{-4}$ and $a_0 = 3.974\times10^{-3}$.

7.5.4 Chloride concentrations

The chloride in concrete is regarded as free or bound

$$c_{tot} = c_f + c_b = p_{sol} c'_f + c_b \tag{7.5.4:1}$$

where c is chloride per m^3 concrete and c' is chloride per m^3 pore solution. The "porosity" p_{sol} represents that part of the pores that contains pore water that acts as a solute. The amount of solute w_{sol} is smaller than the total moisture content w

$$w_{sol} = w - w_{nsol} \tag{7.5.4:2}$$

A possible description of the part of the moisture content w_{nsol} that does not act as a solvent is the moisture content corresponding to 11%RH, Taylor [1990].

7.5.5 Chloride binding

The amount of chloride bound to the cement paste depends on a number of factors, especially the concentration of free chloride in the pore solution, the hydroxide concentration, degree of carbonation and the temperature. If we neglect the "surface effects" due to leaching and carbonation, chloride binding is mainly a function of free chloride concentration and temperature

$$c_b(c'_f, T) \tag{7.5.5:1}$$

For a non-saturated concrete the chloride binding is unclear. It is reasonable to assume that the amount of bound chloride, more or less in the gel, depends mainly on the concentration of free chloride in the pore water filling only part of the pores, since it is the large pores that are empty in a non-saturated concrete and those pores represent only a very small part of the "contact surface" between the pore water and the gel.

The amount of bound chloride will change when:

- The total chloride content, and consequently the free chloride content, changes.
- The moisture content changes and induces changes in the free chloride content.

If the chloride binding relationship is approximated with a linear chloride binding isotherm, starting at an intersect $c_b(c'_f = 0) = c_b(0)$, and with a slope (binding capacity) of dc_b/dc'_f the free chloride concentration may be calculated from

$$\begin{cases} c'_{f,1} = 0, & c_{tot} < c_b(0) \\ c'_{f,2} = \dfrac{c_{tot} - c_b(0)}{\dfrac{w_{sol}}{\rho_w} + \dfrac{dc_b}{dc'_f}}, & c_{tot} > c_b(0) \wedge c'_f < c'_{f,s} \\ c'_{f,3} = c'_{f,s} & c'_{f,2} > c'_{f,s} \end{cases} \tag{7.5.5:2}$$

The temperature effect is not considered in this first version.

An example of a chloride binding isotherm is shown in Figure 7.5.5:1.

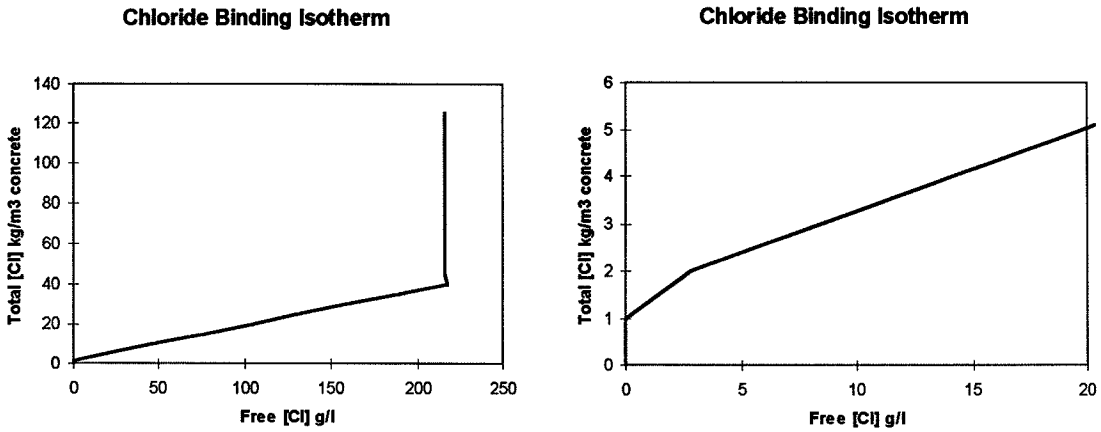

Figure 7.5.5:1. An example of a chloride binding isotherm.

7.6 Numerical solution

The equations are solved by using a Forward Finite Difference Method. To get converging solutions a limited time-step is calculated in every time-step. Usually the liquid flow decides the required time-step

$$\Delta t < \frac{(\Delta x)^2 \frac{\partial w}{\partial \varphi}}{2k_{RH}(\varphi_{eq})} \tag{7.6:1}$$

For extreme values, the required time-step can be as low as one minute!

7.6.1 Flow chart

The model calculates the moisture and chloride distributions in this way:

1. Input data for material parameters and environmental conditions are given.
2. Initial conditions for $w(x, t = 0)$ and $c(x, t = 0)$ are chosen.
3. A new time-step is estimated.
4. The boundary conditions are taken from a climate file containing $T(t)$, $\varphi(t)$ and $c'_f(t)$.
5. The temperature $T(x, t)$ is taken as $T(t)$.
6. The moisture content $w(x, t)$ and the chloride distribution $c'_f(x, t)$ gives the $\varphi(x, t)$ in each cell.
7. With $T(x, t)$, the $\varphi(x, t)$ gives the vapour content $v(x, t)$ in each cell.
8. With $w(x, t)$, the equivalent relative humidity $\varphi_{eq}(x, t)$ is calculated in each cell.
9. For the time t the flows are calculated.
10. The gradients of vapour contents $v(x, t)$ give the vapour flow.
11. The gradients of pore water pressure $P_w(x, t)$ give the liquid flow.

12. The total flow of moisture is the sum of vapour and liquid flow between the cells.
13. The net flow of moisture to each cell gives a change in moisture content $\Delta w(x, t)$ and a new moisture content $w'(x, t)$.
14. The convective flow of chloride is calculated from the liquid moisture flow and the free chloride contents. Depending on the direction of the liquid flow, the chloride content to the left or right of each cell is used.
15. The diffusion of chloride between the cells is calculated from the distribution of free chloride $c'_f(x, t)$ and the moisture distribution $w(x, t)$.
16. The net flow of chloride to each cell gives a change in total chloride content $\Delta c_{tot}(x, t)$ and a new chloride content $c_{tot}(x, t)$.
17. The new chloride content $c_{tot}(x, t)$ is divided into new contents of free $c'_f(x, t)$ and bound chloride $c_b(x, t)$ in each cell.
18. With the new moisture and chloride distributions a new time-step is estimated.
19. The calculations are repeated from point 4.
20. The calculated results are stored at certain times for display.
21. The calculations continue until a certain calculation time is reached.
22. Calculation results are copied and labelled

This procedure was run in an Excel Workbook.

7.7 Examples of results

A number of interesting calculations have been made with the convection model to examine its capability of predicting some of the experimental results, involving convection, that can be found in literature.

7.7.1 Capillary suction of a salt solution

Pure convection with a liquid flow during wetting by a salt solution has been simulated, see Figures 7.7.1:1-3. The moisture content increases at large depths very fast, but the free and bound chloride are "trapped" close to the surface. The results are very similar to the experimental results by Volkwein, cf. Nilsson et al. [1996]. The explanation is of course the binding of chloride to the gel and the "dilution" of the salt solution penetrating into a pore system that already contains a pore solution without chloride.

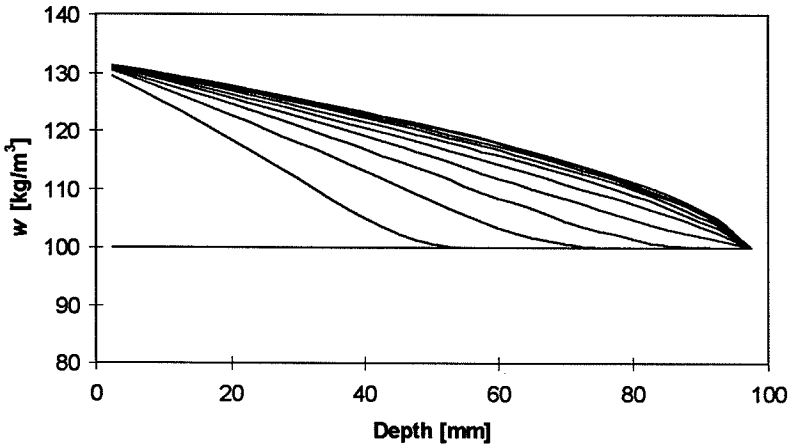

Figure 7.7.1:1. Prediction of profiles of moisture during suction of a salt solution with a concentration of 100 g Cl/l.

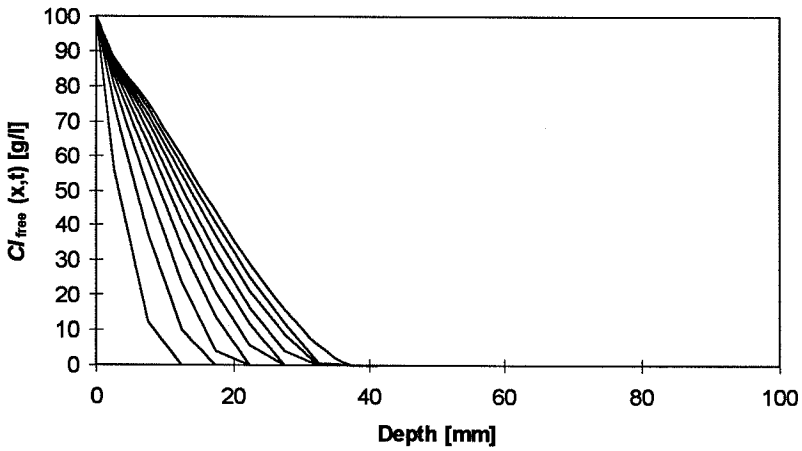

Figure 7.7.1:2. Prediction of profiles of free chloride during suction of a salt solution with a concentration of 100 g Cl/l.

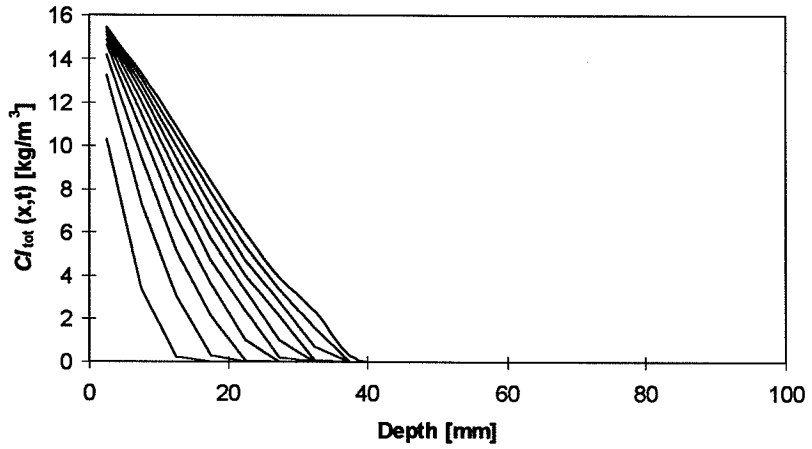

Figure 7.7.1:3. Prediction of profiles of total chloride during suction of a salt solution with a concentration of 100 g Cl/l.

7.7.2 Convection versus diffusion

For comparison the results from a calculation of pure diffusion in a solution with 100 g/l are shown in Figure 7.7.2:1. By comparing with Figure 7.7.1:3, the effect of convection of chloride is shown. The penetration depth is somewhat larger with capillary suction of a salt solution compared with the pure immersion test. The difference, however, is not very large.

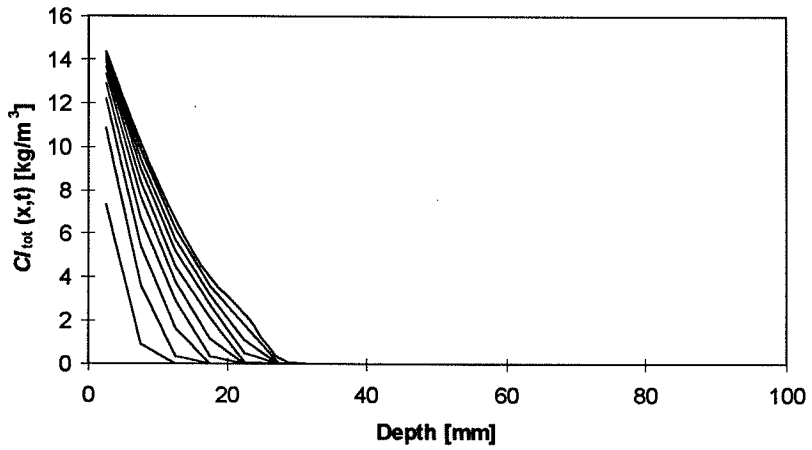

Figure 7.7.2:1. Prediction of profiles of total chloride during an immersion test in a salt solution with a concentration of 100 g Cl/l.

7.7.3 Drying of a salt solution

The predicted profiles during drying of a solution with total 20 kg Cl/m^3 concrete and a moisture content of 100 kg/m^3 at the start are shown in Figures 7.7.3:1-2.

The chloride accumulates at the evaporation front; in this case at the concrete surface and to a depth of 20-40 mm. It is obvious that the chloride is taken from the deeper parts and that the total amount of chloride remain constant during the drying process.

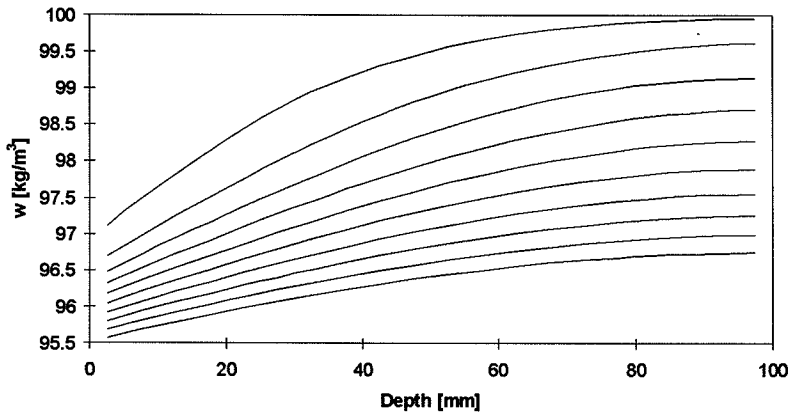

Figure 7.7.3:1. Prediction of profiles of moisture during a drying test.

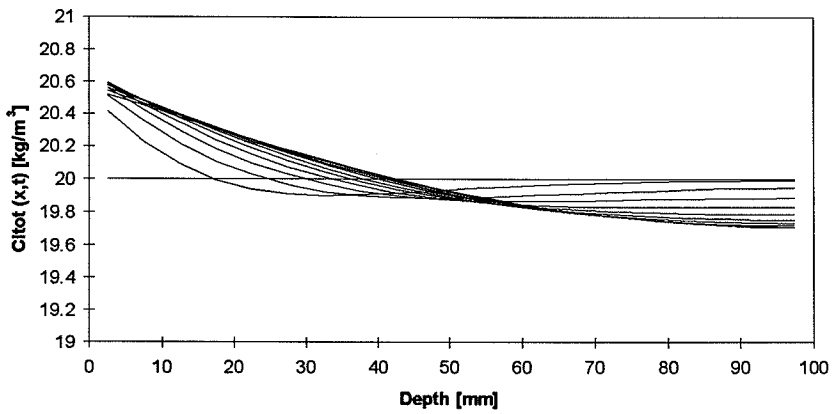

Figure 7.7.3:2. Prediction of profiles of total chloride during a drying test.

7.7.4 Steady-state flow in a humid atmosphere

Steady-state flow with a source of saturated chloride solution at the right boundary was simulated with the results in Figures 7.7.4:1-3. The drying conditions at the left surface were $\varphi(x = 0) = 70$ %.

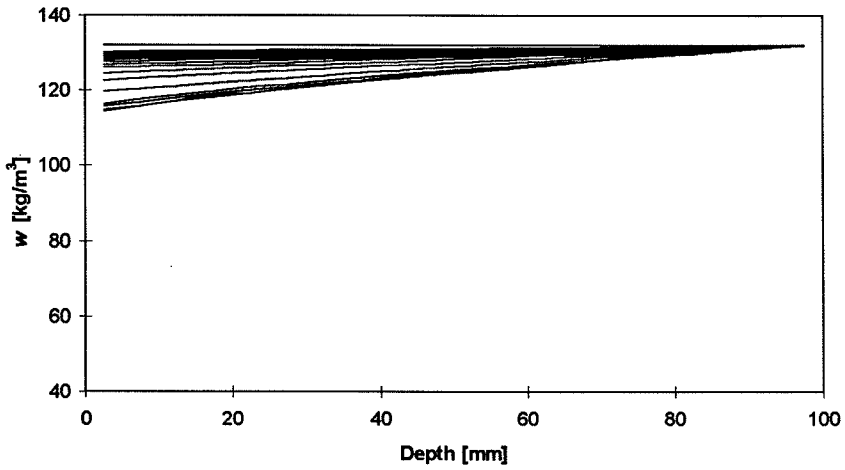

Figure 7.7.4:1. Predicted moisture profiles during a steady-state experiment with a humid left surface. The moisture content drops with time from w(x, t = 0) = 132 kg/m^3.

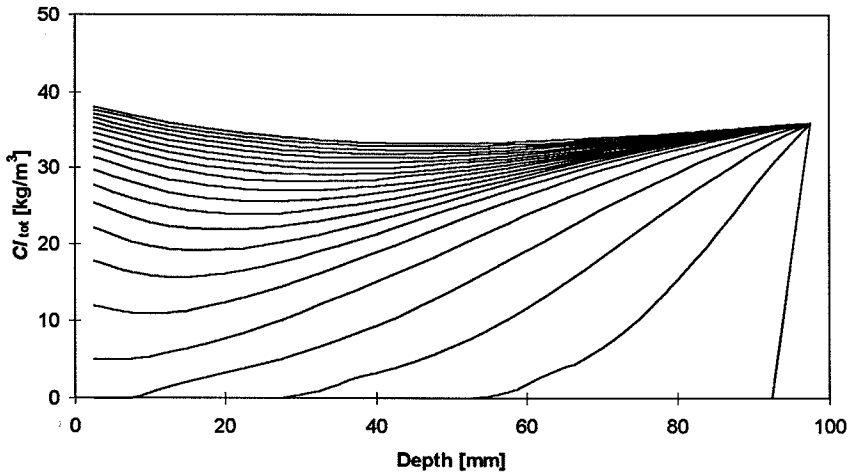

Figure 7.7.4:2. Predicted profiles of total chloride during a steady-state experiment with a humid left surface. The chloride content increases with time from c(x < L, t = 0)=0 and c(x = L, t) = 36 kg/m^3.

It seems as if the evaporation front is fairly close to the left surface and the chloride start to deposit. More and more chloride solution is transported from right to left and the chloride content increase at all depths.

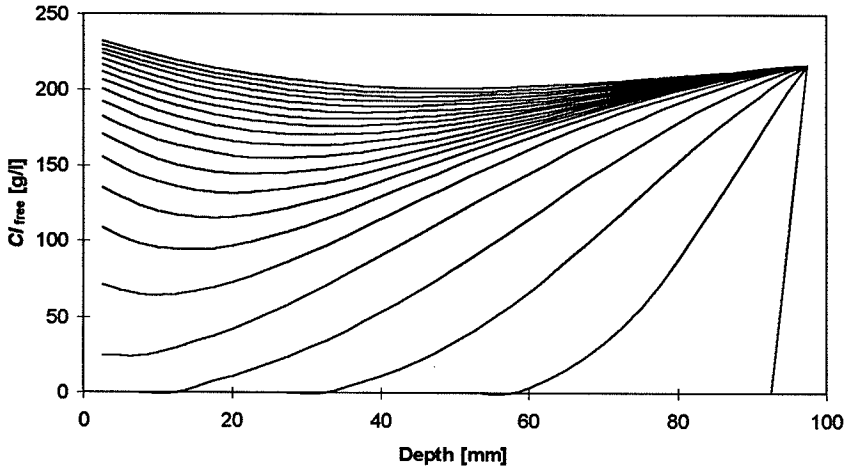

Figure 7.7.4:3. Predicted profiles of free chloride during a steady-state experiment with a humid left surface.

7.7.5 Steady-state flow in a dry atmosphere

A similar calculation as in section 7.7.4, but in a dry atmosphere, was done in the same way. The drying condition at the left surface was $\varphi(x = 0) = 40$ %. The results are shown in Figures 7.7.5:1-3.

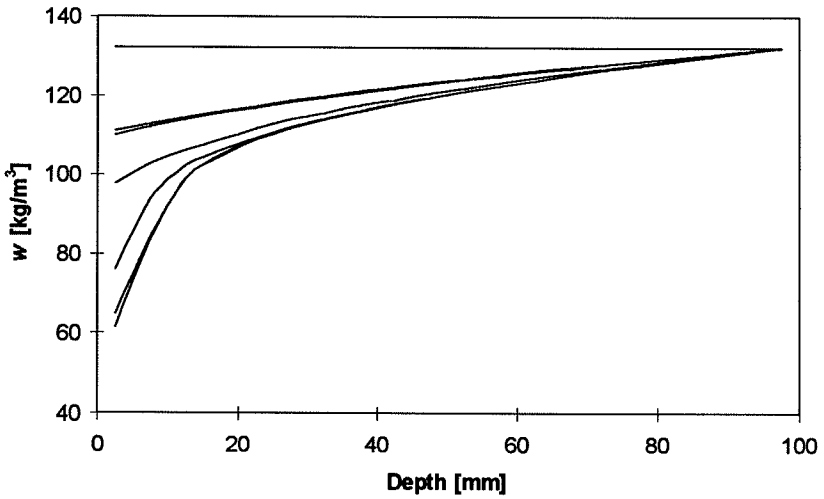

Figure 7.7.5:1. Predicted moisture profiles during a steady-state experiment with a dry left surface. The moisture content drops with time from $w(x, t = 0) = 132$ kg/m^3.

The evaporation front is deeper into the concrete in this case and the chloride deposit at a larger depth. The results are very similar to the measured chloride profiles by Tuutti [1982].

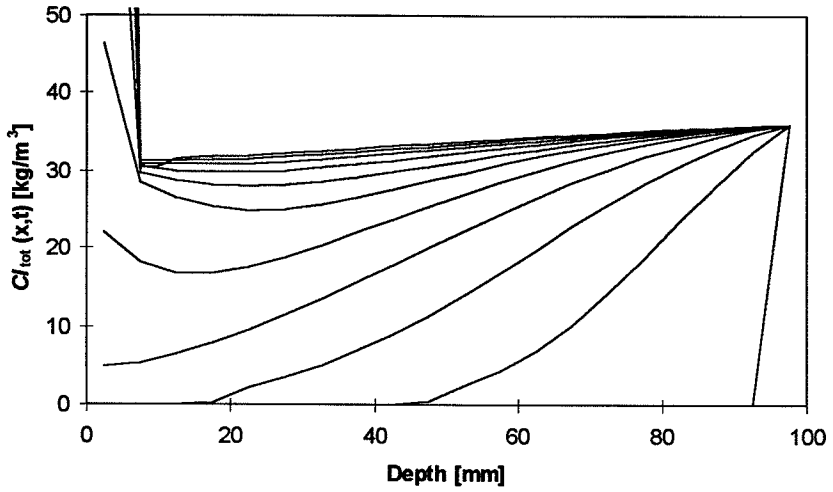

Figure 7.7.5:2. Predicted profiles of total chloride during a steady-state experiment with a dry left surface. The chloride content increases with time from c(x < L, t = 0) = 0 and c(x = L, t) = 36 kg/m^3.

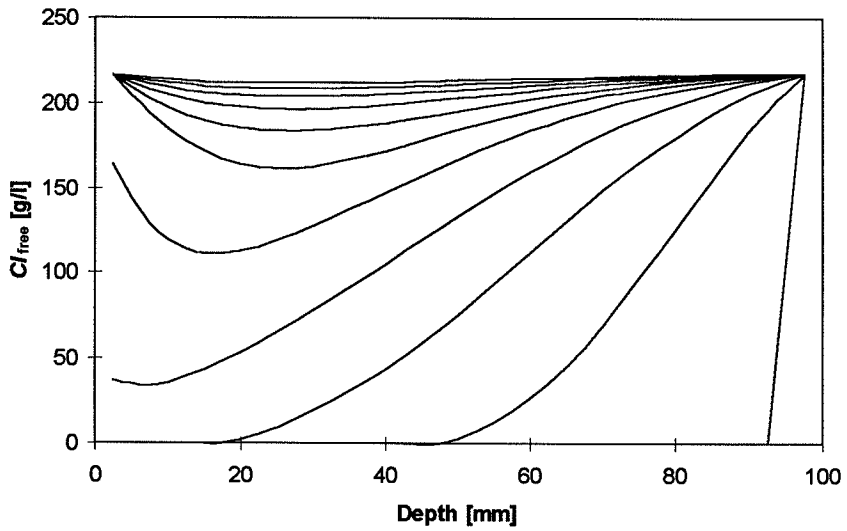

Figure 7.7.5:3. Predicted profiles of free chloride during a steady-state experiment with a dry left surface.

7.7.6 De-icing salt exposed concrete

To simulate the convection and diffusion of chloride in a concrete exposed to de-icing salt, the boundary conditions were described as in Figure 7.4:1. First wetting by a saturated salt solution, then exposed to wet conditions without salt, subsequent drying and occasional wetting by pure rain water was described to simulate a year cycle of the conditions in a bridge exposed to de-icing salts in winter time. The results are shown in a number of figures.

The predicted moisture conditions are shown in Figures 7.7.6:1-3. The initial moisture content is dried out during the first year. After that the moisture content varies during a year cycle up to a depth of some 50-70 mm.

The relative humidity has strange profiles according to the predictions. Up to a depth equal to the depth of chloride penetration, see below, the relative humidity increases with depth. This is due to the increasing concentration of chloride with depth. This is not what is observed in field conditions, Andersen [1996], but should follow from the assumptions made for the convection model. This has to be further examined.

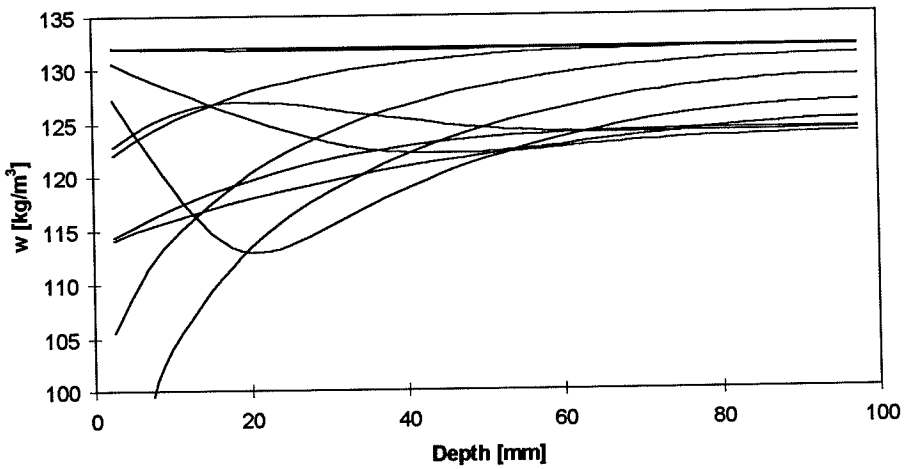

Figure 7.7.6:1. Predicted moisture profiles during the first year of a concrete structure exposed to de-icing salt.

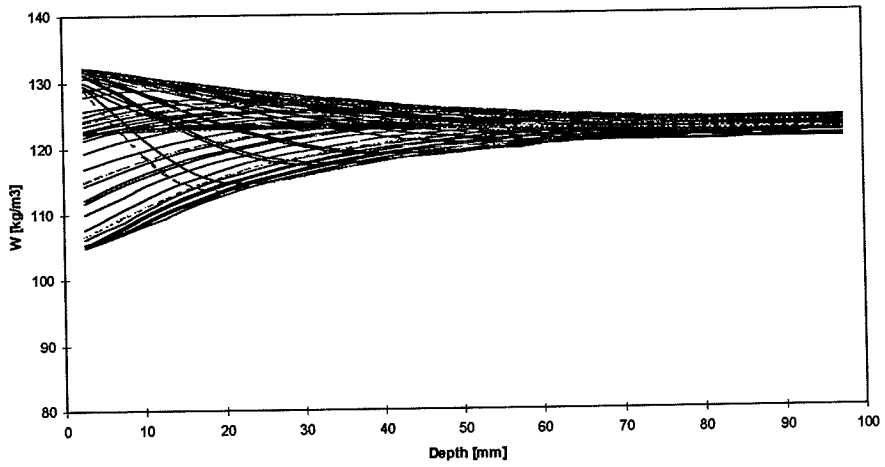

Figure 7.7.6:2. Predicted moisture profiles during three years of a concrete structure exposed to de-icing salt.

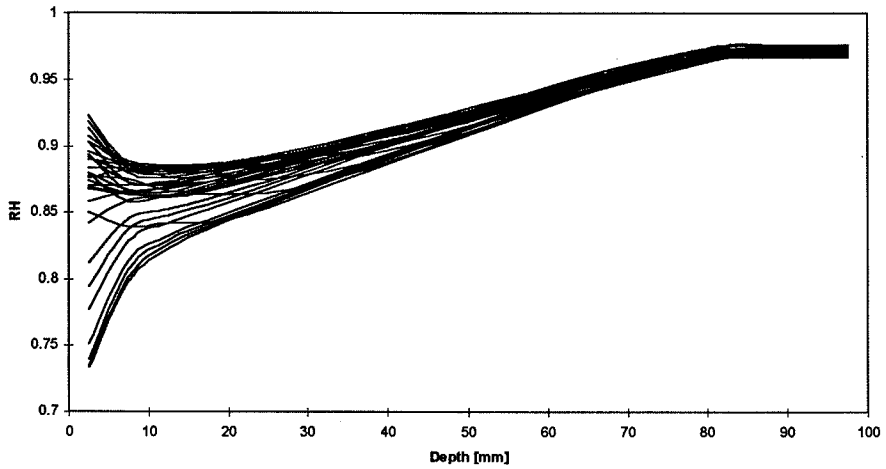

Figure 7.7.6:3. Predicted relative humidity profiles during three years of a concrete structure exposed to de-icing salt.

The predicted chloride profiles during the first two years, during the 10th year and the 40th year are shown in Figures 7.7.6:4-7. For the boundary conditions chosen in this calculation, where the concrete constantly is rather wet, chloride will penetrate deeper and deeper each year. A certain washing out effect is visible during the first and second year, but after some time it is obvious that this effect is only present very close to the surface, cf. Figures 7.7.6:5-7.

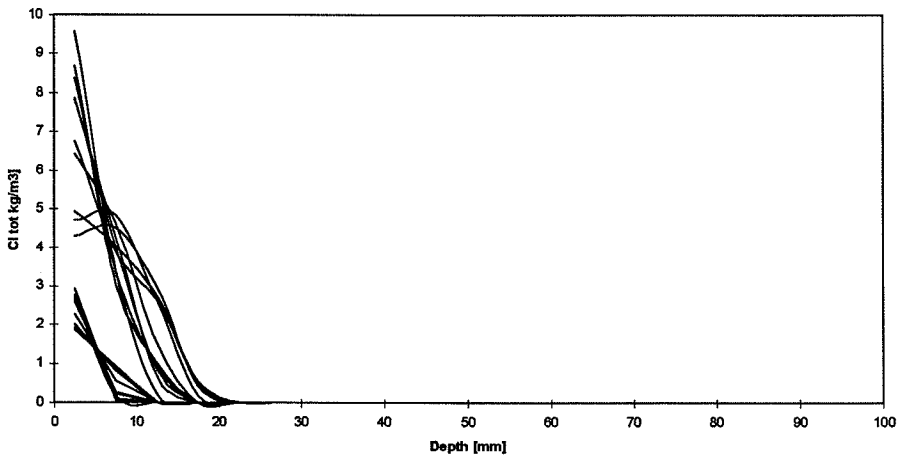

Figure 7.7.6:4. Predicted profiles of total chloride during the first two years in a concrete structure exposed to de-icing salt.

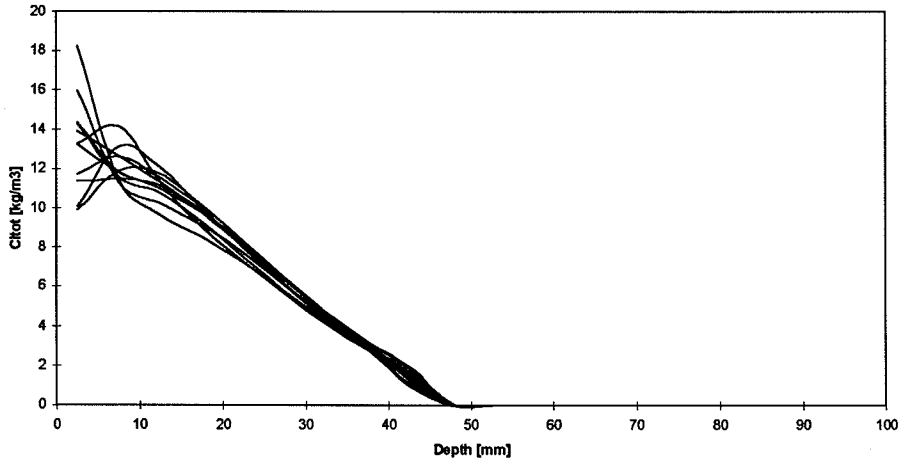

Figure 7.7.6:5. Predicted profiles of total chloride during the tenth year in a concrete structure exposed to de-icing salt.

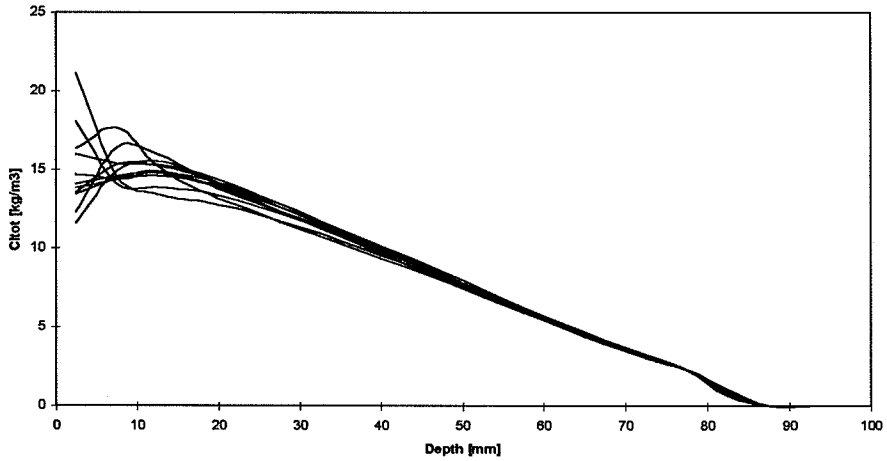

Figure 7.7.6:6. Predicted profiles of total chloride during the 40th year in a concrete structure exposed to de-icing salt.

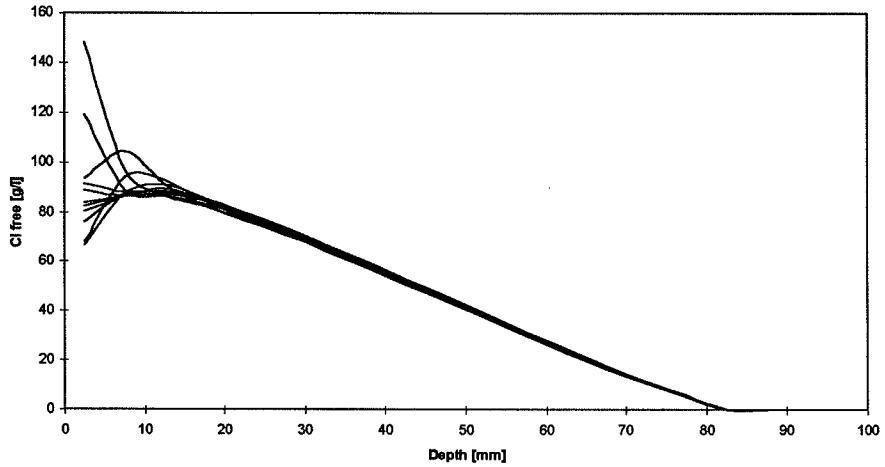

Figure 7.7.6:7. Predicted profiles of free chloride during the 40th year in a concrete structure exposed to de-icing salt.

To see the penetration process, the chloride profiles just before a series of winters are shown in Figures 7.7.6:8-9.

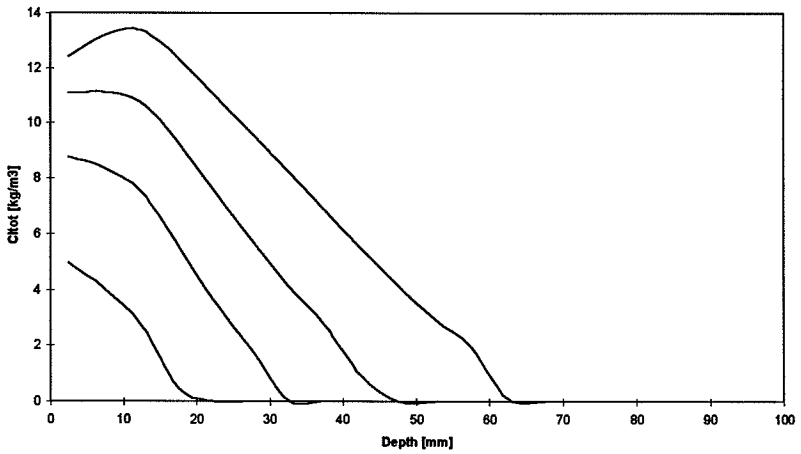

Figure 7.7.6:8. Predicted chloride profiles just before the 2nd, 5th, 10th and 20th winter.

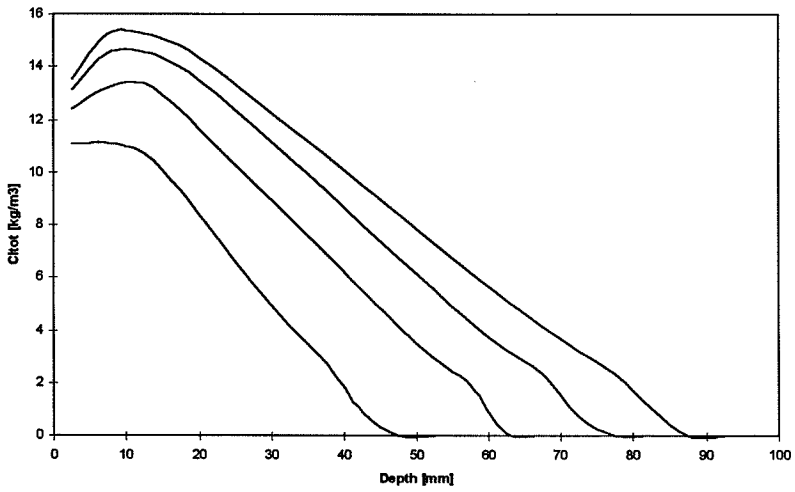

Figure 7.7.6:9. Predicted chloride profiles just before the 10th, 20th, 30th and 40th winter.

The predicted chloride profiles have very little in common with the error function solution of Fick's 2nd law. The profiles look more like straight lines and that is in contradiction with scarce field observations, Andersen [1996]. Several explanations for the deviation in the shape of the predicted profiles compared to the profiles measured in the field can be given:

- The shape of the chloride binding isotherms could have an effect on the shape of the chloride profiles.
- The possible existence of a time-dependent chloride binding may contribute to the explanation, as this was not included in the model.
- The possibly restricted connectivity of the water filled pores, in fairly dry field conditions, may be part of the explanation.

The key factor, however, seems to be the moisture conditions. The level of moisture must be predicted accurately; if not the chloride transport will be under- or over-estimated. The moisture conditions depend very much on the real environment for the particular part of the structure that is treated. Whether the concrete surface is exposed to direct splash of salt water, and direct driving rain, and for how long periods during a year cycle, will be decisive.

7.8 Conclusion

The first version of the new convection model seems to be very promising for predicting experimental results involving convection of chloride. It was demonstrated that the model is also capable of predicting the moisture and chloride profiles in concrete exposed to varying salt and moisture conditions during year cycles as for structures exposed to de-icing salts.

However, the model gives so far only qualitative results. No calibration against measured data, where material properties are available, was possible in this project. Further developments of the model and associated test methods are required if better descriptions and actual predictions should be made.

The presented model supports the findings by Andersen [1996] that the moisture conditions are the key factor for the chloride ingress in the road environment.

8 Theoretical effects of cracks on chloride penetration

Simulation of the effects of cracks perpendicular to the surface on chloride penetration into the concrete cover

8.1 Introduction

The typical size of cracks in concrete may be described as in Table 8.1:1.

Table 8.1:1. Typical sizes of cracks in concrete.

Width	< 0.01 mm	0.01 - 0.1 mm	>0.1 mm
Cause	self-desiccation hydration	shrinkage/temperature damages	mechanical loading damages
Crack depth	< 2 mm	< 50 mm	> 100 mm
Crack distance	5 - 40 mm	10 - 200 mm	30 - 200 mm

Literature information gives contradictory conclusions on the effect of cracks on chloride penetration. An additional examination is required. One important parameter is of course the size of the cracks and the source of the cracks. Micro cracks (width less than 0.01 mm) should be regarded as a natural part of (high quality) concrete and their effect is included when properties of such a concrete is measured.

Larger cracks from loading, shrinkage, temperature stresses etc. are, however, (planned or non-planned) defects in a concrete and their effect should be quantified. The effect of cracks that reach the reinforcement is discussed in Chapter 9 on chloride threshold levels and rates of corrosion. Here the geometrical effect of cracks on chloride penetration is estimated.

8.2 Calculation procedure

A 2D simulation of chloride penetration was done by using VADAU, a 2D simulation software developed by Hedberg [1989], for diffusion problems. The DDX version was used assuming the chloride binding capacity to be constant and equal to 1, i.e. solving the Fick's 2nd law of diffusion in two dimensions with a constant diffusion coefficient D.

The simulation was done on a section of concrete with a thickness L_y = 200 mm. The chloride distribution when the chloride reaches a penetration depth equal to the thickness, i.e. when the semi-infinite conditions are no longer valid, was used for the evaluation of the effect of the crack. The concentration of chloride at the exposed surface of the concrete was assumed to be 20 g/l.

The crack was simulated as a series of cells with a width of 1 mm and a depth that was varied from 20 to 40 mm. The crack intensity is defined here by the distance L_x between the cracks. In those cells defined as the crack the diffusion coefficient was varied linearly to decrease from $2 \cdot 10^{-9}$ (approximately the diffusivity of chloride in water) at the surface to $2 \cdot 10^{-12}$ m^2/s (approximately the diffusivity of chloride in

concrete) at the tip of the crack. In order to simplify the calculations the initial concentration of chloride in the water in the crack was assumed to be equal to the concentration in the sea water. This simplification may overestimate the effect of the crack.

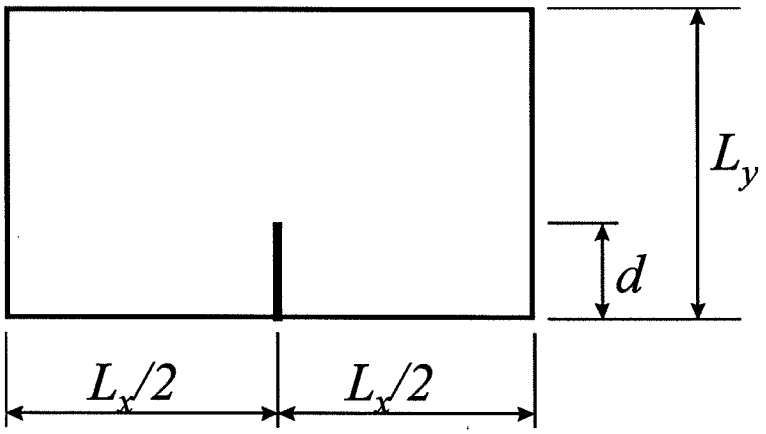

Figure 8.2:1. The geometry of the crack and its position.

The latter assumption means that the penetration of chloride through the crack itself is not considered. In this way the calculations will be on the safe side. In those cases where the penetration of chloride through the crack will be a pure diffusion process, the resistance to penetration of chloride of the crack itself could be a significant part of the penetration process. This is also where the width of the crack should have an effect, cf. Mangat & Gurusamy [1987].

8.3 Calculation results

Examples of results of the calculations are shown in Figures 8.3:1-8.3:6.

The effect of assuming a linear decreasing D or a constant D in the crack is negligible, cf. Figure 8.3:1 and Figure 8.3:2. The effect of crack depth is seen from comparing Figure 8.3:2 and Figure 8.3:3. The effect of crack intensity is seen from comparing Figure 8.3:2, Figure 8.3:4 and Figure 8.3:5. The ingress into concrete without cracks using similar parameters is seen from Figure 8.3:6.

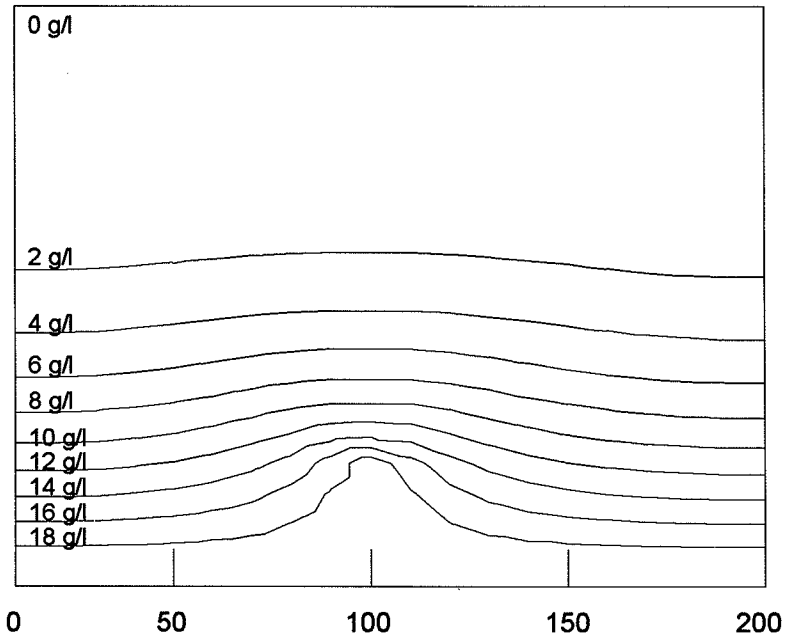

Figure 8.3:1. Chloride distribution around a crack with width 1 mm, depth 40 mm and crack intensity L_x = 200 mm: Chloride diffusion coefficient D constant through the crack. $F_0=Dt/L_y^2=11.7$.

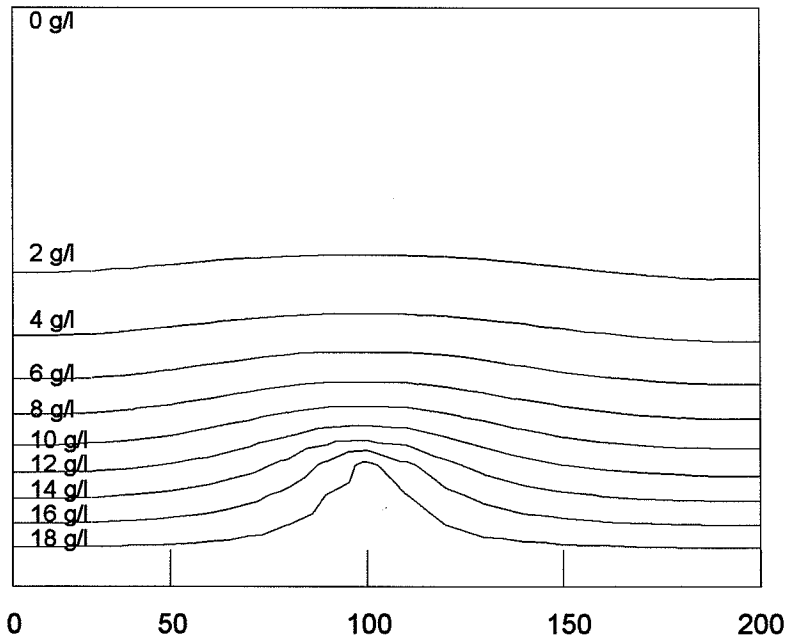

Figure 8.3:2. Chloride distribution around a crack with width 1 mm, depth 40 mm and crack intensity L_x = 200 mm: Chloride diffusion coefficient D linearly decreasing through the crack. $F_0=Dt/L_y^2=11.7$.

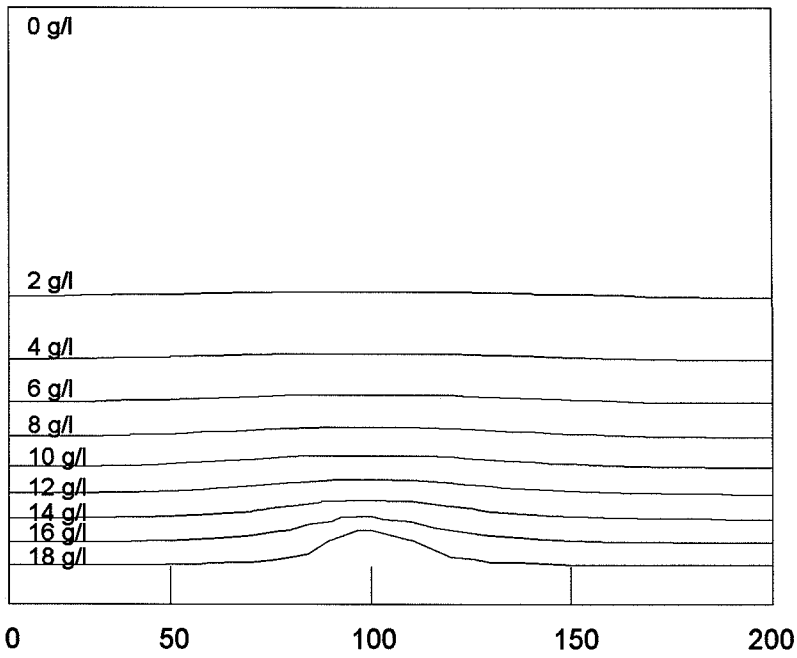

Figure 8.3:3. Chloride distribution around a crack with width 1 mm, depth 20 mm and crack intensity L_x = 200 mm: Chloride diffusion coefficient D linearly decreasing through the crack. $F_0=Dt/L_y^2=11.7$.

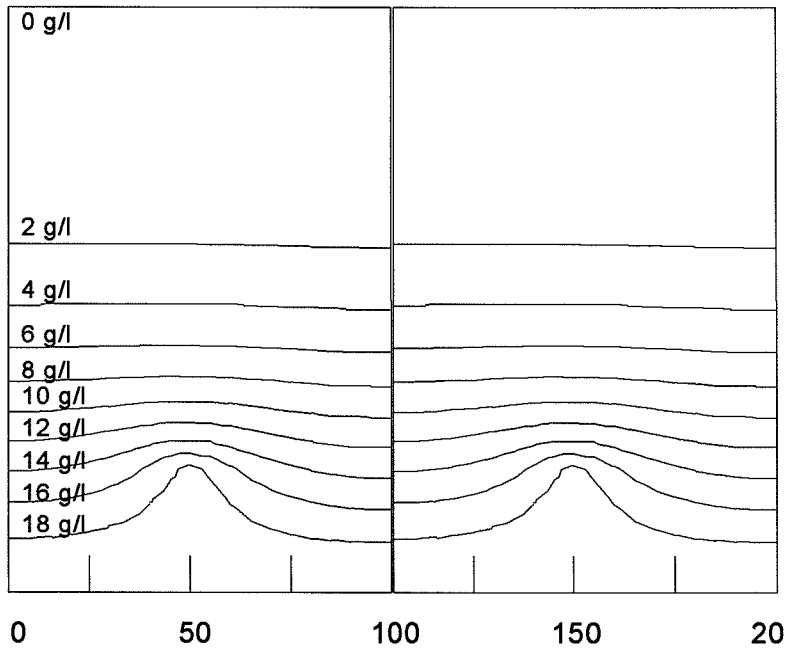

Figure 8.3:4. Chloride distribution around a crack with width 1 mm, depth 40 mm and crack intensity L_x = 100 mm: Chloride diffusion coefficient D linearly decreasing through the crack. $F_0=Dt/L_y^2=11.7$.

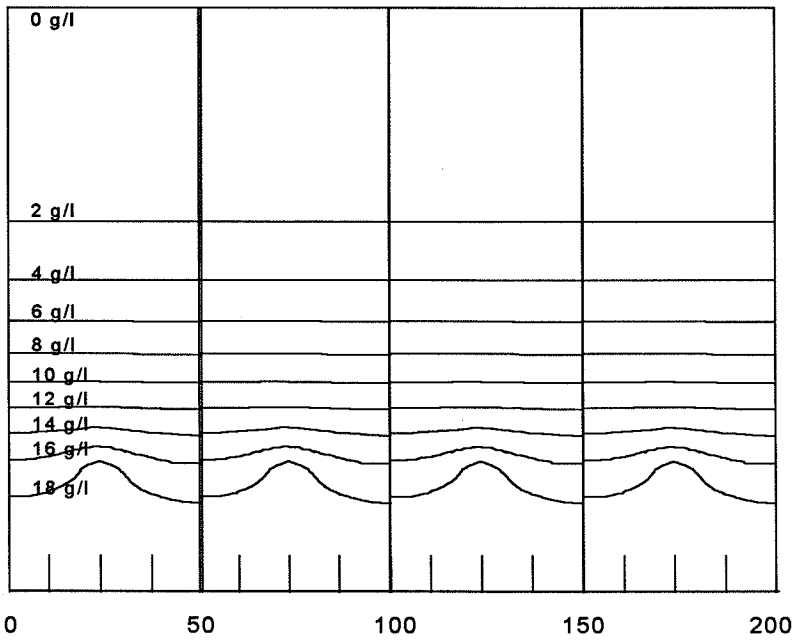

Figure 8.3:5. Chloride distribution around a crack with width 1 mm, depth 40 mm and crack intensity L_x = 50 mm: Chloride diffusion coefficient D linearly decreasing through the crack. $F_0=Dt/L_y^2=11.7$.

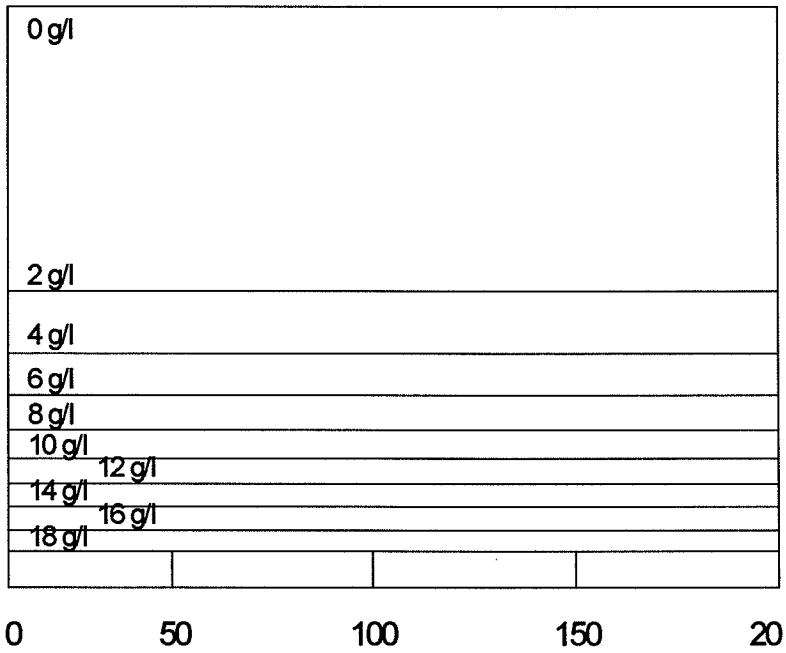

Figure 8.3:6. Chloride distribution in concrete without cracks. $F_0=Dt/L_y^2=11.7$.

8.4 Evaluation

The calculated 2D chloride distributions have been analysed to give an "equivalent cover thickness" when the cover contains cracks. This was done by comparing the calculated chloride concentrations ahead of the crack tip at a depth of 60 mm to the concentration at different depths in the uncracked case.

The depth where the concentration in the uncracked case is equal to the concentration at a depth of 60 mm ahead of the crack tip in each case, is defined as the "equivalent cover thickness".

Calculations were done for various crack depths and crack intensities. The results of the evaluation are shown in Figure 8.4:1.

It is obvious from the results that the pure geometrical effect of a crack is dominated by the depth of the crack and the spacing between cracks, the crack intensity. A single crack that goes through some 50 % of the cover does not reduce the effective cover more than some 20 %. Cracks that are deeper than some 70-80 % of the cover, however, give an effective cover that is less than half of the actual cover.

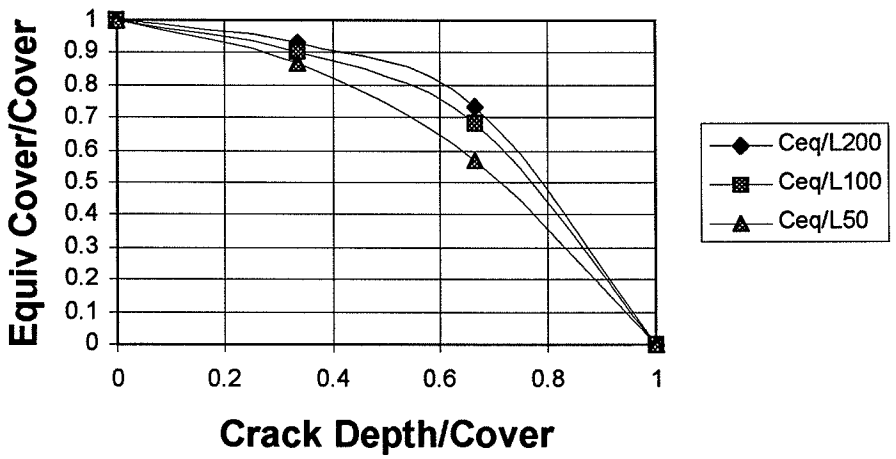

Figure 8.4:1. The "equivalent concrete cover" for cracked concrete with different crack depths and crack intensities L.

The spacing between cracks becomes important mainly when the spacing is equal to the cover thickness or smaller.

The results that are shown are for concretes with diffusion coefficients of $2 \cdot 10^{-12}$ m^2/s (63 mm^2/year). For more dense concretes a single crack will have a relatively larger effect.

8.5 Conclusion

This chapter deals only with cracks that do not reach the reinforcement and are perpendicular to the surface. The importance of cracks for chloride penetration should depend on the geometrical effect of the cracks acting as defects in the cover. The calculations show that a single crack does not significantly reduce the equivalent cover thickness until the depth of the crack is deeper than some 50 % of the actual cover, but the larger the crack intensity is, the smaller the equivalent cover thickness will be. The calculations are done for a crack where the supply of chloride is unlim-

ited. In natural exposure this is uncommon due to self-healing and blocking effects and due to effects from the environment.

Whether the cracks will contain chloride at all is of course more important. Some findings in the literature indicates that salt spray or splash do not necessarily penetrate through a crack, Relling & Sellevold [1996]. The effect of cracks on chloride penetration in different environments is obviously *not only* a geometrical effect. To be able to accept a certain degree of cracking in a particular environment, more knowledge is needed on the penetration mechanisms and the environmental conditions in and close to the cracks.

9 Effect of cracks on chloride threshold levels and corrosion rates

This Chapter outlines a descriptive model for the corrosion behaviour of the reinforcement. Special attention has to be drawn to the danger of macro cell corrosion in macro cracked marine concrete structures.

A descriptive model for the corrosion behaviour of the reinforcement is outlined, based on the more comprehensive information given in Nilsson et al. [1996]. The effect of macro cracks (>0.1 mm wide) is specially addressed.

Special attention has to be drawn to the danger of macro cell corrosion in macro cracked marine concrete structures.

The information available regarding chloride thresholds in uncracked (<0.1 mm wide cracks) concrete has been processed into suggested design values as presented in Table 10.2.6:1.

9.1 Effects of macro cracks on the initiation time

The effect of macro cracks (> 0.1 mm wide) on the initiation time is controlled by the cover size, the crack geometry, the concrete composition (mainly the resistivity and the self healing capacity) and by the local exposure conditions. As described in Nilsson et al. [1996], the crack geometry and the local exposure conditions may vary extensively, and in an uncontrolled way. The self healing capacity of concrete in a marine environment is enlarged by the interactions between sea water ions and cement hydrates. The exposure conditions are fairly constant in sea water submerged cracks without streaming water, and the measured chloride threshold levels are not as low as for macro cracked concrete exposed to wetting and drying, Figure 9.1:1.

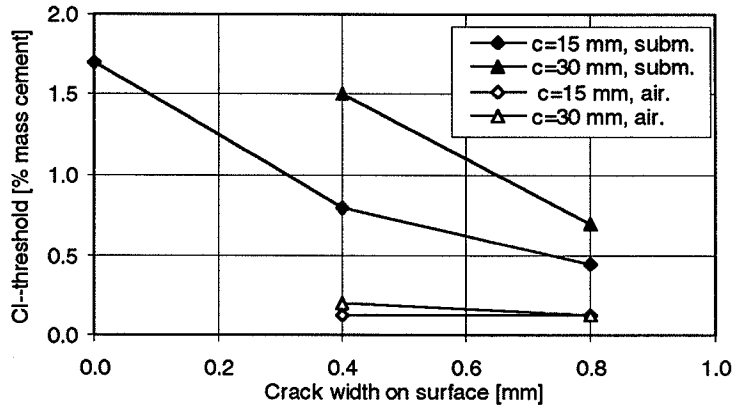

Figure 9.1:1. Chloride threshold levels for laboratory submerged or wet/dry exposed high performance concrete, w/(CE+SF) = 0.30, 15 and 30 mm cover. Pettersson and Sandberg [1996].

9.1.1 Threshold levels in cracked concrete exposed to wetting and drying

The micro environment and the corrosion properties may vary extensively in macro cracks (> 0.1 mm wide) exposed to wetting and drying. Oxygen is abundant, local carbonation is possible and chloride content may be enriched due to the wetting and drying. The chloride threshold levels reported are low and vary extensively under such conditions, from almost zero to some 25 % of the levels measured in uncracked concrete.

As a consequence of the large variations it is very difficult to predict the initiation time in macro cracked reinforced concrete exposed to wetting and drying. However, it is clear that the initiation time for cracked concrete depends on the cover thickness, but the initiation time is substantially lower as compared to uncracked concrete. On the other hand the square root tendency for the propagation rate indicates that a certain degree of corrosion could be accepted, provided that the corrosion process is not leading to any spalling and/or accelerated corrosion rates within the specified service life.

9.1.2 Threshold levels in deep submerged cracked concrete

If the concrete structure is fully submerged, i.e. no reinforcement is present in concrete exposed to the atmosphere, the chloride thresholds can be very high also for cracked concrete. The role of oxygen is important, since it controls the passive steel potential and thereby apparently the chloride threshold for pitting corrosion.

The very high chloride threshold levels in fully submerged but macro cracked concrete is probably a result of a lack of oxygen in combination with a high pH and precipitation of calcium carbonates and hydroxides in the crack. If the oxygen concentration at the reinforcement is very low, pitting corrosion cannot be initiated.

9.2 Effects of macro cracks on the propagation rate

In general, the main parameters controlling the corrosion rate in concrete exposed to the atmosphere, with a given crack pattern, are the cover thickness and the concrete resistivity. In fully submerged concrete, however, the lack of oxygen at the reinforcement will depress the corrosion rate to insignificant levels, provided that no reinforcement is in metallic connection with reinforcement in concrete exposed to the atmosphere.

9.2.1 Corrosion rates in cracked concrete exposed to wetting and drying

The corrosion propagation rate in a macro crack exposed to air decreases over time. The accumulated corrosion depth in a corrosion pit is shaped similar to a square root function, Figure 9.2.1:1 Verbetskii et al. [1989].

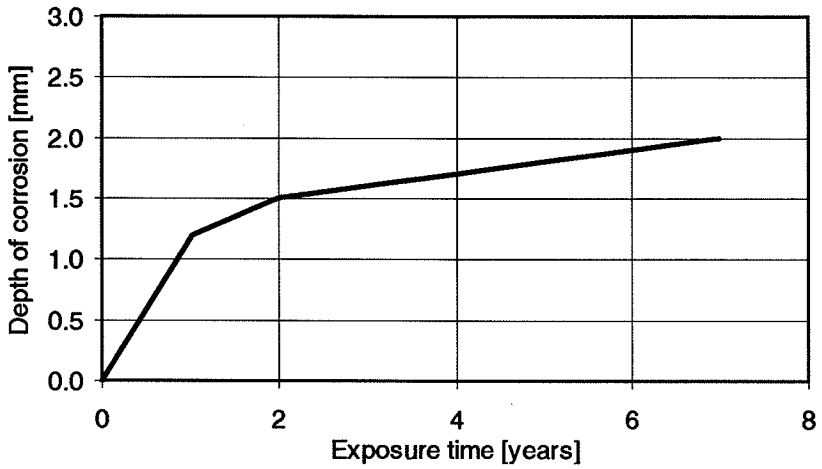

Figure 9.2.1:1. Accumulated corrosion depth as a function of time in macro cracked concrete exposed to periodic wetting by 3% NaCl and drying in laboratory exposure, Verbetskii et al. [1989].

The decreasing corrosion rate over time is mainly attributed to the clogging of cracks with corrosion products and self healing of cracks, Ewertson [1995], thereby stabilising the micro environment in the crack and inhibiting the anodic process. However, if the corrosion process leads to a spalling of the cover, the microstructure around the corrosion cell is opened, and the corrosion process is sometimes accelerated.

Naturally, the propagation rate also vary extremely upon wetting and drying on the short term. But the general square root tendency illustrated in Figure 9.2.1:1 seems to be valid in the long term for concrete exposed to air as long as the corrosion process is not leading to any spalling and/or accelerated corrosion. However, the lack of reliable models and reliable field data for the propagation period makes it very difficult to design for an allowed corrosion attack within the service life.

9.2.2 Corrosion rates in deep submerged cracked concrete

If the concrete structure is *fully submerged,* i.e. no reinforcement is present in, or in metallic contact with reinforcement in concrete exposed to the atmosphere, the propagation rate will be insignificant in a 100 years service life. This seems to be valid also in the presence of macro cracks, provided that the reinforcement is properly embedded in concrete. Repassivation of the reinforcement in cracks as wide as 1-2 mm seems to occur in fully submerged high performance concrete as a consequence of self healing and realkalisation of the crack, Pettersson [1996a]. At very low potential where pitting corrosion cannot occur, a general but extremely slow type of corrosion can be initiated (also in uncracked concrete) if the oxygen level is too low to maintain passivity. However, this type of corrosion is so slow that it does not have any practical consequences within a hundred years of service of normal structures.

9.3 Macro cell corrosion

The macro cell type of corrosion is the most rapid corrosion attack on steel in concrete. It occurs most rapidly in cracks reaching the reinforcement in wet concrete exposed to

chloride. However, the macro cell corrosion only occurs if the reinforcement in the wet concrete is in metallic connection with reinforcement in concrete exposed to the atmosphere, for instance if reinforcement in the atmospheric zone is in metallic contact with the reinforcement in the submerged zone.

However, macro cell corrosion in wet concrete of good quality can fairly easily be prevented by a simple cathodic protection system, provided that all reinforcement has metallic connection to the system.

9.3.1 Initiation times in a macro corrosion cell

Cracks in water saturated concrete, even a few meters below the water level, may initiate macro cell pitting corrosion, if some reinforcement is in metallic contact with reinforcement in concrete exposed to the atmosphere. The initiation period can be zero, if the cracks facilitate rapid chloride transport to the naked steel inside a macro crack.

9.3.2 Corrosion rates in a macro corrosion cell

The macro cell corrosion rate can be extremely high also in silica fume - fly ash concrete with a very low *w/b* ratio, several mm/year pit growth can be found. The cover size and the concrete resistivity seems to be the most important factors controlling the macro cell corrosion rate.

The macro cell corrosion rate is accelerated by the large potential variations between the reinforcement in the relatively dry and oxygen rich concrete just above the splash zone, and the reinforcement in the wet concrete. The size of the macro cell is controlled by the concrete resistivity, which is relatively low in wet, chloride rich concrete. As a consequence, cracks in submerged concrete can initiate rapid corrosion down to several meters below the water level. The phenomenon is illustrated in Figure 9.3.2:1.

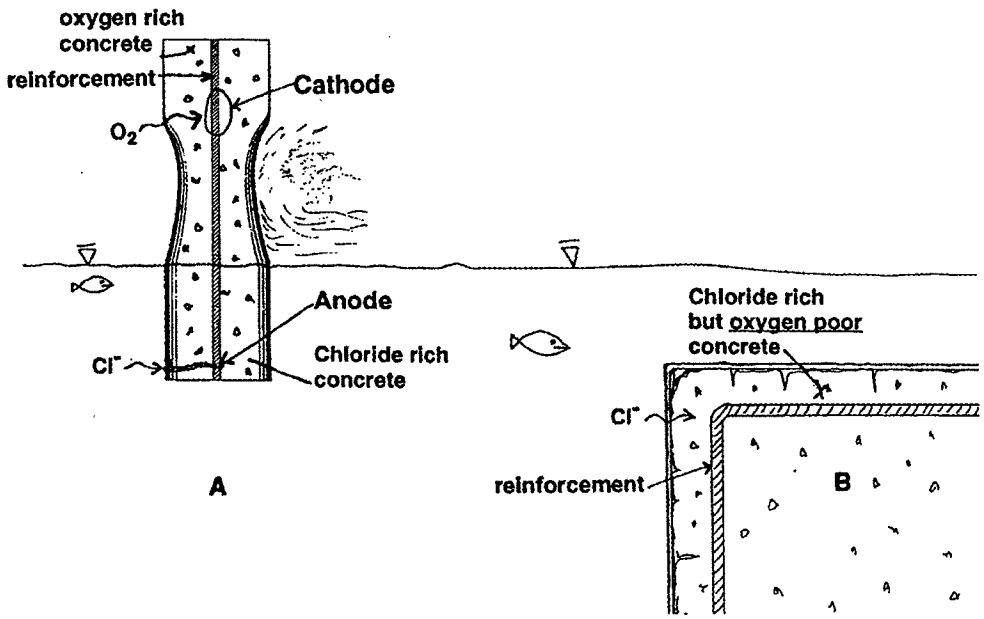

Figure 9.3.2:1. ***A:*** *Macro cell corrosion in partly submerged marine concrete.* ***B:*** *Insignificant corrosion attack in fully submerged concrete.*

9.3.3 Prevention of macro cell corrosion in marine concrete

Macro cell corrosion of reinforcement properly embedded in good quality concrete exposed in a marine environment can be prevented fairly easily at a low cost, by the installation of a sacrificial anode system. The system requires that all reinforcement have metallic connection to the anode, and that the concrete is wet enough to allow electrons to flow from the corroding anode through the concrete to the protected reinforcement. Sacrificial anodes are easy to install and do not normally require any maintenance except for the replacing of anodes.

PART B. DATA

Part B covers Chapters 10-12, describing available data on chloride threshold levels and analysis and compilation of environmental data from marine and road structures.

10 Corrosion data for design in a saline environment

10.1 Introduction

Unfortunately no simple way exists for the translation of short term corrosion data from the laboratory, or even short term data from field exposure, into values that can describe the long term behaviour of a field exposed structure.

Chloride threshold levels and active corrosion rates depend strongly on the cover thickness, for a given concrete quality exposed in a given set of exposure conditions. Therefore it is not possible to obtain quantitative corrosion data from direct measurements on high performance concrete with thick covers, because of the very long initiation period required.

10.2 Chloride threshold levels

10.2.1 Evaluation of published chloride threshold levels

Modern concrete structures exposed in a severe environment typically have a low water to binder ratio (often less than $w/b = 0.40$) and a thick specified cover (often more than 45 mm). These measures does not only increase the penetration time for the chloride to reach the steel surface, they also minimise moisture and temperature variations at the depth of the reinforcement, thereby increasing the chloride threshold.

Unfortunately field exposure tests with such thick covers would be extremely time consuming, before any chloride thresholds could be evaluated. As a consequence, chloride thresholds have been estimated in basically 4 different ways of testing, none of them being capable alone to simulate the field conditions in a modern structure:

A) Field testing of modern low *w/b* ratio laboratory cast concrete specimen, with small covers (normally in the range 10-20 mm) - *missing the effects of cover and of variable compaction in practise.*

B) Laboratory testing of modern low *w/b* ratio concrete, sometimes with the environmental impact simulated by potentiostatically controlled steel potentials. - *missing the effects of cover and of variable compaction, and usually also the effect of a varying microclimate and of leaching of alkali hydroxide.*

C) Field studies of existing good quality old structures, with covers > 30 mm but with higher *w/b* ratios (typically > 0.5) - *missing the effect of a low w/b ratio and the effect of new binders.*

D) Laboratory or field testing of concrete with cast-in chloride, thereby allowing for the use of low *w/b* ratio concrete and a thick cover - *missing the effect of steel passivation in chloride free concrete.*

Procedure D) is considered to be the most erroneous one, since the presence of cast in chloride decrease the ability of the cement paste to passivate the steel. Furthermore, the concrete porosity and the composition of some of the cement hydrates are altered if cast-in chloride are present during most of the curing.

Results from procedure A) - C) will all give some erroneous conclusions if not evaluated with care. No procedure yet exists which has been proven to be scientifically correct for the evaluation of long term threshold levels. Therefore, an engineering approach has been used as shown by the following examples:

Example 1

OPC Concrete with *w/b* = 0.50 exposed in a marine splash zone, reported results on chloride threshold levels by weight of cement, according to procedure A-C):
A) 0.6-1.9 % Cl. Thomas [1995], Pettersson [1996b].
B) 1.1-2.7 % Cl. Arup [1996], Breit [1994].
C) 0.3-1.4 % Cl. Henriksen [1993], Lukas [1985]. Vassie [1984].

Chloride threshold levels < 0.4 % Cl reported from existing structures (procedure C) are generally associated with failure to comply with required cover, or associated with large compaction voids, a high w/c ratio, and similar major defects. On the other hand, threshold levels from "macro defect free" specimens exposed in the laboratory at constant exposure conditions seems to indicate far too optimistic threshold levels for a dynamic exposure zone such as the splash zone. The threshold levels obtained by field exposure of laboratory cast specimens seems to be the most suitable values for describing chloride threshold in high performance concrete which is cast and placed properly. Chloride thresholds according to procedure A should be on the safe side, since they do not take the stabilising effect of a thicker cover into account.

Example 2

OPC Concrete with *w/b* = 0.50 exposed in a marine submerged zone, reported results on chloride threshold levels by weight of cement, according to procedure A-C):
A) 1.5-2.0 % Cl. Pettersson [1996b].
B) 1.6-2.5 % Cl. Arup [1996], Breit [1994].
C) > 2.0 % Cl. Sandberg [1995], Pettersson [1996b].

The chloride threshold levels found in submerged concrete with procedure A-C seems to vary less as compared to the thresholds in the splash zone. This is probably because of the stable and relatively similar exposure conditions. The lower values according to procedure A are probably a result of smaller cover and of hydroxide leaching in the field exposure test. Therefore these values should be on the safe side.

10.2.2 Compilation of chloride threshold levels

Some measured ranges of chloride threshold levels (black steel) in macro crack free concrete or mortar in various exposure regimes have been compiled and analysed in an excellent review by Glass and Buenfeld [1995], as shown in Table 10.2.2:1. Some additional chloride threshold levels have been reported as shown in Table 10.2.2:2

Table 10.2.2:1. Measured ranges of chloride threshold levels (black steel) in macro crack free concrete in various exposure regimes, Glass & Buenfeld [1995].

Total Chloride %wt. cement.	Free Chloride Mole/l	[Cl] / [OH]	Exposure Type	Reference
0.17 - 1.4			Field	Stratful et al. [1975]
0.2 - 1.5			Field	Vassie [1984]
0.25			Field	West & Hime [1985]
0.25 - 0.5			Laboratory	Elsener & Böhni [1986]
0.3 - 0.7			Field	Henriksen [1993]
0.4			Outdoors	Bamforth & Chapman-Andrews [1994]
0.4 - 1.6			Laboratory	Hansson & Sørensen [1990]
0.5 - 2			Laboratory	Schiessl & Raupach [1990]
0.5			Outdoors	Thomas et al. [1990]
0.5 - 1.4			Laboratory	Tuutti [1993]
0.6			Laboratory	Locke & Siman [1980]
1.6 - 2.5		3 - 20	Laboratory	Lambert et al. [1991]
1.8 - 2.2			Field	Lukas [1985]
	0.14 - 1.8	2.5 - 6	Laboratory	Pettersson [1993]
		0.26 - 0.8	Laboratory	Goni & Andrade [1990]
		0.3	Laboratory	Diamond [1986]
		0.6	Laboratory	Hausmann [1967]
		1 - 40	Laboratory	Yonezawa et al. [1988]

Table 10.2.2:2. Additional chloride threshold levels (black steel) in macro crack free concrete in various marine or laboratory exposure regimes, Pettersson [1996b], Pettersson and Sandberg [1996], Sandberg [1995], Arup [1996], Thomas [1995] and by Breit [1994].

	Submerged zone C_{cr} - %Cl of cement		Splash zone C_{cr} - %Cl of cement		Atmospheric zone C_{cr} - %Cl of cement	
Concrete type	Range	Procedure	Range	Procedure	Range	Procedure
w/b = 0.50						
100 % CEM I	1.5-2.0	A	0.6-1.9	A		
100 % CEM I	1.6-2.5	B	1.2-2.7	B	1.5-2.2	B
100 % CEM I	>2.0	C	0.3-1.4	C		
5 % SF	1.0-1.9	A				
5 % SF	0.8-2.2	B				
20 % FA			0.3-0.8	C		
w/b = 0.40						
100 % CEM I	>2.0	A	0.9-2.2	A		
100 % CEM I	>2,2	B				
5 % SF	>1.5	A				
w/b = 0.30						
100% CEM I	>2.2	A	>1.5	A		
5% SF	>1.6	A	>1.0	A		
20 % FA	1.4	A	0.7	A		

10.2.3 The effect of the concrete moisture state

The effect of relative humidity on the chloride threshold level in laboratory exposed mortars is shown in Figure 10.2.3:1, as presented by Pettersson [1996b].

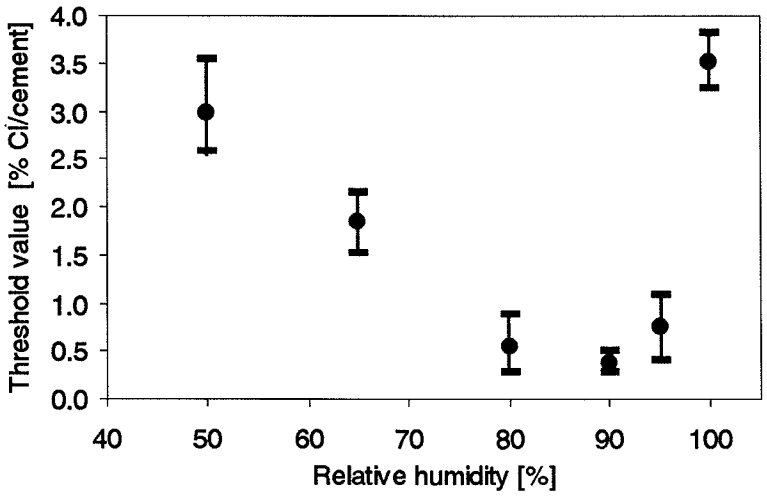

Figure 10.2.3:1. The effect of relative humidity on the chloride threshold level in laboratory exposed mortars, w/c ratio = 0.50, Pettersson [1996b].

10.2.4 The effect of water to binder ratio

The effect of water to binder ratio on the chloride threshold was illustrated by Pettersson and Sandberg [1996] as shown in Figure 10.2.4:1.

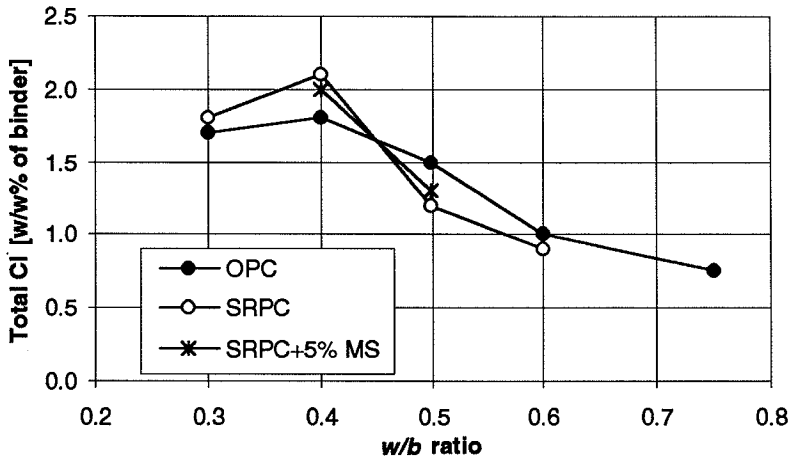

Figure 10.2.4:1. Chloride threshold levels measured on submerged concrete or mortar. Experimental results. Cover = 15 to 20 mm. Pettersson and Sandberg [1996].

10.2.5 The effect of mineral admixtures in concrete

Mineral admixtures have been found to decrease the chloride threshold level, as illustrated by Thomas [1996] for fly ash exposed in a marine splash zone, Figure 10.2.5:1. Similar results have been reported for the effect of fly ash and silica fume by Pettersson [1993], [1996b].

Note that several investigations have indicated a very positive and decreasing effect of mineral admixtures on the corrosion rate. These findings are in most cases not related to direct studies of the chloride threshold, rather obtained from studies of the corrosion behaviour in the active state. The positive effect of mineral admixtures on the corrosion rate is attributed to the increase in concrete resistivity.

The negative effect of mineral admixtures on the chloride threshold level is attributed to the decrease in alkalinity of the concrete pore solution, and to the decrease in calcium hydroxide at the steel-concrete interface, Sandberg [1995].

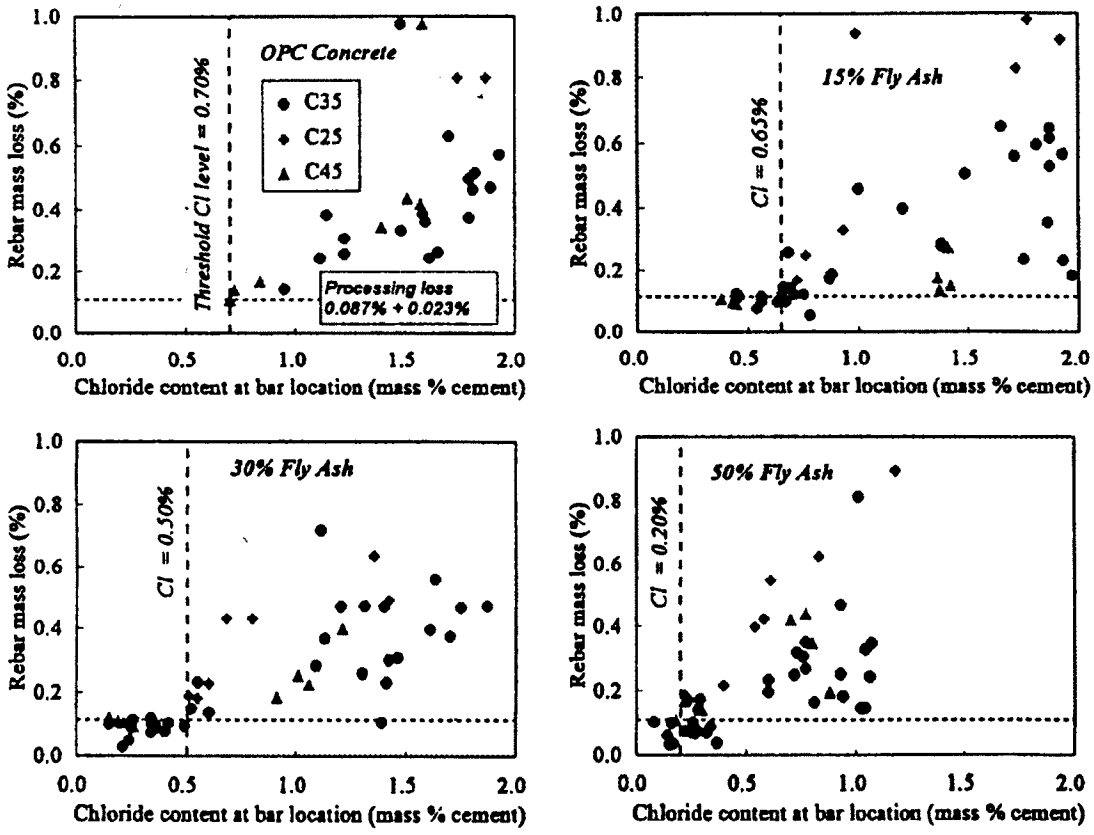

Figure 10.2.5:1. Chloride threshold levels and corrosion rates for OPC and fly ash concrete exposed in a marine splash zone in Canada, Thomas [1996].

10.2.6 The development of chloride threshold levels for design purposes

The chloride threshold levels presented in Table 10.2.2:2 and Figures 10.2.4:1 and 10.2.5:1 indicate that the chloride threshold level tend to decrease with the incorporation of mineral admixtures, and with an increasing *w/c* ratio. This behaviour is attrib-

uted to the decrease in the pH of the concrete pore solution caused by the incorporation of mineral admixtures, and by the diluting effect of an increasing *w/c* ratio, Sandberg [1995] and Pettersson [1996b].

The threshold levels given in Table 10.2.2:1 are unfortunately presented in several different ways and sometimes lacking relevant information, which makes it very difficult to evaluate the results in a statistically correct way for design purpose. Therefore, a conservative engineering approach has been used as illustrated in the previous examples 1 and 2, to establish chloride threshold levels for design purpose as shown in Table 10.2.6:1. The relative differences in threshold levels between OPC and FA-concrete, between OPC and SF-concrete, and between OPC concrete of various *w/c* ratio, as found by Thomas [1996] and Pettersson [1996b] respectively, has been maintained in the development of Table 10.2.6:1.

Table 10.2.6:1. Suggested design values for chloride threshold levels (black steel) in various Nordic exposure zones.*

Concrete type	**submerged zone** C_{cr} %Cl of CE	**marine splash zone** C_{cr} %Cl of CE	**de-icing salt splash zone** C_{cr} %Cl of CE	**atmospheric zone marine/de-icing** C_{cr} %Cl of CE
w/b 0.50				
100 % CEM I	*1.5 %*	*0.6 %*	*0.4 %*	*0.6 %*
5 % SF	*1.0 %*	*0.4 %*	*0.3 %*	*0.4 %*
10 % SF	*0.6 %*	*0.2 %*	*0.2 %*	*0.2 %*
20 % FA	*0.7 %*	*0.3 %*	*0.2 %*	*0.3%*
w/b 0.40				
100 % CEM I	*2.0 %*	*0.8 %*	*0.6 %*	*0.8 %*
5 % SF	*1.5 %*	*0.5 %*	*0.4 %*	*0.5 %*
10 % SF	*1.0 %*	*0.3 %*	*0.2 %*	*0.3 %*
20 % FA	*1.2 %*	*0.4 %*	*0.3 %*	*0.4 %*
w/b 0.30				
100% CEM I	*2.2 %*	*1.0 %*	*0.8 %*	*1.0%*
5% SF	*1.6 %*	*0.6 %*	*0.5 %*	*0.6 %*
10% SF	*1.2 %*	*0.4 %*	*0.3 %*	*0.4 %*
20 % FA	*1.4 %*	*0.5 %*	*0.4 %*	*0.5 %*

*Chloride threshold levels vary extensively in field exposed concrete exposed to the air, as a consequence of the varying micro climate at the steel surface. As a consequence the chloride threshold level depends on the cover thickness and on the physical bonding between concrete and reinforcement. The chloride threshold levels are only valid for "macro crack free" concrete with a maximum crack width of 0.1 mm and a minimum cover of 25 mm. The data are not valid for calculations of the initiation time in cracked concrete with crack widths > 0.1 mm.

11 The road environment

Environmental data for road structures are scarce. What is actually available and what can be concluded from them?

11.1 Introduction

The conditions in the road environment are summarised in Nilsson et al. [1996]. The distribution of chloride (concentrations at different depths) is a function of the environmental conditions, the design of the structure and the material properties. The mechanisms of chloride transport and binding involved are complicated and usually combined in a complicated way, cf. Chapter 7.

The transport and distribution of chloride in a concrete structure is very much a function of the environmental conditions, mainly the duration of the contact and the concentration of the solutions in contact with the concrete surface. The conditions are quite different in different exposure situations.

Salt water can be sucked into the concrete surface. Rain water washes the surface free from chloride and may remove some. Evaporation increases the chloride concentration. Chloride move inwards and outwards due to moisture flow and ion diffusion.

The conditions are different at different heights from the road level. A maximum chloride content may be found at a height where salt water is frequently supplied to the surface but where the surface intermittently dries out.

Bridges and road structures that are exposed to de-icing salts have boundary conditions that vary extensively with time. In wintertime parts of the structure are exposed to saturated salt solutions that are rapidly diluted as the ice and snow melts. This exposure can be repeated frequently, sometimes once a day. Rain water washes the surfaces and move salt water to drains and/or other parts of the structure.

Salt water penetrates cracks and joints. Consequently, the occurrence and the effect of defects must be considered in the evaluation of the behaviour of a structure. These effects are described in Chapter 8 and 9.

The following Section will isolate and describe decisive environmental parameters for RC structures in the road environment.

11.2 The meteorological environment

Statistical data can be obtained from The Danish Meteorological Institute. Table 11.2:1 contains some data from Copenhagen as an example of what type of environmental data is available. More detailed data are also available but it will require some processing to be useful for this purpose. Frequent combinations of wind speed, wind direction and rain intensity are useful information for this purpose.

Table 11.2:1. Meteorological data from Copenhagen, The Danish Meteorological Institute [1994].

	Jan	Feb	Mar	Apr	May	Jun	Jul	Aug	Sep	Oct	Nov	Dec
T_{mean}	0	0	2	7	12	16	18	17	14	9	5	3
T_{max}	2	2	5	10	16	19	22	21	18	12	7	3
T_{min}	-2	-3	-1	4	8	11	14	14	11	7	3	1
Rain (mm)	49	39	32	38	40	47	71	66	62	59	48	49
Rain (days)	17	13	12	13	11	13	14	14	15	16	16	17
Sun (hours)	36	55	118	161	245	245	239	207	157	87	34	19
RH (%)	87	85	83	76	68	68	71	74	78	83	87	88
Wind direction	SW	W	W	W	W	W	W	W	W	SW	SW	SW
Wind(m/s)	4	3	3	3	3	3	3	3	3	3	4	4
Days with frost	20	19	16	4	<1	0	0	0	0	1	4	12

11.2.1 Rain

It rains statistically 11 to 17 days each month in Copenhagen.

11.2.2 Wind

The wind direction in the Copenhagen area is SW to W most of the time and with a moderate wind speed.

11.2.3 Sea salt exposure

The sea salt exposure is a function of the distance to the sea and the frequency of higher wind speeds. Sea salt exposure could be relatively high close to the coastline even at moderate wind speeds. The sea salt exposed area reaches up to a distance of 10 km, and in high wind forces the salt could be carried even longer distance from the coast line. One single storm could be responsible for large part of the annual chloride depositions. According to Gustafsson [1995] typical values from the Swedish west coast indicates a deposition of sea salt around 100 g/(m^2year) close to the coastal line.

11.2.4 Radiation

Radiation give a major contribution to the energy balance of surfaces. The radiation is traditionally divided into two components: Short wave radiation from the sun and long wave radiation which have origin in "black body" radiation from surfaces and long wave transparent volumes. Long wave radiation are a function of surface temperature end emission properties.

The long-wave radiation exchange with the sky lowers the temperature in night time on horizontal surfaces. To predict the energy balance of structures, information on the cloudiness is needed. Bridge columns are often covered by the bridge deck and are therefore protected both from driving rain and long wave radiation exchange with sky, the so called sky temperature are normally several degrees lower than the ambient

temperature. But the columns still absorbs the short-wave solar radiation from the low standing sun. Such parts of a bridge could therefore be warmer than the surrounding air. This can explain the low relative humidity measured in columns under Danish road bridges by Andersen [1996]. The bridge deck is extremely exposed to radiation. Both short-wave radiation from the sun and to long-wave radiation towards a clear sky. That lead to extreme variations in surface temperature over a 24 h period every cloud-free day of the year.

11.3 The artificial environment

The environment can change locally due to activities on the road. A local climate and environmental loads on the area close to the road could be expressed. In this Section information is gathered on the de-icing salts in general, exhaust gases, water and the movement of de-icing salts from the road by car tires and by the air drag from moving vehicles.

11.3.1 De-icing salts

When the temperature drops below 0°C or if its raining under cold rain, de-icing salts (NaCl) are sprayed on the road as a NaCl solution or as dry salt. Sometimes de-icing salts are applied in the beginning of a snow period. Salting are mostly performed in night time or in the early morning hours. In the Nordic countries de-icing salts are spread around 30 to 60 times each season and each time 10 to 25 g/m^2 NaCl are spread depending on the meteorological conditions.

There could be a relationship between the frequency of de-icing salt exposure and chloride penetration according to Kamiya et al. [1995]. The transport of the salt from the road surface will be discussed in Section 11.4.

11.3.2 Exhaust from vehicles

Exhaust from vehicles can change the pH value in the area close to the road, which could affect leaching of salts and ions from the concrete surface. An ongoing investigation by Paulsson [1996] indicate pH-values from 6.8 to 7.9 in free water collected on a concrete bridge in the central area of Stockholm. Data will be published in 1997.

11.4 Transport proeesses from the road surface

Transport of rain water, snow, de-icing salt and other agents from the road surface to the close surrounding environment of the road, could be described with the following mechanisms and maybe combinations of them. The principal transport mechanisms are drainage, splash and aerosols. The aerosols are transported with the moving air due to the wind or drag from vehicles.

11.4.1 Drainage

Most roads has a drainage system with defined elevation and ditches at the road side to take care of the drained water. Some asphalt have a open pore structure which allows drainage trough the road surface.

The drainage mechanism is only active when the road surface has a layer of free water. In winter-time salt water will flow periodically towards the lower parts of a structure.

11.4.2 Splash

When a car drives trough water or wet snow, the tires drainage system generates a flow from the contact surface between the tire and the road. The majority of the flow is directed from the car towards the side of the road. The direction of the splash and the distance it could travel are functions of car speed, Eliasson [1996].

Combined effects of splash and air-borne salt are studied by Tang [1996]. The experimental set-up cf. Figure 11.4.2:1 collects the salt water and chloride content are analysed, and the total chloride exposure on a vertical surface close to the road were calculated. Wirje [1996] measured the adsorption of chloride in mortar specimens on the same location. The correlation between in chloride exposure and absorption in mortar specimens are shown in Figure 11.4.2:1.

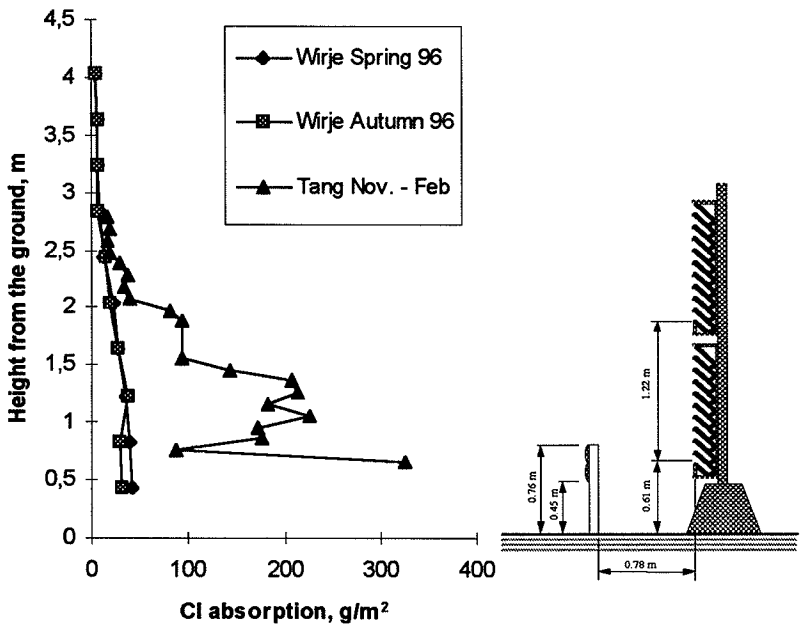

Figure 11.4.2:1. Chloride exposure on a vertical surface at Rv40, SW part of Sweden. Under the winter 1995-1996 869g Cl/m² (1432 g NaCl/m²)was applied. Tangs [1996] experimental set-up measures the chloride exposure. Wirjes [1996] experimental set-up measures the chloride absorbed into mortar specimens.

11.4.3 Air borne salt

Small water drops will be created when mechanical energy or moving air are added to wet surfaces or to larger water drops. Small water drops do not have enough kinetic energy and will easily follow moving air.

In the road environment the definition of "air borne salt" should be used on small salt water drops and dry salt that easily follow the drag from vehicles, They move parallel to the traffic and can be lifted in the turbulent zone behind the car. When the car has

passed, it will follow the wind and be deposited close to the road. At a distance of more than 100 m from the road the airborne salt level is close to the background level, Eliasson [1996]. About 20% of the salt will deposit within 3 meters from the road according to Dragstedt [1980], and 25% will deposit within 7 meters according to Pedersen & Forstad [1994].

11.5 The road bridge environment

The micro environment surrounding a road bridge could be divided into two principal zones, the dry zone and the zone exposed to rain. These zones could be identified in data from Wirje [1996] shown in Figure 11.5:1. It is important to note that the data are obtained from only one exposure season and in a location where the other parameters (car speed, location...) are constants.

The height above the road is the most decisive parameter in this and other studies. The C_{sa} value varies from 0.4 % down to 0.05 % in the wet zone and from 0.15% down to the detection limit in the dry zone. The C_{sa} values in Andersen [1996] are higher see section 11.5.3.

This could be explained with the lack of leaching in the dry zone and it would be natural with a slow increase with time in C_{sa} in the dry zone. In the wet zone a steady-state in the C_{sa} value would probably be reached after a couple of seasons due to leaching of chloride out of the concrete in the summer and autumn periods. In Wirje [1996] approximately 20 % of the chloride leached out in the wet zone and less than 5 % in the dry zone during the first season.

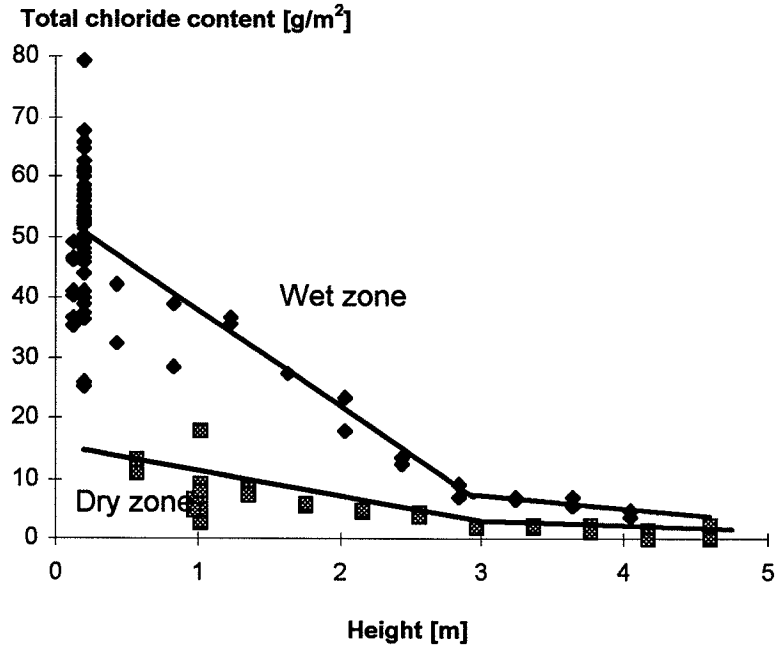

Figure 11.5:1. The amount of chloride absorbed in mortar specimens close to highway Rv40 in Sweden during the winter 1995-1996 as a function of height above the road for dry and wet road structures. Data from Wirje [1996].

11.5.1 The dry road environment

It is characteristic for the dry zone that it is not exposed to direct rain, and therefore the concrete has a relative low relative humidity, less than 90% RH. Sometimes it could have a lower relative humidity than the surrounding air, because of the low radiation from a low standing sun and lack of radiation towards the sky, which leads to a higher temperature than the surrounding air.

Splash and aerosols from the road make the micro climate very complex on these parts of the structure. It is not straight forward to evaluate the chloride penetration in these parts of a bridge structure.

Measurements by Volkwein [1986] and Andersen [1996] indicate that it is not the surface facing the road, the traditionally examined surface, that have the highest chloride penetration depth. Instead, the leeward surfaces have higher chloride contents, this phenomena is also observed in some RC structures exposed to marine environment Maage et al. [1995].

The height dependence is however relatively clear. From the road level up to around 3 meters the chloride exposure decreases to almost a background level, cf. Weber [1982] and Figure 11.5.1:1. This is also confirmed by Wirje [1996], cf. Figure 11.5:1. The salt exposure is relatively low but leaching of salt from the concrete in the dry parts is also low according to Wirje [1996].

Parts of a concrete structure in the dry environment just below joints are exposed to running salt water and are typical damaged areas according to West [1996]. This indicates that special concern should be taken when designing these parts of de-icing salt exposed structures.

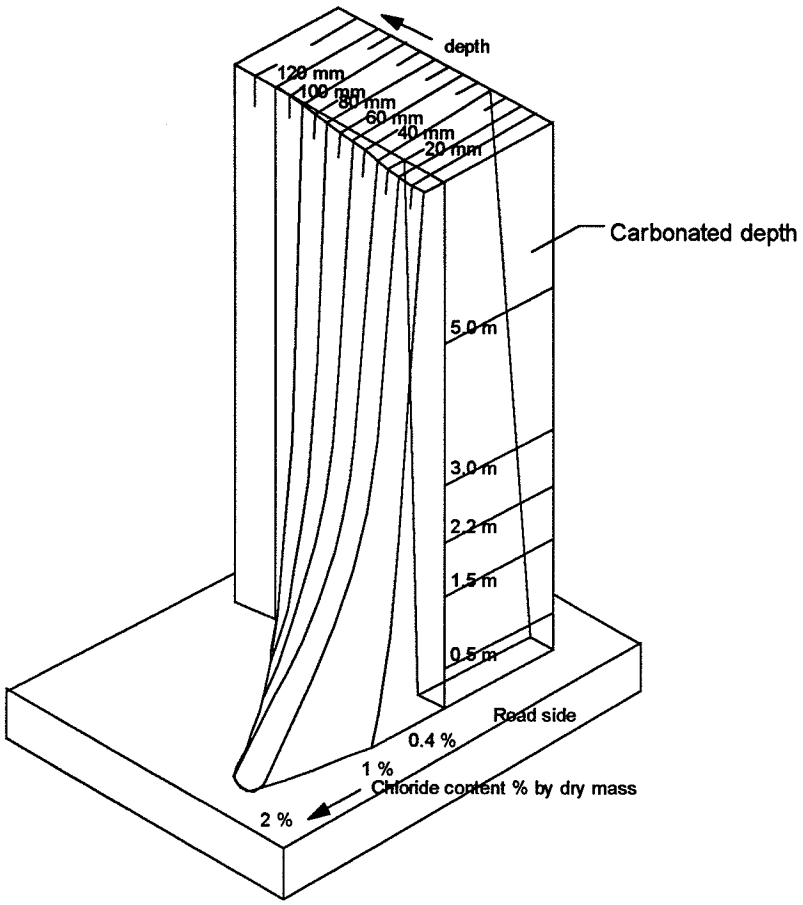

Figure 11.5.1:1. Height dependence of chloride penetration profiles close to a road. Data from Weber [1982].

11.5.2 The wet road environment

The wet road environment is directly exposed to rain, and therefore the relative humidity in the concrete often exceeds 90 % RH. The wet environment is also exposed to radiation which could lead to extreme temperature variations on some of these parts. The road surface is also wet close to these parts. Consequently there will be significant splash of rain water and salt water from the road surface to the concrete surfaces. These parts of the structure often have the highest chloride exposure but chloride could be extensively washed out according to Wirje [1996].

11.5.3 Response from Danish road bridges

The response of road bridges are complex but they seem to follow a pattern. The simplest way to summarise the response is to use the parameters C_{sa} and D_a defined in Chapter 3. The inner part of the chloride profiles from Andersen [1996] fits well the error function. Curve fitting of the inner part of the profile and the outer part of the profile separately gives approximately the same C_{sa} value but the D_a value differs in the

inner and outer part of the profile. One interpretation of this phenomena is the chloride profile's inner part are a response from the bridge's lifetime. The outer part of the chloride profile changes over a year cycle. This change is larger in the wet zone. In the inner part of the structure the chloride transport mechanism is a diffusion process. In the outer part convection contributes to the chloride transport. The cores are all from columns supporting road bridges and they are situated in the dry road environment.

Table 11.5.3:1. Chloride penetration depths, carbonation depths and chloride diffusion coefficients for cores taken from bridges. From Andersen [1996]. The C_{sa} and D_a values are fitted from the inner part of the profiles. The C_{sa} values from the outer part of the profile are almost the same as the C_{sa} values from the inner part.

Bridge built	Sampling date	Core Mark	Height above road level [m]	x_{CO3} [mm]	D_{CTH} [10^{-12} m^2/s]	C_{sa} [% Cl by dry mass]	D_a [10^{-12} m^2/s]
10-0031	960512	1	0.2	2		0.15	0.06
1968	960512	2	0.2	0	8.2	0.33	0.15
	960512	3	0.0	0		0.17	0.8
	9103		0.2			0.17	0.8
30-0016	960425	1	0.5	-	10	0.13	0.18
1972	9103		0.2			0.061	0.049
20-0085	960511	1	0.3	7-14		0.07	0.3
1963	960511	3	0.1	5-15	35 and 32	0.16	0.25
	960511	4	0.7	7-10	79 and 37	0.20	0.40
	9103		0.3			0.065	0.25
40-0004	960526	"20"	0.2	0		0.16	0.19
1956	960526	"33"	0.3	0		0.16	0.22
	9103		0.15			0.12	0.15
14-0036	960619	S	1.3	4	7.5	0.41	0.083
1956	960619	N1	1.3	2	9.0	0.44	0.009
	960619	N3	0.2	2	4.6	0.46	0.086
	960619	N4	1.9	3		0.27	0.035
	911002	S	1.0			0.48	0.042
	911002	N	1.0			0.39	0.021
	920520	S	1.0			0.33	0.066
	920520	N	1.0			0.21	0.033

11.6 Conclusion

A reasonable approach to describe the environment for road structures is to separate the environments into two main groups, each having a height dependent chloride exposure with a maximum chloride exposure at the road level and decreasing almost linearly to near zero at some 3-4 m above road level.

The two environmental areas would be

- wet road structures, parts of structures that are exposed to direct driving rain and direct splash from a wet road surface.
- dry road structures, parts of structures that are exposed to airborne chloride, but sheltered from rain and close to relatively dry road surfaces that are sheltered from rain.

The surface chloride level in these two areas should be quite different, a few examples are given here. The chloride penetration can be predicted by using an improved convection model (Chapter 7) with the moisture conditions taken into account. If using the empirical model for chloride penetration (Chapter 3), the achieved chloride diffusion coefficient should rapidly decrease with time, i.e. $D_a t$ = constant ($\alpha = 1$), in the dry zone. In the wet zone however it should be possible to use the empirical model in the "ordinary" way (see Section 6.6).

12 The marine environment

Concrete responds differently to different environments. The differences from one location to another are not fully understood and cannot be modelled with todays knowledge. Thus studies of the respond in different situations is the key to better understanding. This Chapter presents data from one of the most comprehensive studies of the responses of different concretes to the marine environment.

During the last decade the inspection of marine RC structures (reinforced concrete structures) has increased the number of observations available for design and analysis of new marine RC structures. Therefore, it is expected that in near future the knowledge about the achieved chloride diffusivity of various types of concrete exposed to environments of different chloride exposure will increase remarkably.

12.1 Types of data

The sources of data from concrete exposed to marine environment vary, but they can be divided into the following groups:

- Test on concrete specimens being exposed to seawater by either spray or submerged under laboratory conditions.
- Inspection of concrete specimens exposed to seawater on location at a marine exposure station.
- Inspection of (real) marine RC structures.

12.1.1 Laboratory exposure tests

The laboratory test of concrete exposed to an artificial marine environment has the advantage that small test specimens can be used, i.e. that a test series can contain many types of concrete. This means that the influence of the concrete's properties on its response to the environment can be studied systematically and in details.

The disadvantage of laboratory tests is that seawater exposure will always be established in a much simpler way than in nature. This means that deviations from a real seawater exposure might occur. It is obvious that the casting, compacting and curing of concrete under laboratory conditions will in most cases differ significantly from that of a building site. Since the casting, compacting and curing of concrete are characteristics important for the achieved chloride diffusivity laboratory tests might lead to one-sided deviation from concrete in real marine structures.

However, if the response of the concrete exposed under laboratory conditions is checked against the real exposure conditions and a possible correction is made, this will compensate for such deviations so that many more details can be studied in the laboratory than in the real marine environment.

12.1.2 Marine exposure stations

The test of concrete exposed to seawater at marine exposure stations has the advantage that medium-sized test specimens and concrete structural components can be used. This means that the influence of the concrete's properties and the component's structural and

geometrical details on the response to the environment can be studied systematically and in details.

The disadvantage of marine exposure stations is that it is difficult to create the humidity and temperature conditions in rather small concrete test specimens compared to the conditions present in more massive volumes of concrete found in real marine RC structures.

Tests of concrete at marine exposure stations are more expensive than tests carried out in the laboratory. However, since they are more realistic and reliable than laboratory tests, several marine exposure stations are in function today.

In order to obtain reliable observations, inspections ought to be carried out during a period of at least 5 years and include 3 - 7 observations so that the influence of time (age) can be dealt with. Some marine exposure stations are that old but we have no access to useful data. Thus, the results of tests carried out at many marine exposure stations are still waiting to be presented.

12.1.3 Real marine structures

Marine RC structures have the advantage that there is no doubt about the reality of their seawater exposure. Another advantage is that there are marine concrete structures in a wide range of ages.

However, the disadvantages are that the types of concrete will be very limited. The concrete used has always been chosen for just the purpose of the marine structure itself. Thus, it will not be possible in this way to inspect concrete which is not believed to be durable to seawater attack. Also, the inspection of the concrete must be carried out in-situ, i.e. the drilling of test cores for submerged concrete must be carried out by divers. Inspection of concrete in marine structures is very expensive and all holes left by drilling must be repaired. Furthermore, no building owner likes to drill cores since it will always weaken the structure to a certain extent and also estetic reasons! Therefore, only a limited amount of cores will be available from each marine structure.

12.2 Träslövsläge marine exposure station

The need for a series of observations of chloride ingress into concrete specimens having systematic variation of decisive parameters lead to the establishment of a marine exposure station at Träslövsläge Harbour at the west coast of Sweden, near Varberg. The exposure station was established in 1991 and the first observations collected are very promising and will hopefully fill in the gab between laboratory tests and inspection of the real marine structures.

Here, the first set of observations is presented, but a new inspection is planned during the spring of 1997.

12.2.1 Experimental programme

When the test series of Träslövsläge was planned it was possible to take various decisive parameters into account. However, each of the test series is very time consuming and costly if a detailed inspection is required, e.g. by observing profiles of total and free chloride, moisture, hydroxide ion, sodium and potassium, besides the micro structural analysis of the concrete (intensity of defects and mineralogical and chemical characteristics versus time). A choice of test series had to be made and at the moment three pon-

toons are carring test specimens of concrete of more than 50 mixture recipes with water/binder ratios varying from 0.75 to 0.25.

Environments tested

The concrete test specimens are prismatic having the dimensions: 1000 × 700 × 100 mm. These specimens are mounted at the pontoon in such a way that three local environments are formed:

- Marine atmospheric zone.
- Marine splash zone.
- Marine submerged zone.

With respect to the chloride content the seawater in Träslövsläge Harbour represents an average marine environment from a Danish point of view, i.e. the marine environment lies between the environment of the North sea and the Baltic sea.

Concretes tested

Many different constituent materials and compositions are used for the concretes tested:

- Cement types: OPC and SRPC from various factories.
- Silica fume: Additions in the range of 0 - 10 % by mass binder.
- Flyash: Additions in the range of 0 - 20 % by mass binder.
- Silica fume and fly ash: Simultaneous additions of various amounts of silica fume and fly ash.
- Air entrainment: Air entrained concrete (air content up to 6.6 % by volume of concrete) as well as concrete with no addition of air entraining admixtures are tested.
- Cement content: Concretes having cement contents in the range from 240 kg/m^3 of concrete to 522 kg/m^3 of concrete are tested.
- Water/binder-ratio: Concrete having water/binder ratios in the range from 0.25 to 0.75 by mass are tested.
- 28 days compressive cube strength: Concretes having compressive cube strengths at an maturity age of 28 M-days in the range from 21 MPa to 125 MPa in average are tested.

Basic concrete properties for selected specimens are given in Table 12.2.2:1. A more detailed description of the test programme carried out at the Träslövsläge Marine Exposure Station is given by Sandberg [1996].

Table 12.2.2:1. Basic properties of some of the concretes from the Träslövsläge marine exposure station. The obtained chloride profiles from the natural exposure of these concretes are given in the Appendix.

ID Number	w/b ratio	Cement	Silica fume	Fly ash	Water	Cement paste	Cementitious content	Calculated density
3-75	0.75	232.8	12.3	0.0	184.0	26.3	12%	2109
1-50	0.50	370.0	0.0	0.0	185.0	30.2	17%	2152
2-50	0.50	390.0	0.0	0.0	195.0	31.9	18%	2134
3-50	0.50	351.5	18.5	0.0	185.0	30.5	17%	2145
Ô	0.38	420.0	0.0	0.0	159.6	29.3	19%	2217
2-40	0.40	420.0	0.0	0.0	168.0	30.1	19%	2217
3-40	0.40	399.0	21.0	0.0	168.0	30.4	19%	2210
H4	0.40	399.0	21.0	0.0	168.0	30.4	19%	2210
10-40	0.35	345.0	20.5	75.0	155.2	30.8	20%	2205
12-35	0.33	382.5	22.5	45.0	146.5	29.9	20%	2245
H3	0.30	492.0	0.0	0.0	148.0	30.4	20%	2460
H1	0.30	475.0	25.0	0.0	150.0	31.2	20%	2448
H2	0.30	450.0	50.0	0.0	150.0	31.6	21%	2439
H8	0.26	493.0	0.0	123.0	159.0	37.1	26%	2399
H5	0.25	525.0	26.3	0.0	137.8	31.6	22%	2501
Unit	by mass	kg/m^3 concrete	kg/m^3 concrete	kg/m^3 concrete	kg/m^3 concrete	% volume concrete	% mass concrete	kg/m^3 concrete

Data processing

In order to describe the local environment and the concrete's response by the four parameters used by the Mejlbro-Poulsen Model, selected observations are studied. These observations are selected in such a way that chloride profiles of the concrete are achieved at least at two different periods of chloride exposures. By non-linear regression analyses the values of the parameters S_p, p, D_{aex} and α are obtained and the more convenient parameters D_1, C_1, D_{100} and C_{100} are calculated. Also the more conventional parameters of the error function solution to Ficks 2nd law D_a and C_{sa} are calculated.

A description of the regression analysis is given in Section 6.6 "Prediction with the Mejlbro-Poulsen Model". All the results of the regression analyses are presented in the Appendix of this report, but some of them are being utilised later and those are presented below. How to make use of the mentioned parameters is described in Chapter 15 and 16.

Table 12.2.2:2. Achieved diffusion coefficients for each of the chloride profiles measured on the Träslövsläge concretes defined in Table 12.2.2:1. The values are extracts of the data sheets given in the Appendix.

	Exposure times				Submerged			Splash		Atmosphere	
ID No.	t_{ex}	t_1	t_2	t_3	$D_a(t_1)$	$D_a(t_2)$	$D_a(t_3)$	$D_a(t_1)$	$D_a(t_3)$	$D_a(t_1)$	$D_a(t_3)$
3-75	0.038	0.822		1.241	527.8		244				
1-50	0.038	0.822	1.241	2.184	219.2	313.9	177.5	203.1	101.1	151.2	103.3
2-50	0.038	0.953		1.373	228.6		251.4				
3-50	0.038	0.819	1.238	2.219	204.3	199.5	94.8				
Ô	0.038	0.614	1.033	2.014	106.8	114.2	90.1	95.3	81.4	100.9	33.3
2-40	0.038	1.362		2.4	115.2		94	24.6	54.7	21.9	37.4
3-40	0.038	0.819	1.238	2.277	136.6	50.2	67.2	48	27.5	51.9	16.2
H4	0.038	0.627	1.047	2.027	67.5	37.8	31.5	27	25.7	35.5	34.9
10-40	0.038	0.71		2.11	47.6		28.3	12.2	9	24	23
12-35	0.038	0.726		2.129	61.8		27.9	29.4	32.9	40.7	20.2
H3	0.038	1.047		2.088	82.9		101.2	30.9	41.7	47.4	27
H1	0.038	1.047		2.016	29.4		25	8	6.5	14.4	5.9
H2	0.038	1.047		2.027	13.4		13.9	9.2	10.7	11.7	8.8
H8	0.038	1.047		2.088	62		40.3	35.7	21	20.5	18.9
H5	0.038	1.047		2.074	16.8		16.2	6.1	5.6	16.8	6.1
Unit	year	year	year	year	mm^2/yr	mm^2/yr	mm^2/yr	mm^2/yr	mm^2/yr	mm^2/yr	mm^2/yr

The data and the quality of each fit of the chloride profiles are presented in the Appendix. In Figure 12.2.2:1 is shown an example of good agreement between the data, the fit to the Mejlbro-Poulsen model and the conventional error function solution.

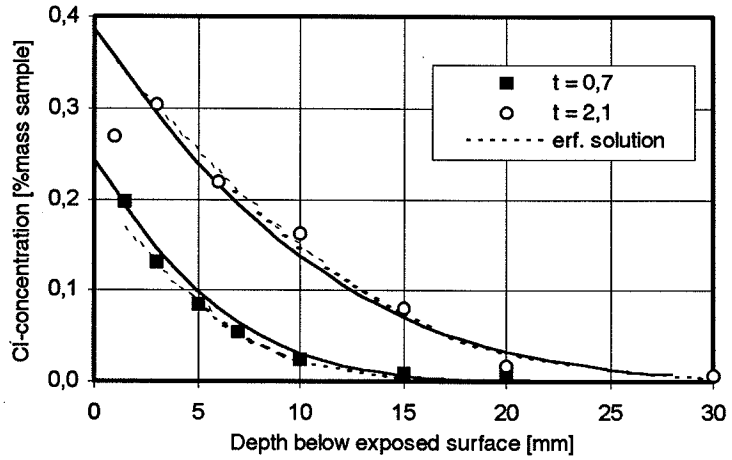

Figure 12.2.2:1. The achieved chloride profiles measured in the the splash zone on the concrete with ID No. 12-35. This is an example of good agreement between the data, the fit to the Mejlbro-Poulsen model and the conventional error function solution.

*Table 12.2.2:3. The derived parameters D_1 and D_{100} of some of the concretes from the Träslövsläge marine exposure station. The obtained values are extracts of the data sheets with the chloride profiles from the natural exposure of these concretes given in the Appendix. The figures in **bold** writing represents samples where the error function solution and the Mejlbro-Poulsen solution almost agree in the fit to the measured profiles.*

ID Number	Marine submerged [mm^2/yr]		Marine splash [mm^2/yr]		Marine atmosphere [mm^2/yr]	
	D_1	D_{100}	D_1	D_{100}	D_1	D_{100}
3-75	340.9	3.4				
1-50	3198.6	33.0	192.0	3.3	**420.0**	**76.1**
2-50	273.5	273.5				
3-50	1017.9	10.8				
Ô	622.8	6.2	884.8	10.3	**93.3**	**5.9**
2-40	**102.7**	**102.7**	55.7	55.7	**50.9**	**50.9**
3-40	162.6	1.6	**34.2**	**34.2**	189.7	2.2
H4	53.2	0.5	**25.6**	**1.6**	**35.1**	**35.1**
10-40	31.5	0.3	**14.2**	**3.9**	**26.2**	**16.5**
12-35	**41.8**	**4.2**	**55.8**	**55.8**	33.6	0.3
H3	55.3	55.3	1271.8	12.7	46.2	2.1
H1	**34.4**	**19.7**	9.5	0.4	**10.6**	**10.6**
H2	**16.3**	**16.3**	10.6	10.6	25.6	0.3
H8	73.2	0.7	40.4	0.4	24.2	24.2
H5	19.9	19.9	8.6	3.4	162.0	1.7

*Table 12.2.2:4. The derived parameters C_1 and C_{100} of some of the concretes from the Träslövsläge marine exposure station. The obtained values are extracts of the data sheets with the chloride profiles from the natural exposure of these concretes given in the Appendix. The figures in **bold** writing represents samples where the error function solution and the Mejlbro-Poulsen solution almost agree in the fit to the measured profiles.*

ID Number	Marine submerged [% of concrete]		Marine splash [% of concrete]		Marine atmosphere [% of concrete]	
	C_1	C_{100}	C_1	C_{100}	C_1	C_{100}
3-75	0.450	0.450				
1-50	0.445	0.716	0.352	0.352	**0.112**	**0.970**
2-50	0.478	2.000				
3-50	0.571	0.927				
Ô	0.635	0.748	0.516	2.000	**0.252**	**0.633**
2-40	**0.402**	**1.151**	0.292	2.000	**0.137**	**1.851**
3-40	0.688	0.722	**0.361**	**2.000**	0.225	0.531
H4	0.713	0.721	**0.399**	**0.399**	**0.219**	**0.219**
10-40	0.586	0.586	**0.385**	**1.141**	**0.214**	**2.000**
12-35	**0.430**	**0.615**	**0.249**	**1.587**	0.173	0.173
H3	0.361	0.462	0.232	2.000	0.161	0.161
H1	**0.485**	**1.279**	0.281	0.281	**0.190**	**1.553**
H2	**0.397**	**2.000**	0.467	2.000	0.211	0.219
H8	0.414	0.414	0.288	0.288	0.213	0.660
H5	0.338	2.000	**0.255**	**1.467**	**0.192**	**0.708**

It is difficult to discover any clear and conclusive system of the data presented above, but the following trends seem to be supported by the data:

- The achieved diffusion coefficient D_a tends to decrease with time for many of the data sets.
- The achieved surface chloride concentration tends to increase with time for many data sets.
- The achieved diffusion coefficient D_a decrease with a lower *w/b* ratio.
- Addition of silica fume has a remarkable decreasing effect of the achieved diffusion coefficient D_a.
- The achieved diffusion coefficient D_a is depending on the type of exposure.

More tendencies can be found, but that is not the aim of this Chapter. This will be treated more systematically in Chapter 13.

PART C. DESIGN

Part C covers chapters 13-18, describing the environmental conditions and giving examples of how to make chloride durability design and how to calibrate the developed models.